Static-Cyclic Shear Tests on Masonry Wallettes with a Damp-Proof Course Membrane

Nebojša Mojsilović, Senior Scientist,
Institute of Structural Engineering, Department of Structural, Environmental and Geomatic Engineering, ETH Zurich, Switzerland

Goran Simundic, Professional Officer,
Centre for Infrastructure Performance and Reliability, School of Engineering, University of Newcastle, Callaghan, NSW, 2308, Australia

Adrian Page, Emeritus Professor,
Centre for Infrastructure Performance and Reliability, School of Engineering, University of Newcastle, Callaghan, NSW, 2308, Australia

Zurich
November 2009

Preface

A joint research project by the University of Newcastle and the ETH Zurich on the structural behaviour of unreinforced masonry elements subjected to cyclic shear is underway at the University of Newcastle, Australia. The main goal of the research project is to investigate the influence of a damp-proof course (DPC) on the structural behaviour of masonry walls subjected to shear when the DPC is placed in a bed joint or at the interface of the masonry and its supporting concrete slab.

Within the framework of the project a series of static-cyclic shear tests on brick masonry wallettes were performed at the University of Newcastle. This report presents and discusses the results obtained from these tests.

This research project extends the previous investigation of a small specimen study of the shear behaviour of masonry walls subjected to static-cyclic shear loading with a DPC incorporated either in a mortar joint or at the masonry-concrete slab interface.

Zurich, November 2009 Dr. Nebojša Mojsilović

Table of contents

1. Introduction

A joint research project by the University of Newcastle and the ETH Zurich on the structural behaviour of unreinforced masonry elements subjected to cyclic shear is underway at the University of Newcastle. The main goal of the research project is to investigate the influence of a damp-proof course (DPC) on the structural behaviour of masonry walls subjected to shear when the DPC is placed in the bed joint or at the interface of the masonry and its supporting concrete slab.

1.1. Background to the project

A damp-proof course (DPC) is frequently placed at the base of masonry walls as a moisture barrier and/or to act a slip joint to allow for differential movements (see Figure 1). Although it is desirable for the DPC to be sandwiched in the mortar joint, in reality it is usually placed in the joint above or below the mortar. In some cases, the DPC alone is used, particularly if it is serving as a slip joint at the interface between a masonry wall and a concrete slab.

Figure 1: Typical DPC practice and earthquake performance

From a structural point of view, it is important to understand the influence of the DPC on structural behaviour, especially on the in-plane shear behaviour of unreinforced masonry walls which often serve as shear walls for the complete structure. Recently, a series of static, static-cyclic and dynamic tests on small masonry elements with different types of damp proof courses were performed (1-4). These tests indicated that shear can be transmitted through a joint containing a DPC. Reasonable hysteretic behaviour was also observed under cyclic loading.

This research project extends a previous small specimen investigation of the study of the shear behaviour of masonry walls subjected to static-cyclic shear loading with a DPC incorporated either in a mortar joint or at the masonry-concrete slab interface.

1.2. Testing programme

Cyclic load tests were performed on two series of masonry elements with a DPC placed into one of the bed joints. Each series consisted of nine 110 mm thick clay brick masonry wallettes with nominal dimensions of 1200x1200 mm. The DPC was placed either between the first two courses (Series A) or between the concrete base and first masonry course (Series B). In addition, three control specimens with the same dimensions and without a DPC were tested (Series C). The specimens were at first subjected to a vertical pre-compression load which was kept constant during the test and then subjected to a cyclic shear load applied in time steps with prescribed horizontal displacements. Three different levels of pre-compression were considered, see Table 1. For each level of pre-compression, three replicates were tested for Series A and B, resulting in a total of 21 tests being performed.

Table 1: Specimen designation for test programme

Series	Pre-compression stress [MPa]		
	0.7	1.4	2.8
A	A3	A1	A2
B	B3	B1	B2
C	C3	C1	C2

2. Masonry materials

2.1. Masonry units

Extruded clay bricks with nominal dimensions of 230x110x76 mm and a void area of 25% (see Figure 2) were used for building the wallette specimens. The compressive strength of brick was determined from 10 brick units in accordance with Australian/New Zealand Standard AS/NZS 4456.4:2003 (5). The mean value obtained from the tests was 39.66 MPa and after applying the aspect ratio factor K_a a mean brick compressive strength of 28.60 MPa was determined. The characteristic compressive strength obtained from the sample was 19.10 MPa. Full details of the compressive strength results are given in Table A1 of Appendix A.

Figure 2: Extruded cored clay bricks

2.2. Mortar

A typical 1:1:6 mortar (cement:lime:sand) was used for building the wallette specimens. One batch of mortar was used for each wallette specimen and prepared in the laboratory by an experienced bricklayer. The mortar compressive strength was determined from six cube specimens with 100 mm sides (see Figure 3). The cubes were cured in air in the laboratory and tested after 28 days. A mean strength of 5.65 MPa was obtained. Detailed results are given in Table A2 of Appendix A.

Figure 3: Mortar test cubes and typical failure

2.3. Damp-proof course membrane

After considering the results of the previous tests on masonry with damp-proof courses (1-4), an embossed polythene membrane was chosen as the damp-proof course for the current tests (see Figure 4). The membrane was placed either between the first two courses (Series A) or between the concrete base and first masonry course (Series B). During the wallette construction the membrane was firstly placed directly on the brick course (Series A) or on the concrete base. The bed joint mortar was then placed on top of the membrane and the bricks of the next course laid on the mortar bed.

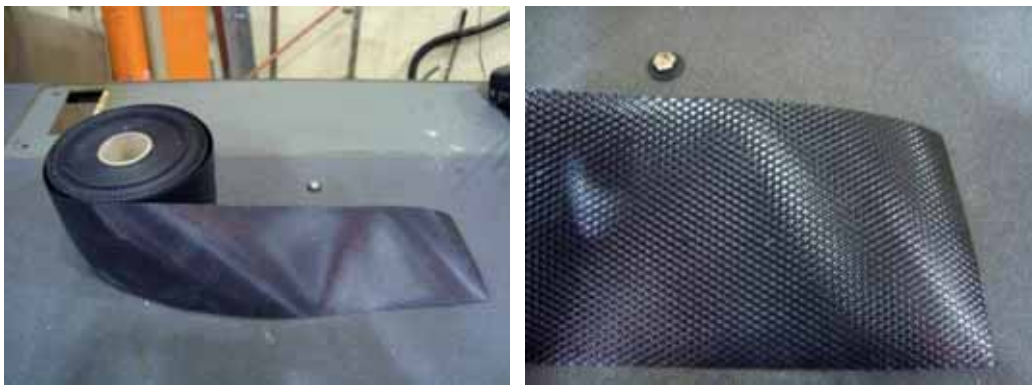

Figure 4: Embossed polythene DPC membrane

2.4. Flexural bond strength (Bond wrench test)

The flexural bond strength of the masonry was determined by means of the bond wrench test in accordance with Australian Standard AS 3700:2001 (6). Each joint of two six-unit high specimens was tested. The testing apparatus and typical joint failure are show in Figure 5. The mean and characteristic flexural tensile strengths were found to be 1.18 MPa and 0.61 MPa respectively. Detailed results are reported in Table A3.

Figure 5: Bond wrench test apparatus and joint failure

2.5. Masonry tensile bond strength (Splitting test)

Because the failure of the wallettes also involved some vertical splitting, for later modelling purposes, it was also useful to determine the transverse strength of the masonry composite. This was achieved using the splitting test reported by Ali (7), see Figure 6, performed on specimens which were built according to reference (7) and were cured in air in the laboratory. Using this procedure, the transverse strength is given by:

$$\sigma_T = \frac{CF}{Dt}$$

where $D = \sqrt{\frac{hl}{\pi / 4}}$ and h and l are the specimen height and width, respectively. In addition, t denotes the specimen thickness; F is the applied load and C a constant of 0.648. This constant depends on brick/joint stiffness and the chosen value was based on moduli of elasticity ratio of brick and mortar, E_b/E_m, of approximately 2, see also (7).

Using this approach, the mean transverse tensile strength of the five specimens was found to be 0.62 MPa with a coefficient of variation of 22.4%. Detailed results are given in Table A4.

Figure 6: Tensile bond test apparatus and splitting failure

2.6. Masonry shear bond strength

The masonry shear bond strength was determined using a triplet test in accordance with the European Testing Standard EN 1052-3 (8), see Figure 7. The mean shear strength was found to be 1.27 MPa (coefficient of variation 11.7%). Full results are given in Table A5 in Appendix A.

Figure 7: Shear bond test apparatus and shear failure

2.7. Masonry compressive strength

Masonry compressive strength was determined in accordance with the provisions of Australian Standard AS 3700:2001 (6). Five tests on three-unit specimens were performed, see Figure 8. The mean value obtained from the tests was 17.75 MPa (coefficient of variation 15.0%). After applying the aspect ratio factor k_a, mean and characteristic masonry compressive strengths of 14.18 MPa and 9.50 MPa were obtained, respectively. The mean value was used to determine the levels of pre-compression for the wallette tests. Detailed results are given in Table A6 in Appendix A.

Figure 8: Compression test on a masonry triplet

In order to obtain information on the in-situ masonry compressive strength of the wallettes, four specimens were cut-out from the undamaged specimen B3_2 after it was tested (failure occurred by sliding over the concrete base). The size of these four specimens corresponded to those stipulated in the European Standard EN 1052-1 (9) with the specimens being two units long and five courses high. In addition, these four specimens were used to determine the modulus of elasticity of the masonry.

Table A7 in Appendix A shows the specimen dimensions, failure loads as well as the compressive strength and modulus of elasticity (as a secant modulus at the load of 30% of the ultimate) for all four specimens. The mean value for the modulus of elasticity E_m obtained from tests on specimens 1 and 4 was 6.81 GPa. The mean value for the masonry compressive strength obtained from the tests was only a half of that obtained from the prism tests in accordance with the Australian code (see Table A6). Apart from any size effects, it is also possible that the specimens may have been damaged during the cutting-out process. The failure modes of these specimens (Figure 9) also differed from that of the masonry triplets indicating that the type of specimen may have also played a role.

Figure 9: Compression test on cut-out specimen and its failure

3. Wallette test specimens

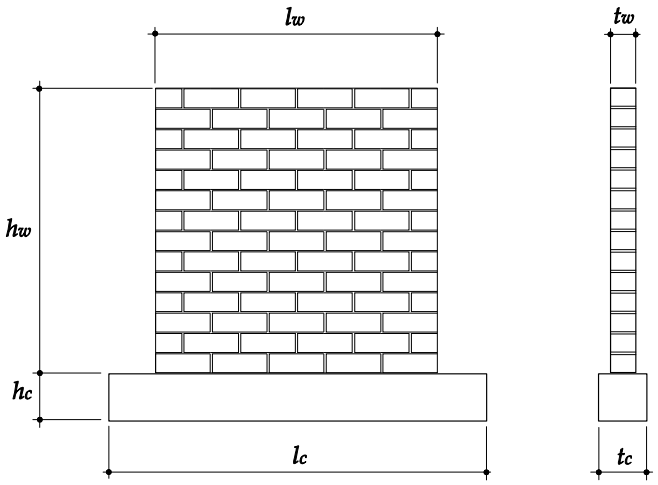

Figure 10: Wallette specimen

The wallette test specimens were built in the laboratory on reinforced concrete beams by a skilled mason. The specimens were nominally 1200 mm wide and 1200 mm high (five units long and 14 courses high). The wallette thickness t_w was 110 mm. These dimensions differed somewhat from specimen to specimen, see Table A8 in Appendix A. The concrete beam had a length l_c of 1600 mm, height h_c of 200 mm and a width t_c of 200 mm. The beam was reinforced with a nominal reinforcing cage consisting of 4/10 mm bars with 8 mm stirrups at 200 mm. The 1:1:6 mortar was prepared in the laboratory and the wallettes built in running bond. Both the bed and the head joints were 10 mm thick and fully filled. All wallettes were cured in air in the laboratory for 28 days before testing. Prior to testing the specimens were painted white in order to follow the crack development during the test. The wallette specimens as well as their construction are shown in Figures 10 and 11.

Figure 11: Construction and completion of wallette specimens

4. Test set-up and procedure

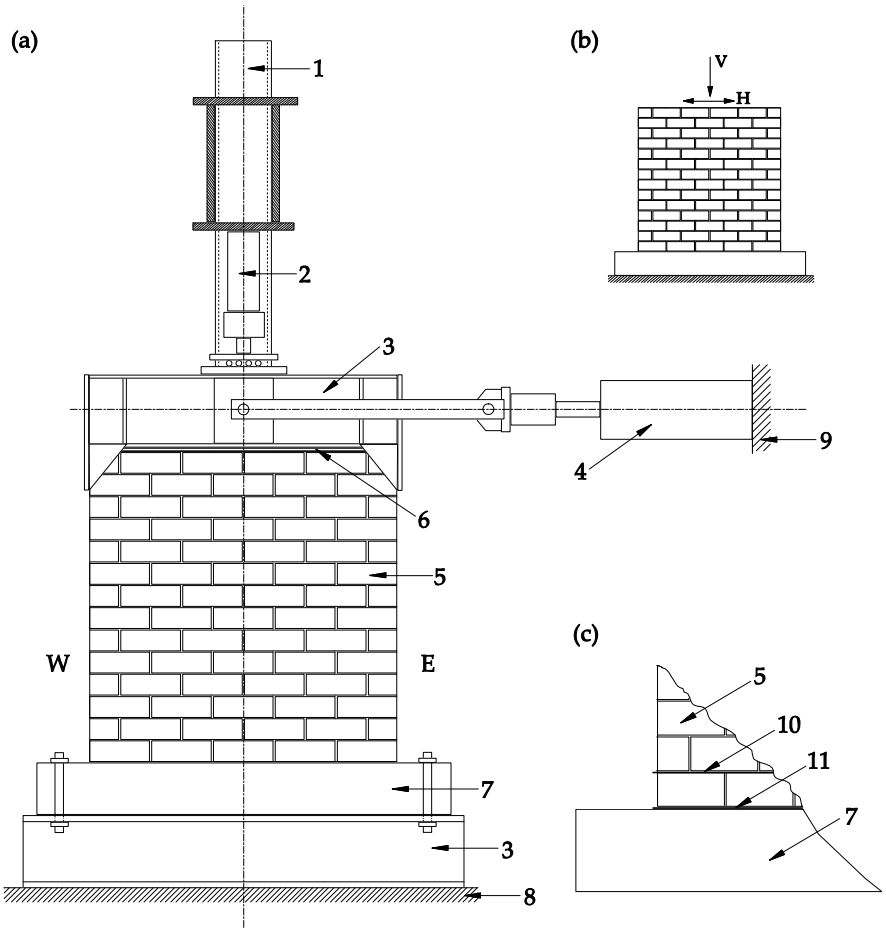

Figure 12: Test set-up: (a) Set-up; (b) Test principle; (c) DPC-detail

Figure 12 (a) shows the test set-up. Twenty-eight days after preparation, the wallette specimens were placed in the test set-up and were initially subjected to the desired level of pre-compression which was kept constant during the test. Three different levels of compression were applied, corresponding to 5%, 10% or 20% of the estimated masonry compressive strength as determined from the prism tests described in Section 2.7. The pre-compression levels imposed were 0.7 MPa, 1.4 MPa and 2.8 MPa, respectively. The axial load was applied by means of the hydraulic jack (2) placed between the support frame (1) and the upper spreader beam (3). The test specimen (5) together with concrete beam (7) was placed between two spreader beams (3). The concrete beam (7) was fixed to the lower spreader beam which in turn lay directly on the laboratory's strong floor (8). A neoprene plate (6) was placed between the specimen (5) and upper spreader beam (3) in order to ensure uniform load distribution over the specimen. After applying the vertical pre-compression load the wallette

specimens were subjected to cyclic shear loading by means of the hydraulic actuator (4) which was fixed to the reaction wall (9). Figure 12 (b) depicts the test principle and Figure 12 (c) shows the damp-proof course positions for both Series A (10) and B (11). A general overview of the set-up is shown in Figure 13. Further details of the test set-up are given in Figures 14 and 15.

Figure 13: Test set-up: overview

Figure 14: Test set-up: details

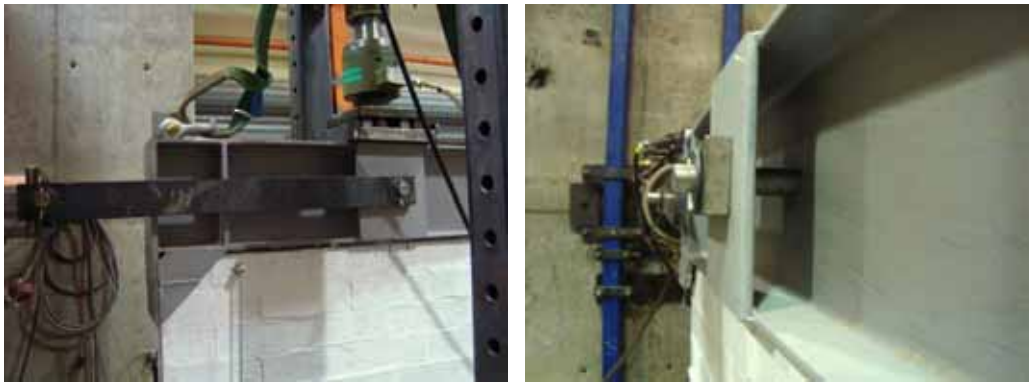

Figure 15: Test set-up: shear force introduction

The cyclic shear load was applied using computer controlled displacement steps. Each step was repeated three times in a form of a sinusoidal wave. A typical displacement history of shear displacement, v, versus time, t, is shown in Figure 16.

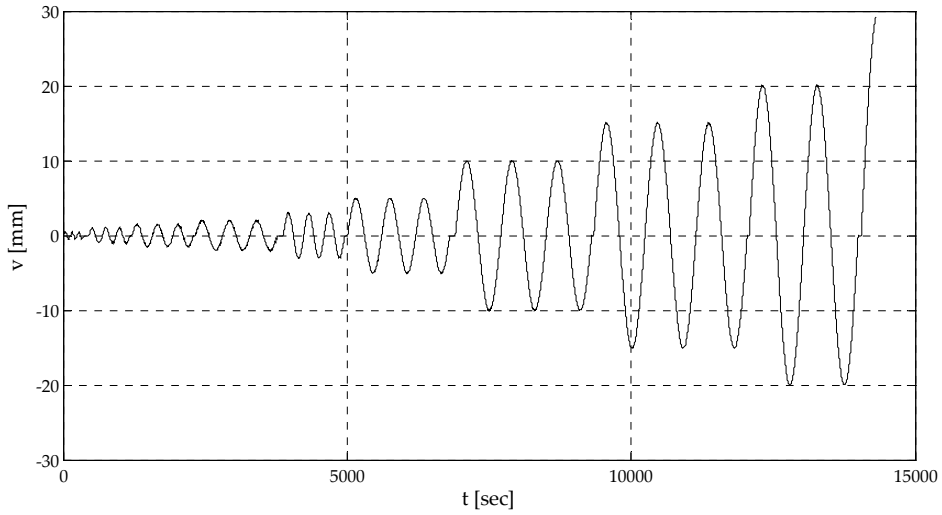

Figure 16: Typical displacement history

At the beginning of the test, i.e. for small displacements, the loading speed was only 1 mm/min. For the larger displacement steps the loading speed was gradually increased up to 5 mm/min for the maximum applied displacement of 30 mm, see also Table 2. This Table also provides information on the duration (period length) of each load step. Using this procedure, the test duration varied from 135 to 290 minutes depending on the pre-compression level.

Table 2: Loading history

Travel [mm]	0.5	1	1.5	2	3	5	7.5	10	12.5	15	20	25	30
Loading speed [mm/min]	1	1	1	1	2	2	2	3	4	4	5	5	5
Period [min]	2	4	6	8	6	10	15	13.3	12.5	15	16	20	20

Apart from the applied vertical and horizontal loads and displacement (jack travel) measurements included vertical (north face) and diagonal (south face) deformations of the wallette specimen, see Figure 17. Vertical deformations of the masonry were measured by means of two potentiometers, POT5 and POT6 which had a gauge length of 1115 mm. Diagonal deformations were measured by means of another two potentiometers, POT3 and POT4 which had a gauge length of 1453 mm, cf. Figure 17. Slip of the wallette specimen over the joint with damp-proof course membrane (POT 9 or POT10, depending on the position of DPC) as well as the uplift of the wallette toes (POT7 and POT8) were measured in relation to the concrete beam which was assumed to be static, see also Figure 17. All measuring devices were connected to a personal computer, which processed the data in real time. The potentiometer measurements were started after the vertical pre-compression was applied. As stated earlier, another personal computer was used to control the application of the horizontal displacements. During the tests, the nature and extent of the cracking was continuously observed and noted.

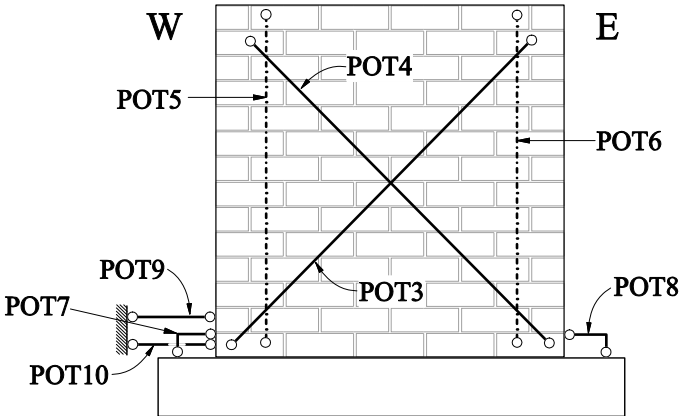

Figure 17: Potentiometer positions

5. Wallette test results and behaviour

Table 3 shows the values of the extreme (maximum and minimum) horizontal forces, H, recorded during the testing and their ratio to the applied vertical force, V. The total number of the load cycles as well as maximum horizontal displacement (jack travel), v, is also given. The failure modes for each wallette together with applied level of pre-compression, σ_{pc}, are also presented.

Table 3: Wallette test results

Specimen	σ_{pc} (MPa)	Number of cycles	max v [mm]	min H [kN]	max H [kN]	ext H/V	Failure mode
C1	1.4	27	30	-93.28	89.17	0.499	compression
C2	2.8	28	15	-157.71	145.89	0.422	compression
C3	0.7	25	30	-51.58	53.37	0.568	rocking
A1_1	1.4	27	15	-72.86	88.55	0.473	sliding
A1_2	1.4	28	20	-82.10	80.48	0.439	sliding
A1_3	1.4	27	20	-77.09	79.19	0.423	sliding
A2_1	2.8	28	15	-141.45	153.92	0.412	compression
A2_2	2.8	27	12.5	-125.49	125.35	0.336	compression
A2_3	2.8	24	10	-117.90	112.48	0.315	compression
A3_1	0.7	19	15	-42.80	45.53	0.484	sliding
A3_2	0.7	18	10	-43.41	44.73	0.476	sliding
A3_3	0.7	18	10	-44.73	44.00	0.476	sliding
B1_1	1.4	24	10	-87.95	85.47	0.470	sliding
B1_2	1.4	25	12.5	-77.98	81.38	0.435	sliding/compression
B1_3	1.4	33	20	-87.96	87.81	0.470	sliding/compression
B2_1	2.8	24	10	-132.32	139.61	0.373	compression
B2_2	2.8	27	12.5	-144.81	150.33	0.402	compression
B2_3	2.8	28	15	-150.24	149.59	0.402	compression
B3_1	0.7	21	15	-42.83	45.18	0.481	sliding
B3_2	0.7	21	15	-43.56	43.80	0.466	sliding
B3_3	0.7	22	20	-41.56	44.58	0.474	sliding

Note: Wallettes 'C' – no DPC; wallettes 'A' – DPC in the joint between first and second course; wallettes 'B' – DPC between masonry wallette and the concrete base.

Appendix B presents plots which show the relationship between the horizontal force and the previously mentioned potentiometer measurements. Appendix C presents the crack patterns for the tested specimens and Appendix D contains the photo archive of the tests.

In the following, the behaviour of the test specimens under different pre-compression levels will be discussed under consideration of failure modes, crack patterns and DPC influence.

5.1. Low pre-compression level, σ_{pc} = 0.7 MPa (Series A3, B3 and C3)

Typical cyclic behaviour (hysteresis curves) for this level of pre-compression is shown on Figures 18 and 19 for both wallettes with DPC (B3_1) and without DPC (C3), respectively. As can be seen from Figure 18 wallettes with DPC exhibited considerable energy dissipation and behaved in a quasi ductile manner. On the other hand, the wallette without a DPC (C3) exhibited a typical rocking behaviour and almost no ductility.

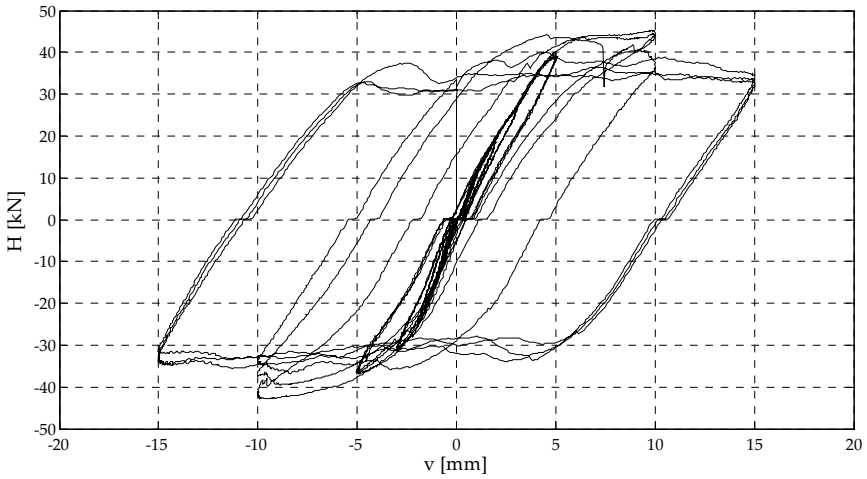

Figure 18: Hysteresis (H/v relationship) for typical wallette with DPC (B3_1)

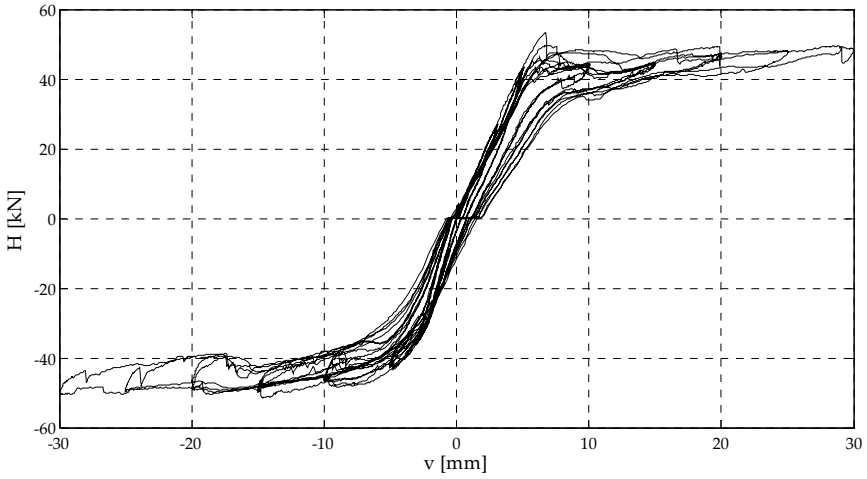

Figure 19: Hysteresis (H/v relationship) for wallette without DPC (C3)

Figure 20 shows envelopes of hysteresis curves for all test series, A3, B3 and C3. The influence of DPC in wallettes A3 and B3 can be clearly seen.

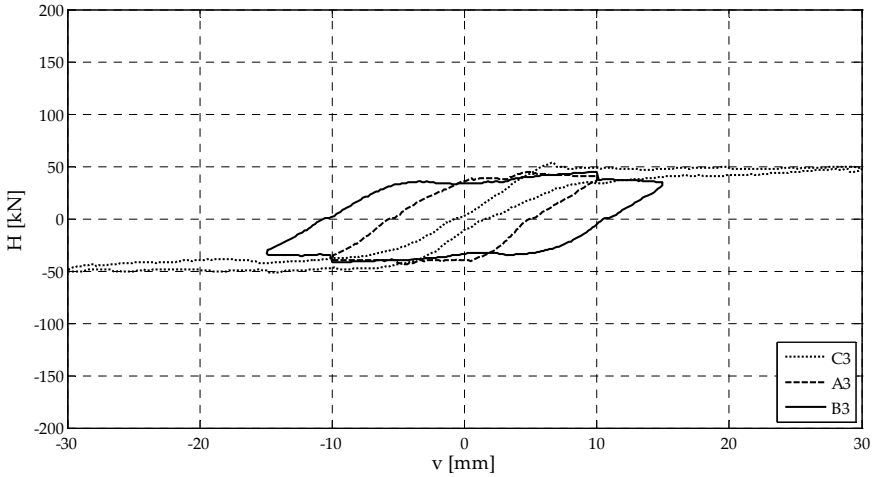

Figure 20: Hysteresis envelopes for wallettes under low pre-compression

Wallettes of both Series A3 and B3 failed by sliding over the DPC and accordingly developed a horizontal crack along the bed joint containing the DPC. Series A wallettes had additional vertical cracks in the first course (between the concrete base and the bed joint with the DPC) induced by cycling movement of the upper part of the wallette over the DPC (see also photos in Appendix D). Figure 21 shows the failure of the wallette A3_1 which was typical.

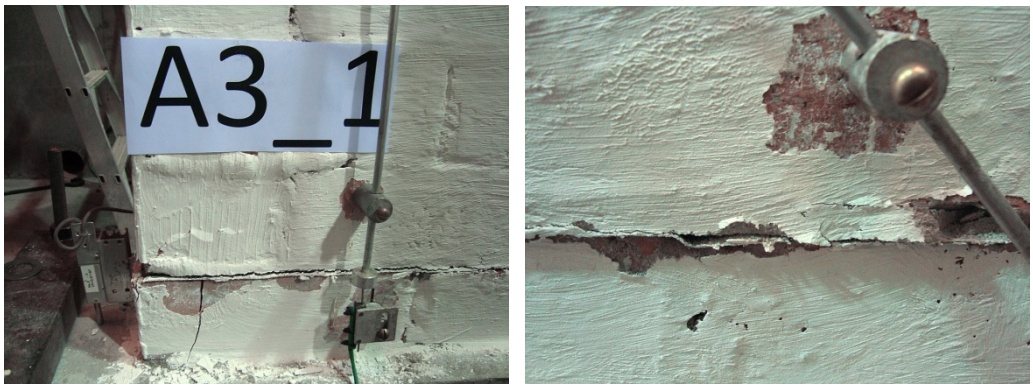

Figure 21: Sliding failure of the specimen A3_1

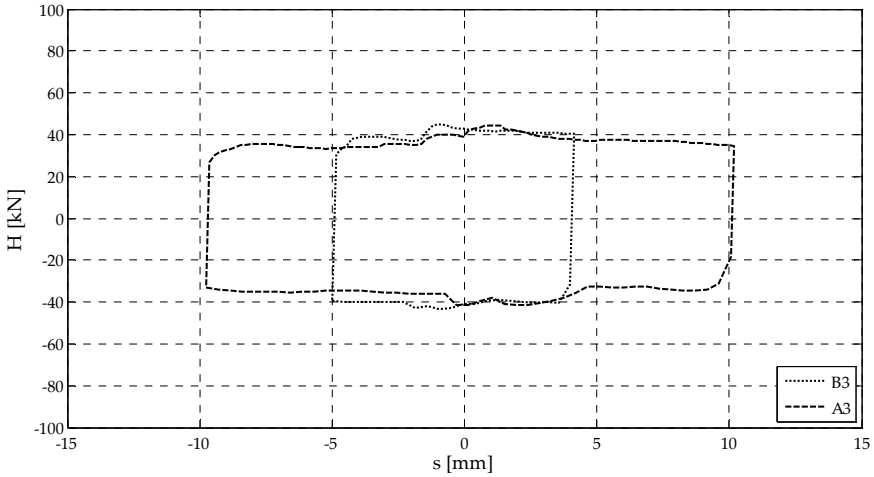

Figure 22: Slip envelopes of the wallettes A3 and B3

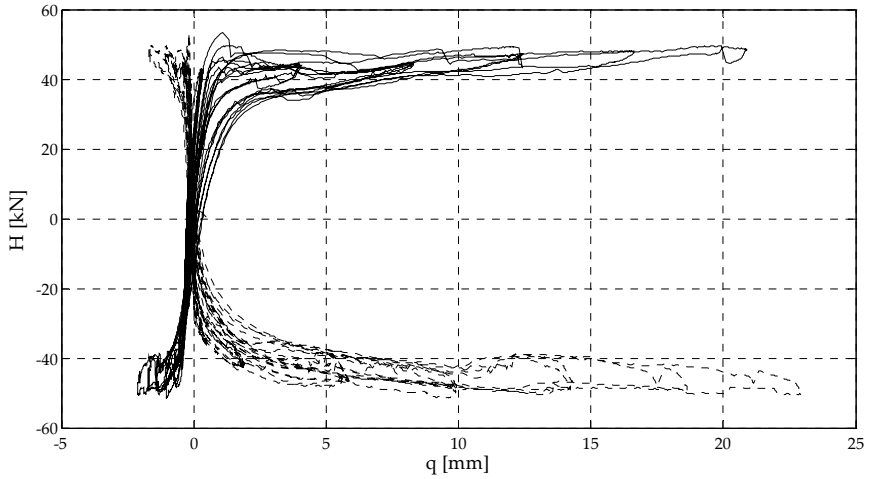

Figure 23: Uplift of the wallette toes for specimen C3

Figure 22 shows envelopes of the horizontal displacements i.e. slip, *s*, over the DPC for the wallettes A3 and B3. The corresponding control specimen without a DPC, C3, failed in a rocking mode and acted as a rigid body which rocked on the concrete base. Figure 23 shows the uplift measurements at each end of the wallette (the dashed line represents the uplift of the east side of the wallette and the full line that of the west side of the wallette, potentiometer positions 7 and 8 in Figure 17).

5.2. Medium pre-compression level, σ_{pc} = 1.4 MPa (Series A1, B1 and C1)

The typical cyclic behaviour (hysteresis curves) for this level of pre-compression is shown in Figures 24 and 25 for both wallettes with the DPC between the first two courses (A1_2) and between the concrete base and wallette (B1_3), respectively. Figure 26 shows the behaviour of the control wallette C1. As can be seen from these Figures, the wallettes with the DPC between the first two masonry courses showed considerable energy dissipation and behaved in a quasi ductile manner. On the other hand, the wallette without the DPC as well as wallettes with the DPC between the wallette and the concrete base exhibited almost no ductility.

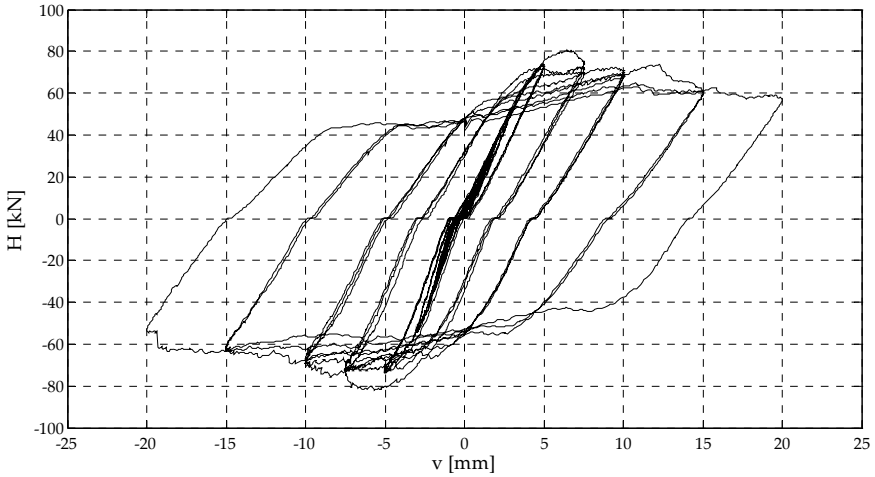

Figure 24: Hysteresis (*H*/*v* relationship) for wallette with DPC between firs two courses (A1_2)

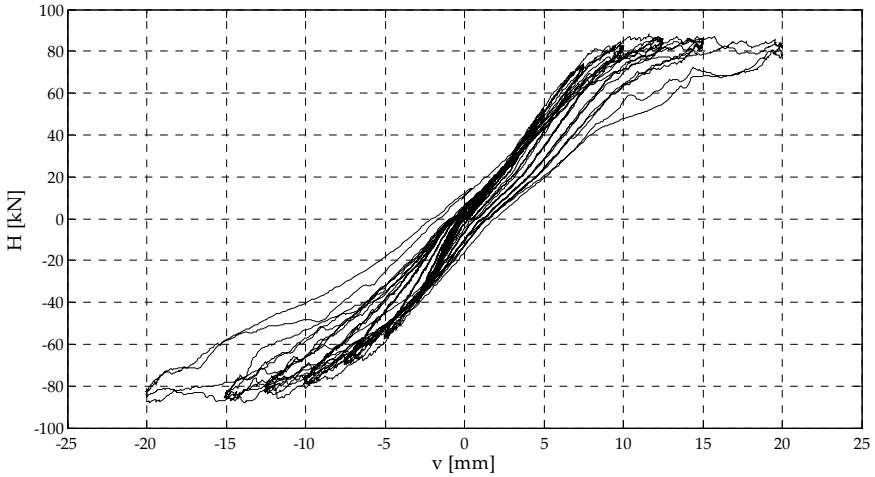

Figure 25: Hysteresis (H/v relationship) for wallette with DPC between concrete and wallette (B1_3)

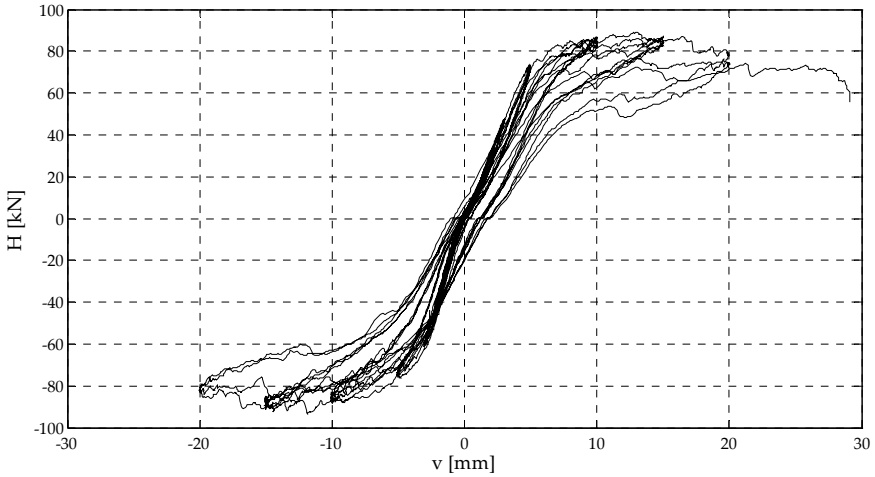

Figure 26: Hysteresis (H/v relationship) for control wallette (C1)

Figure 27 shows envelopes of hysteresis curves for all of the test series, A1, B1 and C1. The influence of DPC presence and position can be clearly seen.

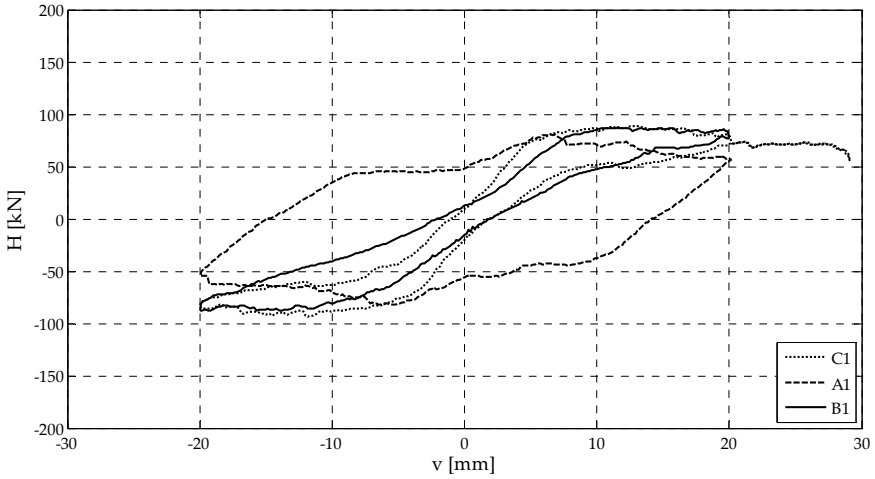

Figure 27: Hysteresis envelopes for wallettes under mid-level pre-compression

Figure 28: Failure of the specimens A1_2 and B1_2

The wallettes of Series A1 and B1 under the middle level of pre-compression failed mostly in a sliding mode, except for walls B1_2 and B1_3 which had a combined sliding and compression failure. The corresponding wallette without a DPC, C1, failed in compression. Wallettes which failed in compression developed mostly vertical cracks. The location of these cracks moved towards the wallette toes during the testing as the applied displacements increased. Wallettes which failed by sliding developed horizontal cracks in the bed joint containing the DPC. Wallettes of Series A had additional vertical cracks in the first course (between the concrete base and the bed joint with the DPC) induced by the cyclic movement of the upper part of the wallette over the DPC. Figure 28 shows the failure of the wallettes A1_2 and B1_2.

Figure 29 shows envelopes of the horizontal displacements i.e. slip, *s*, over the DPC for the wallettes A1 and B1. It can be seen that the area of the envelope for the A1 specimen that failed in sliding is considerably larger than that for the B1 wallette which failed predominantly in compression with minimal sliding.

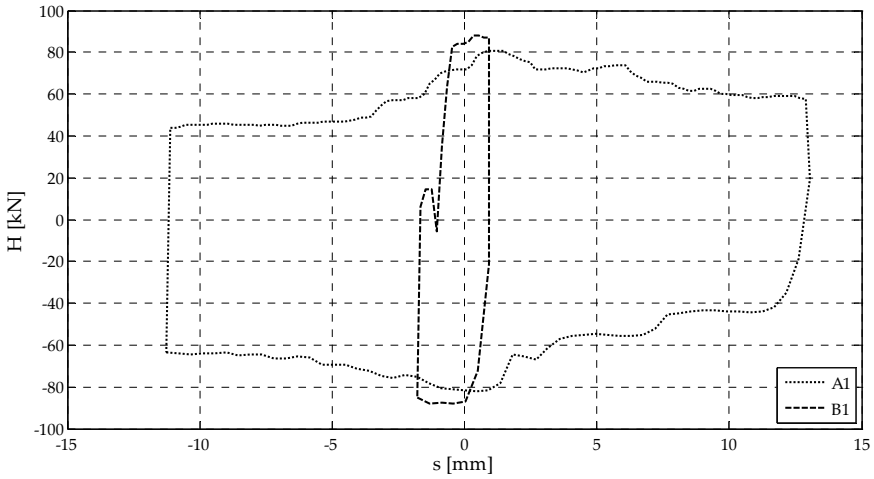

Figure 29: Slip envelopes of the wallettes A1 and B1

5.3. High pre-compression level, σ_{pc} = 2.8 MPa (Series A2, B2 and C2)

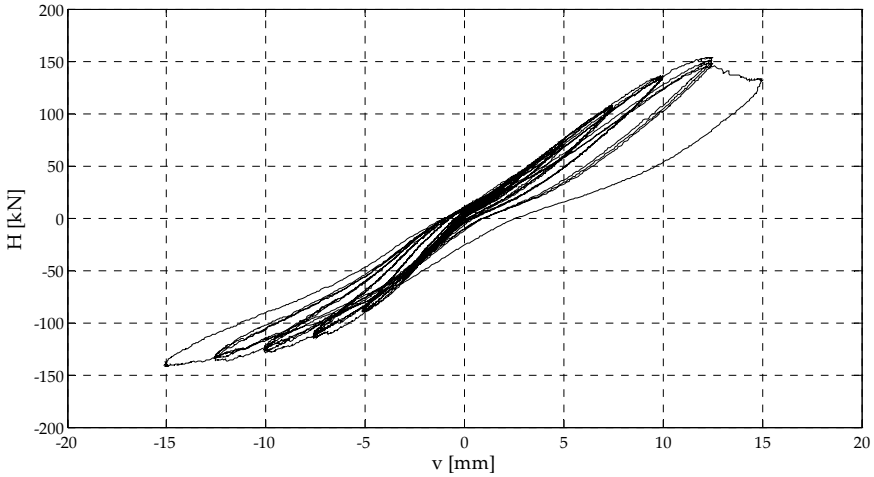

Figure 30: Hysteresis (*H*/*v* relationship) for typical wallette with DPC (A2_1)

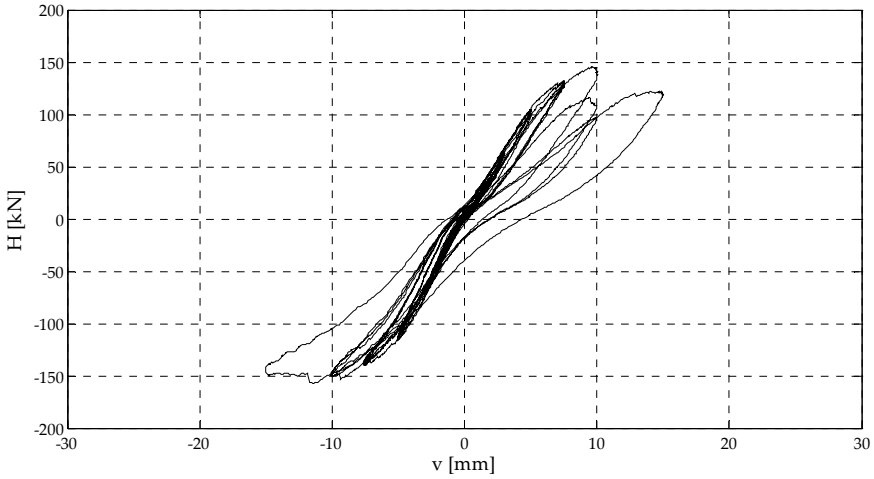

Figure 31: Hysteresis (*H*/*v* relationship) for wallette without DPC (C2)

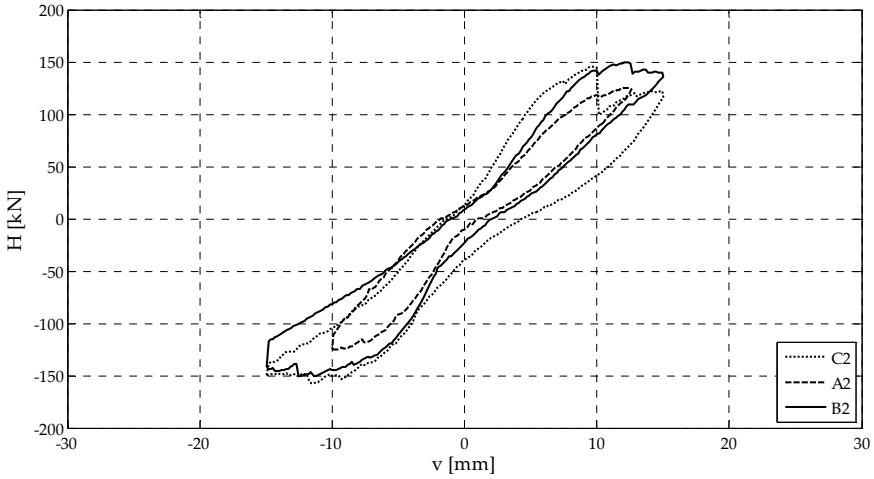

Figure 32: Hysteresis envelopes for wallettes under high pre-compression

Typical cyclic behaviour (hysteresis curves) for this level of pre-compression is shown on Figures 30 and 31 for both wallettes with the DPC (A2_1) and without the DPC (C2), respectively. As can be seen

from these Figures, because of the higher level of pre-compression, both wallettes with and without a DPC displayed similar behaviour with small energy dissipation and almost no ductility. This is also obvious from the envelopes of hysteresis curves for all test series, A2, B2 and C2 shown in Figure 32.

The wallettes with a high pre-compression level for all Series failed in compression. One of them, wallette A2_2, failed suddenly and practically exploded, see Figure 33. Because of the high level of pre-compression the presence of a DPC appeared to have little influence on the wallette behaviour.

Figure 33: Failure of the specimens A2_2 and B2_3

5.4. Additional considerations

Figures 34, 35 and 36 show the hysteresis envelopes of all the wallettes grouped in terms of the position of the DPC. The influence of pre-compression level on the cyclic behaviour of masonry for different DPC positions can be clearly seen.

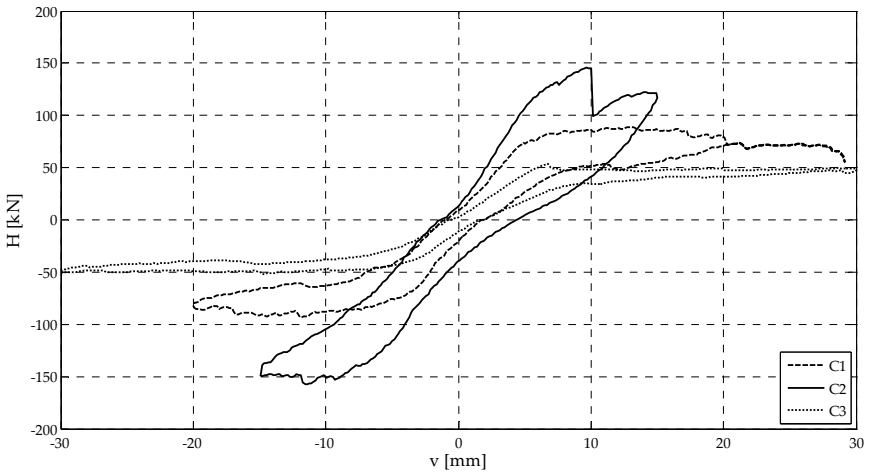

Figure 34: Hysteresis envelopes for wallettes without DPC

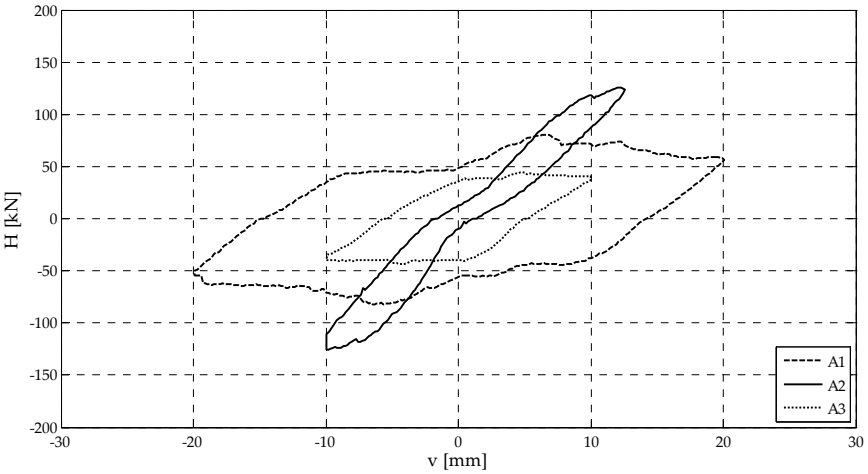

Figure 35: Hysteresis envelopes for wallettes with DPC between first two courses

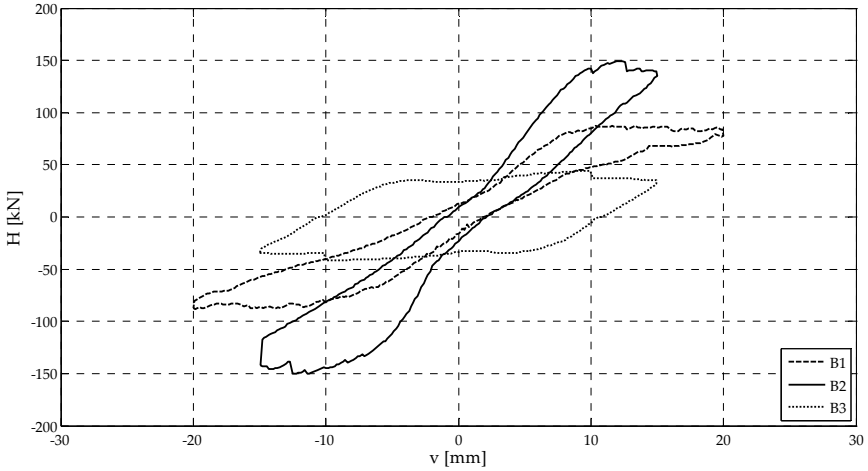

Figure 36: Hysteresis envelopes for wallettes with DPC between the concrete base and wallette

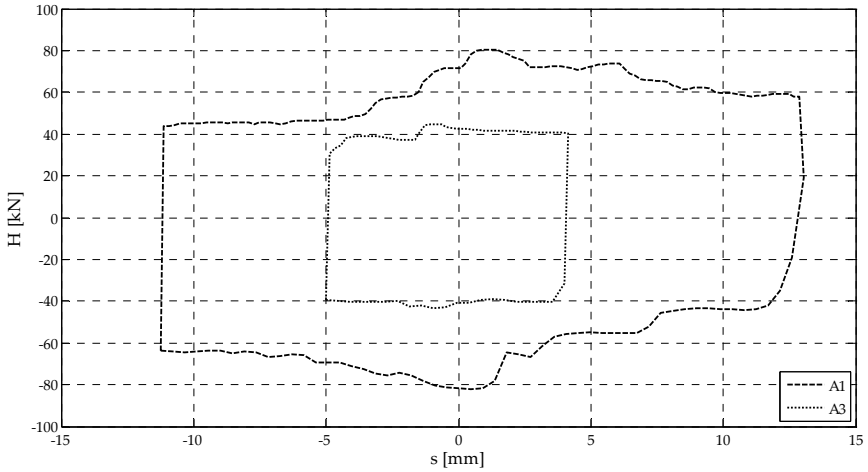

Figure 37: Slip envelopes for wallettes with DPC between first two courses

For all the wallettes it can be seen that higher levels of pre-compression reduce the area of the envelope i.e. reducing the amount of energy dissipation of the specimen. Furthermore, to achieve the

same horizontal displacement, the higher level of pre-compression required higher levels of applied horizontal load. Similar conclusions can de drawn from the slip envelopes which are shown in Figures 37 and 38.

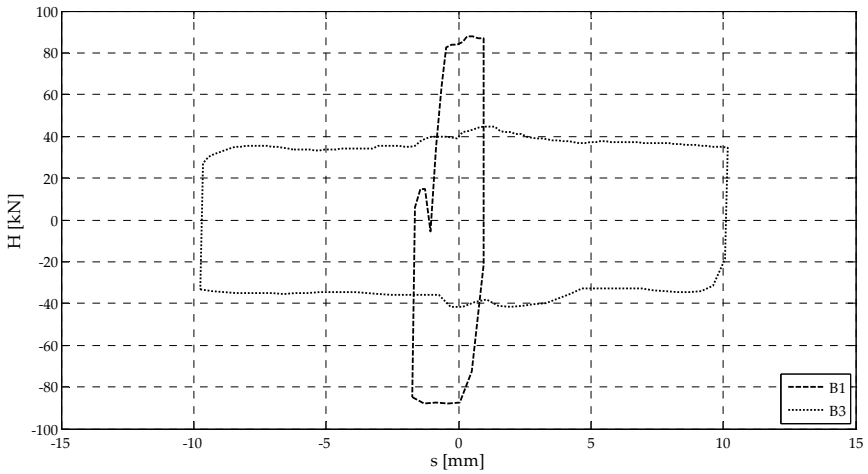

Figure 38: Slip envelopes for wallettes with DPC between the concrete base and wallette

The influence of the pre-compression level on uplift of the wallette toes is shown in Figure 39 which shows the uplift envelopes of wallettes without DPC for the east corner of the wallette. From this Figure it can be seen that the higher pre-compression levels reduce the toe uplift at cyclic loading.

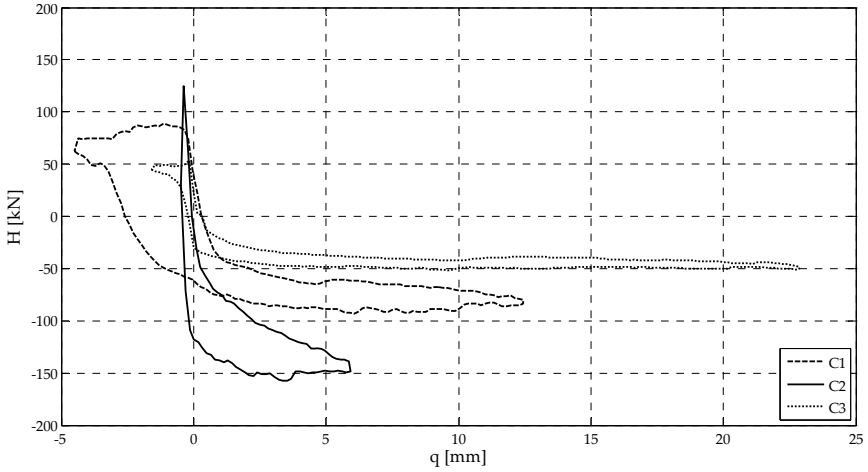

Figure 39: Toe uplift envelopes for wallettes without DPC

5.5. Friction coefficient in bed joint with DPC

Taking into consideration tests on wallette specimens which failed through sliding, cf. Table 3, a friction coefficient in the bed joint with DPC can be estimated from the levels of compression and shear in the joint once sliding has occurred. This resulting shear stress-normal stress graph is shown in Figure 40. The mean value of the coefficient of friction was found to be 0.425. In addition, cohesion of 0.038 MPa could be estimated. This small value can be neglected, especially for practical applications.

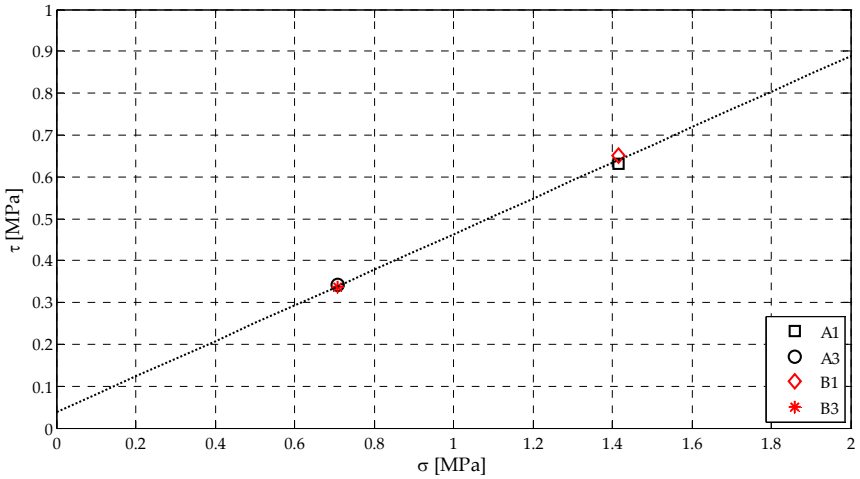

Figure 40: Relationship between normal and shear stresses

5.6. Structural behaviour of wallettes

The behaviour of the wallettes was highly influenced by the pre-compression level. Furthermore, the presence and position of the DPC had a considerable influence on the behaviour of the wallettes, especially on their failure mode. Two types of failure were observed, namely sliding and compression failure. In general, all the wallettes initially showed some uplift at the corners. In the case of the sliding failure this uplift diminished. When compression failure was the governing mode, the uplift had the effect of reducing the compression area of the wallette available to carry the compressive load. Wallettes which failed in compression developed mostly vertical cracks which moved towards the wallette toes during the testing with increasing imposed displacements. Furthermore, wallettes that failed in compression exhibited almost no ductility. Wallettes which failed through sliding developed horizontal cracks in the bed joint containing the DPC. These wallettes also displayed a considerable energy dissipation capacity and behaved in a quasi ductile manner. Greater ductility was observed in the wallettes with the DPC in the bed joint (Series A) rather than at the wallette-slab interface (Series B), indicating that the former detail would be more desirable for enhanced seismic performance.

Summary

A joint research project by the University of Newcastle and the ETH Zurich on the structural behaviour of unreinforced masonry elements subjected to cyclic shear is underway at the University of Newcastle, Australia. The main goal of the research project is to investigate the influence of a damp-proof course (DPC) on the structural behaviour of masonry walls subjected to shear when the DPC is placed in a bed joint or at the interface of the masonry and its supporting concrete slab. This research project extends a previous small specimen investigation of the study of the shear behaviour of masonry walls subjected to static-cyclic shear loading with a DPC incorporated either in a mortar joint or at the masonry-concrete slab interface.

Within the framework of the project a series of static-cyclic shear tests on brick masonry wallettes were performed at the University of Newcastle. The present report shows and discusses the results obtained from these tests.

Cyclic load tests were performed on two series of masonry elements with a DPC placed into one of the bed joints. Each series consisted of nine 110 mm thick clay brick masonry wallettes with nominal dimensions of 1200x1200 mm. The DPC was placed either between the first two courses (Series A) or between the concrete base and first masonry course (Series B). In addition, three control specimens with the same dimensions and without a DPC were tested (Series C). The specimens were at first subjected to a vertical pre-compression load, which was kept constant during the test and then subjected to a cyclic shear load applied in time steps with prescribed horizontal displacements. Three different levels of pre-compression were considered. For each level of pre-compression, three replicates were tested for Series A and B, resulting in a total of 21 tests being performed.

The behaviour of the wallettes was highly influenced by the pre-compression level. Furthermore, the presence and position of the DPC had a considerable influence on the behaviour of the wallettes, especially on the failure mode. Two types of failure were observed, namely sliding and compression failure. In general, all the wallettes initially showed some uplift of the corners. In the case of the sliding failure this uplift diminished. When compression failure was the governing mode, the uplift had the effect of reducing the compression area of the wallette available to carry the compressive load. Wallettes which failed in compression developed mostly vertical cracks which moved towards the wallette toes during the testing with increasing applied displacements. Furthermore, wallettes that failed in compression exhibited almost no ductility. Wallettes which failed through sliding developed horizontal cracks in the bed joint containing the DPC. These wallettes also displayed a considerable energy dissipation capacity and behaved in a quasi ductile manner. Greater ductility was observed in the wallettes with the DPC in the bed joint (Series A) rather than at the wallette-slab interface (Series B), indicating that the former detail would be more desirable for enhanced seismic performance.

Zusammenfassung

Im Rahmen eines gemeinsamen Forschungsprojekts zwischen der University of Newcastle, Australien und der ETH Zürich wird das Tragverhalten von unbewehrten Mauerwerkswänden unter statisch-zyklischer Schubbeanspruchung untersucht. Das Hauptziel des Forschungsprojekts ist es, den Einfluss einer Feuchtigkeitssperre in der untersten Lagerfuge der Wand oder zwischen der Wand und untenliegenden Betondecke auf der auf zyklischen Schub beanspruchten Wand zu untersuchen. Das Projekt baut auf den vorher durchgeführten Schubversuchen an kleinen Mauerwerkselementen auf.

Im Rahmen des Projekts wurden Versuche an kleinen Mauerwerkswänden an der University of Newcastle durchgeführt. Die vorliegende Publikation berichtet über die Versuchsergebnisse und diskutiert diese eingehend.

Es wurden Versuche an zwei Serien durchgeführt, in welchen jeweils neun unbewehrten 110 mm dicken Backsteinmauerwerkswänden geprüft wurden. Die Versuchskörperabmessungen betrugen 1200x1200 mm. Die Feuchtigkeitssperre wurde entweder in der untersten Lagerfuge (Serie A) oder am Übergang zwischen der Wand und dem Betonsockel (Serie B) eingebaut. Zusätzlich wurden drei Kontrollkörper ohne Feuchtigkeitssperre (Serie C) geprüft. Die Wände wurden zunächst einer Vertikallast unterworfen, welche im Laufe des Versuchs konstant gehalten wurde. Anschliessend wurde die statisch-zyklische Schubbelastung in den Zeitschritten durch vordefinierte horizontale Verschiebungen aufgebracht. Es wurden drei verschiedene Vertikallastniveaus berücksichtigt und es wurden jeweils drei Replikate in den Serien A und B getestet. Somit wurden insgesamt 21 Wandelemente geprüft.

Das Tragverhalten der Wände wurde sowohl durch das Vertikallastniveau als auch durch die Präsenz und der Lage der Feuchtigkeitssperre massgeblich bestimmt. Es wurden zwei verschiedene Brucharten festgestellt, nämlich das Gleiten entlang der Lagerfuge mit der Feuchtigkeitssperre und der Druckbruch. Bei allen Wänden wurde anfänglich das Abheben der Ecken festgestellt, welche im Falle eines Bruchs durch das Gleiten im Laufe des Versuchs verschwand. Im Falle eines Druckbruchs reduzierte das Abheben der Ecken die für den Transfer der Druckresultierende zur Verfügung stehende Wandfläche. Dabei beobachtete man vertikal verlaufende Risse, welche sich mit steigender horizontaler Verschiebung gegen die Ecken der Wand verschoben. Des Weiteren verhielten sich diese Wände wenig duktil. Die Wände, welche durch das Gleiten versagten, entwickelten einen horizontalen Riss in der Lagerfuge mit der Feuchtigkeitssperre und zeigten eine beachtliche Energiedissipation bzw. ein quasi duktiles Verhalten. Die Wände der Serie A, mit der Feuchtigkeitssperre in der untersten Lagerfuge, zeigten eine größere Duktilität verglichen mit denjenigen der Serie B. Somit ist im Bezug auf das seismische Verhalten der Wände ein Einbau der Feuchtigkeitssperre wie bei der Serie A zu bevorzugen.

Acknowledgements

This was a joint project involving the University of Newcastle and ETH Zurich, and the support of both organisations is acknowledged. Funding and support for the program was also provided by Think Brick Australia and its member companies and the Centre for Infrastructure Performance and Reliability in the School of Engineering at the University of Newcastle. The assistance of the Civil Engineering laboratory staff is gratefully acknowledged, particularly that of Mr Ian Jeans in preparing the specimens.

References

1. Page, A.W. and Griffith, M.C., "A Preliminary Study of the Seismic Behaviour of Slip Joints Containing Membranes in Masonry Structures", The University of Newcastle and University of Adelaide, Research Report 160.02.1998, December 1997.

2. Simundic, G., Page, A.W. and Chen, Q., "The Cyclic and Long Term Behaviour of Slip Joints in Load-Bearing Masonry Construction", Proceedings, 12th International Brick/Block Masonry Conference, Madrid, Spain, June 2000, Vol. 2, pp. 1409-1420.

3. Totoev Y.Z., Page A.W. and Simundic G., "Shear Transfer Capacities of Horizontal Slip Joints in Masonry at Different Levels of Vertical Load", Proceedings, 9th North American Masonry Conference, Clemson, South Carolina, June 2003, pp. 791-800.

4. Totoev Y.Z. and Simundic G., "New Test for the Shear Transfer Capacity of Horizontal Slip Joints in Load-Bearing Masonry", Proceedings, 10th Canadian Masonry Symposium, Banff, Alberta, June 8 – 12, 2005, pp. 863-872.

5. Australian/New Zealand Standard AS/NZS 4456.4:2003 "Masonry units, segmental pavers and flags - Methods of test - Determining compressive strength of masonry units", Standards Australia, Sydney.

6. Australian Standard AS3700:2001 "Masonry Structures", Standards Australia, Sydney.

7. Ali S., "Concentrated Loads on Solid Masonry", PhD Theses, The University of Newcastle, February 1987.

8. European standard EN 1052-3:2002, "Methods of Test for Masonry – Part 3: Determination of Initial Shear Strength", The European Committee for Standardization, Brussels.

9. European standard EN 1052-1:1998, "Methods of Test for Masonry – Part 1: Determination of Compressive Strength", The European Committee for Standardization, Brussels.

Appendix A: Tables

Table A1: Compressive strength of unit (AS4456.4:2003); tested on 11.03.2009

Specimen	F [kN]	f [MPa]	b [mm]	h [mm]	t [mm]	h/t	k_a	f_b [MPa]
B1	790.2	31.10	231	79	110	0.71	0.61	22.33
B2	786.0	31.22	231	78	109	0.72	0.61	22.34
B3	950.0	37.89	230	80	109	0.73	0.61	27.81
B4	1080.0	42.69	230	78	110	0.71	0.60	30.27
B5	1026.8	40.96	230	79	109	0.72	0.61	29.68
B6	994.2	39.66	230	78	109	0.72	0.61	28.38
B7	1122.0	45.20	232	78	107	0.73	0.61	32.95
B8	853.4	33.75	232	78	109	0.72	0.61	24.15
B9	1229.0	48.81	231	79	109	0.72	0.61	35.38
B10	1150.4	45.69	231	78	109	0.72	0.61	32.69
mean value		39.70						28.60
standard deviation		6.20						4.50
characteristic value		26.60						19.10

Table A2: Compressive strength of mortar

Specimen	Date built	Date tested	F [kN]	f [MPa]
M1	24.02.2009	02.03.2009	28.0	5.71
M2	24.02.2009	02.03.2009	28.0	5.71
M3	24.02.2009	02.03.2009	27.4	5.59
M4	24.02.2009	02.03.2009	29.4	6.00
M5	24.02.2009	02.03.2009	26.8	5.47
M6	24.02.2009	02.03.2009	26.6	5.43
mean value				5.65
standard deviation				0.21

Table A3: Flexural bond strength (AS3700:2001)

Specimen	Date built	Date tested	F [N]				
BW1	20.02.2009	03.03.2009	437	393	492	547	426
BW2	20.02.2009	03.03.2009	462	483	378	290	293

Table A4: Tensile bond strength (with C=0.648); tested on 25.05.2009

Specimen	F [kN]	h [mm]	l [mm]	t [mm]	D [mm]	σ_T [MPa]
TB1	33.90	248	231	108	270.10	0.75
TB2	28.09	250	231	105	271.19	0.62
TB3	21.08	250	231	106	271.19	0.46
TB4	34.43	249	231	106	270.65	0.76
TB5	22.58	248	231	108	270.10	0.50
mean value						0.62
standard deviation						0.14

Table A5: Shear bond strength (EN 1052-3); tested on 25.05.2009

Specimen	F [kN]	l [mm]	t [mm]	Mode of failure*	τ_T [MPa]
SB1	28.920	231	109	A1-2	1.15
SB2	38.277	231	109	A1-2	1.52
SB3	29.617	231	109	A1-1	1.18
SB4	32.830	231	109	A1-2	1.30
SB5	30.691	231	109	A1-2	1.22
mean value					1.27
standard deviation					0.15

*A1-1: Shear failure in the unit/mortar bond area on one unit face
A1-2: Shear failure in the unit/mortar bond area divided between two unit faces

Table A6: Masonry compressive strength (AS3700:2001)

Specimen	Date built	Date tested	F [kN]	f [MPa]	h [mm]	t [mm]	h/t	k_a	f_m [MPa]
FX1	20.02.2009	02.03.2009	486.2	19.40	247	108	2.29	0.80	15.46
FX2	20.02.2009	02.03.2009	435.4	18.03	247	105	2.35	0.80	14.45
FX3	20.02.2009	02.03.2009	373.4	15.32	245	106	2.31	0.80	12.23
FX4	20.02.2009	02.03.2009	484.8	19.89	248	106	2.34	0.80	15.92
FX5	20.02.2009	02.03.2009	400.4	16.12	246	108	2.28	0.79	12.83
mean value				17.75					14.18
standard deviation				2.00					1.61
characteristic value				11.90					9.50

Table A7: Masonry compressive strength (EN 1052-1); tested on 29.05.2009

Specimen	F [kN]	h [mm]	l [mm]	t [mm]	f_m [MPa]	E_m [GPa]
CFX1	539.6	430	480	110	10.22	7.59
CFX2	385.5	425	475	110	7.38	-
CFX3	330.0	430	480	110	6.25	3.20
CFX4	304.3	440	480	110	5.76	6.04
mean value					7.40	6.81*
standard deviation					2.00	

*mean value from tests on CFX1 and CFX4

Table A8: Wallette specimens' dimensions

Specimen	Date built	Date tested	h_w [mm]	l_w [mm]	t_w [mm]	A [m²]
C1	13.02.2009	24.03.2009	1200	1207	110	0.1328
C2	13.02.2009	01.04.2009	1198	1204	110	0.1324
C3	17.02.2009	16.04.2009	1195	1206	110	0.1327
A1_1	20.02.2009	26.03.2009	1201	1201	109	0.1309
A1_2	24.02.2009	30.03.2009	1200	1200	110	0.1320
A1_3	25.02.2009	31.03.2009	1204	1205	110	0.1326
A2_1	26.02.2009	02.04.2009	1200	1200	110	0.1320
A2_2	03.03.2009	03.04.2009	1198	1196	109	0.1304
A2_3	10.03.2009	09.04.2009	1210	1205	109	0.1313
A3_1	11.03.2009	17.04.2009	1204	1200	108	0.1296
A3_2	11.03.2009	18.04.2009	1203	1197	109	0.1305
A3_3	17.03.2009	20.04.2009	1215	1185	109	0.1292
B1_1	18.02.2009	04.04.2009	1205	1202	110	0.1322
B1_2	19.02.2009	06.04.2009	1205	1205	109	0.1313
B1_3	26.02.2009	07.04.2009	1200	1195	110	0.1314
B2_1	17.03.2009	15.04.2009	1205	1200	108	0.1296
B2_2	18.03.2009	15.04.2009	1200	1208	109	0.1317
B2_3	26.03.2009	21.04.2009	1205	1200	107	0.1284
B3_1	24.03.2009	20.04.2009	1200	1210	107	0.1295
B3_2	30.03.2009	27.04.2009	1205	1205	107	0.1289
B3_3	31.03.2009	28.04.2009	1210	1200	107	0.1284

6. Appendix B: Test results

This Appendix contains six different diagrams per each test performed. The data is shown as measured, i.e. without any intervention on data files. The potentiometer measurements were started after the desired level of pre-compression was applied. A short description for each of six diagrams is given hereinafter:

- First diagram shows the applied horizontal displacement, v, depending on the time, t, given in seconds; the sinusoidal wave form of applied deformation, in general repeated three times for each displacement step, is depicted on this diagram.
- On the second diagram the load hysteresis, i.e. dependence of the horizontal force, H, on the applied horizontal displacement, v, is shown.
- Third diagram shows the measured slip, s, on the damp-proof course membrane against the horizontal force, H. For Series A the slip is recorded by means of the potentiometer POT9 (slip between the first two courses of the wallette) and for Series B and C by means of the POT10 (slip between the masonry wallette and concrete base).
- The toe uplift of the wallette specimen, q, against the horizontal force, H, is depicted on the fourth diagram. This diagram represents two measurements, i.e. contains two curves. The dashed line represents the measurement of POT8 (east side of the wallette) and the full line shows the measurements of POT7 (west side of the wallette), cf. also Figure 17.
- Vertical deformation of the wallette, f, which was captured by means of the potentiometers POT5 (west side of the wallette) and POT 6 (east side of the wallette) is shown against the horizontal force, H on the fifth diagram. The POT5 measurements are represented by the dashed line and those of POT6 by the full line.
- The last diagram displays the diagonal deformation of the wallette, d, which was captured by means of the potentiometers POT3 and POT 4, against the horizontal force, H, whereas the dashed line shows the measurements recorded by POT3 and the full line those recorded by POT4.

The axis marking is chosen in such a way that all diagrams showing the same relationship for the walls with same pre-compression load within one Series has the same marks, e.g. diagrams for the hysteresis for the tests A1_1, A1_2 and A1_3 has the same axis marking.

Test A1_1

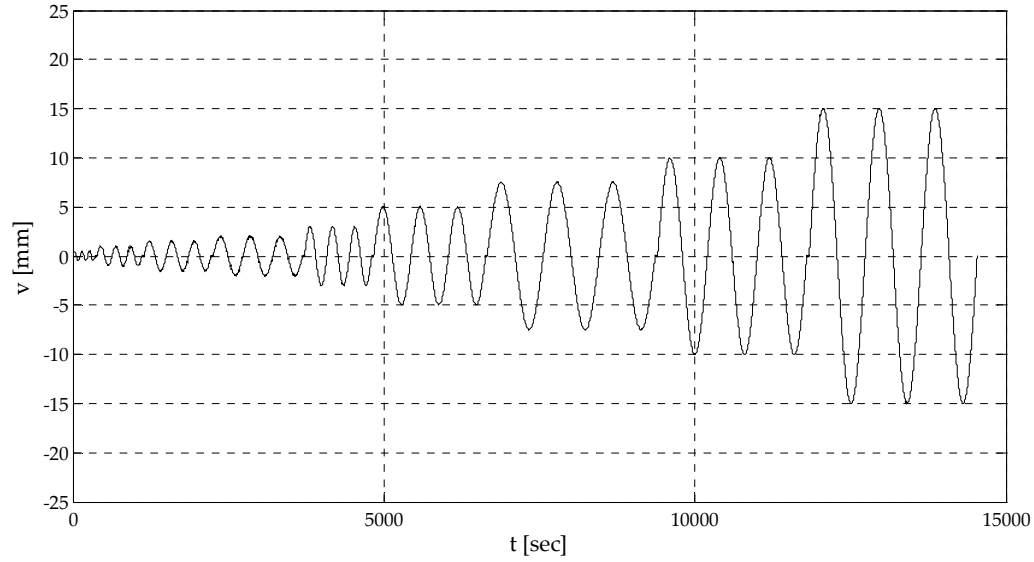
v [mm]
t [sec]
25
20
15
10
5
0
-5
-10
-15
-20
-25
0
5000
10000
15000

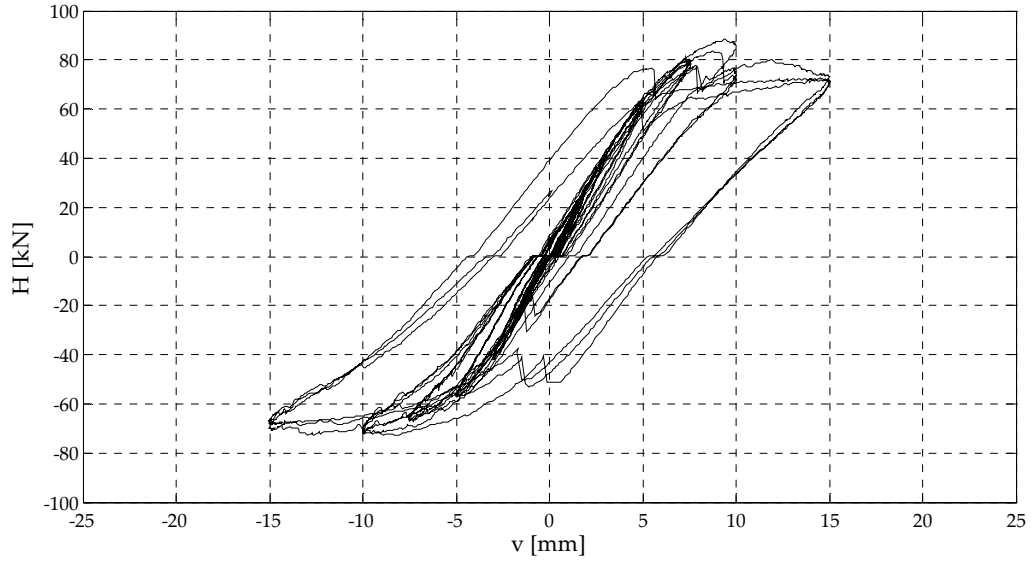
H [kN]
v [mm]
100
80
60
40
20
0
-20
-40
-60
-80
-100
-25
-20
-15
-10
-5
0
5
10
15
20
25

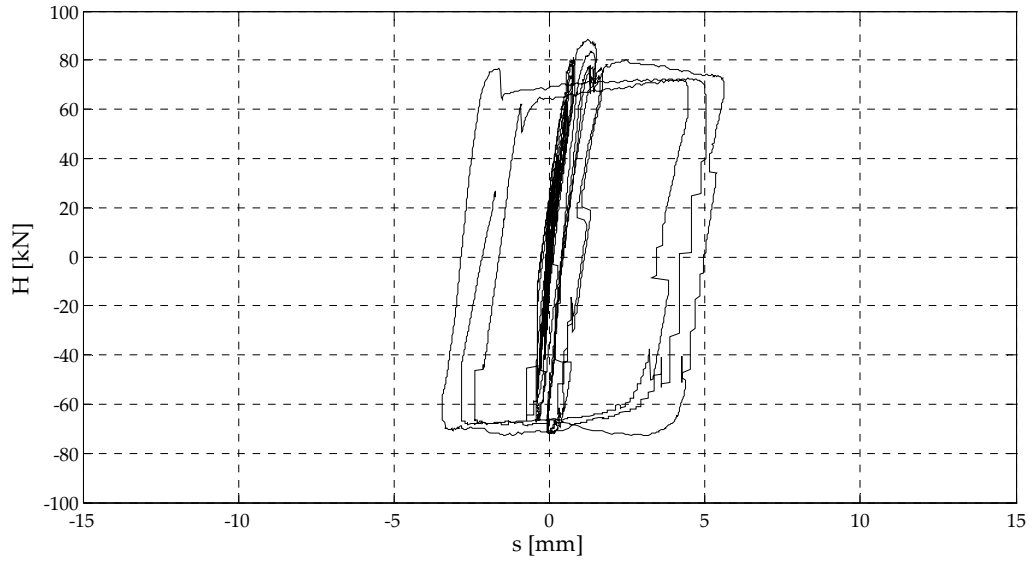
H [kN]
s [mm]
100
80
60
40
20
0
-20
-40
-60
-80
-100
-15
-10
-5
0
5
10
15

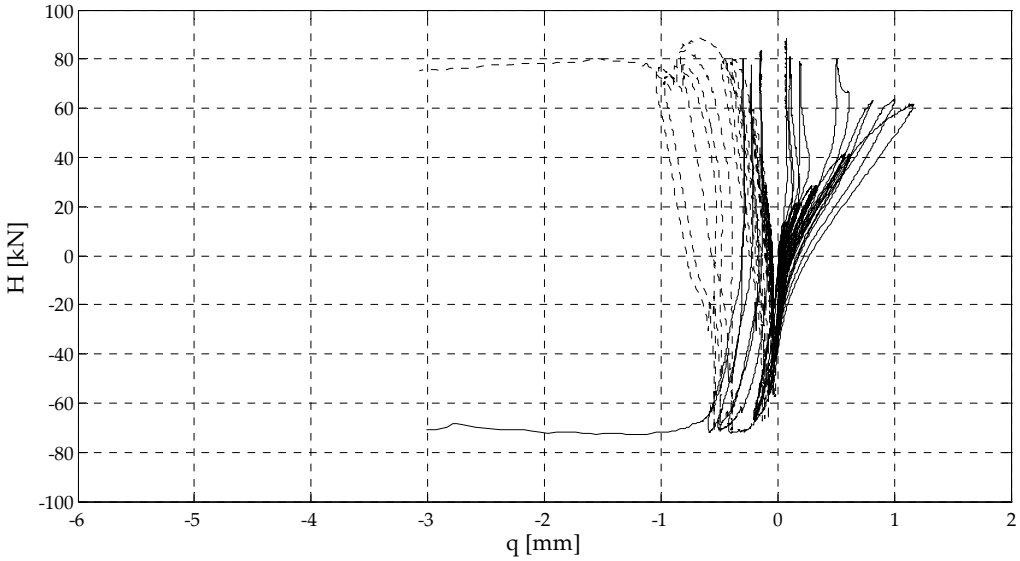
H [kN]
q [mm]

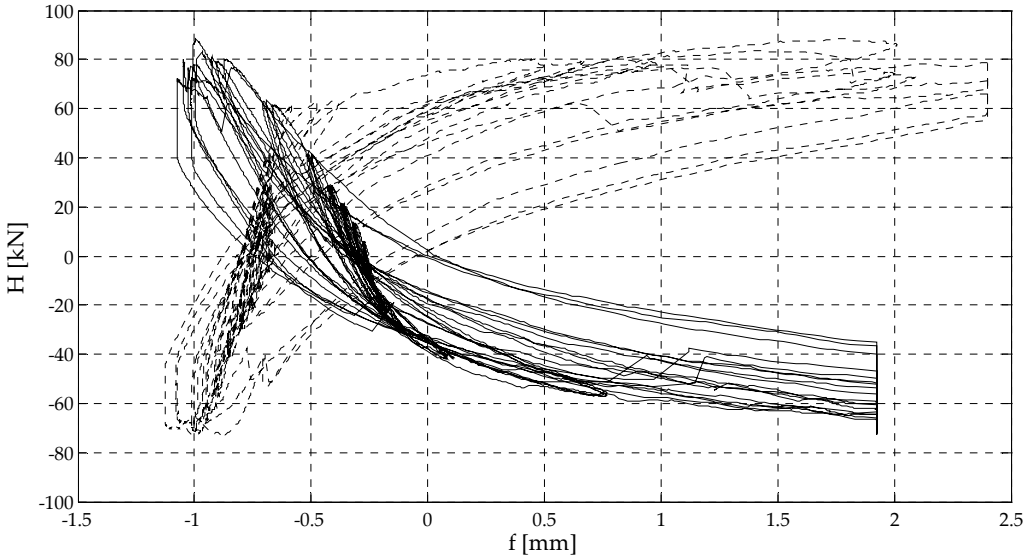
H [kN]
f [mm]

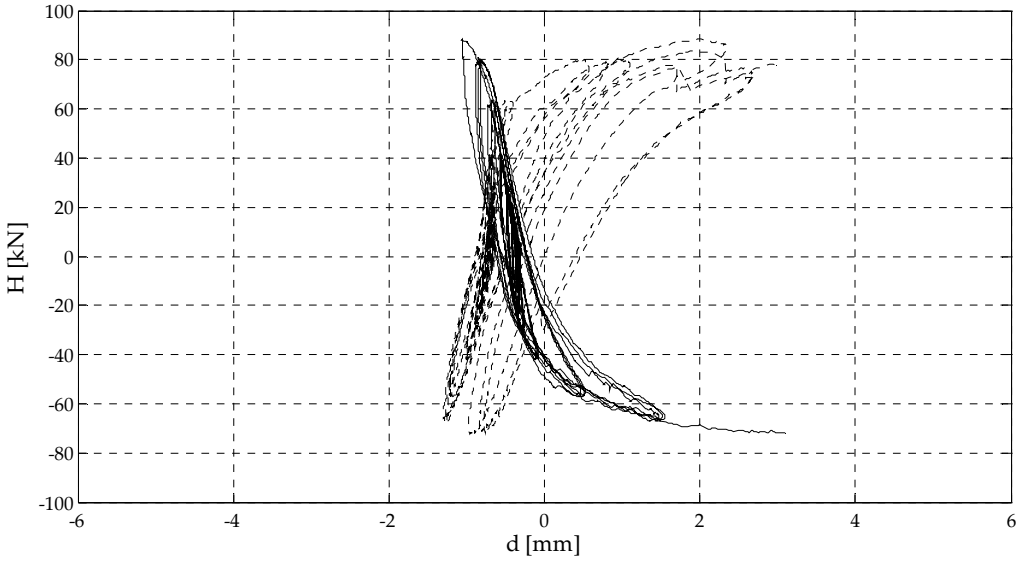
H [kN]
d [mm]

Test A1_2

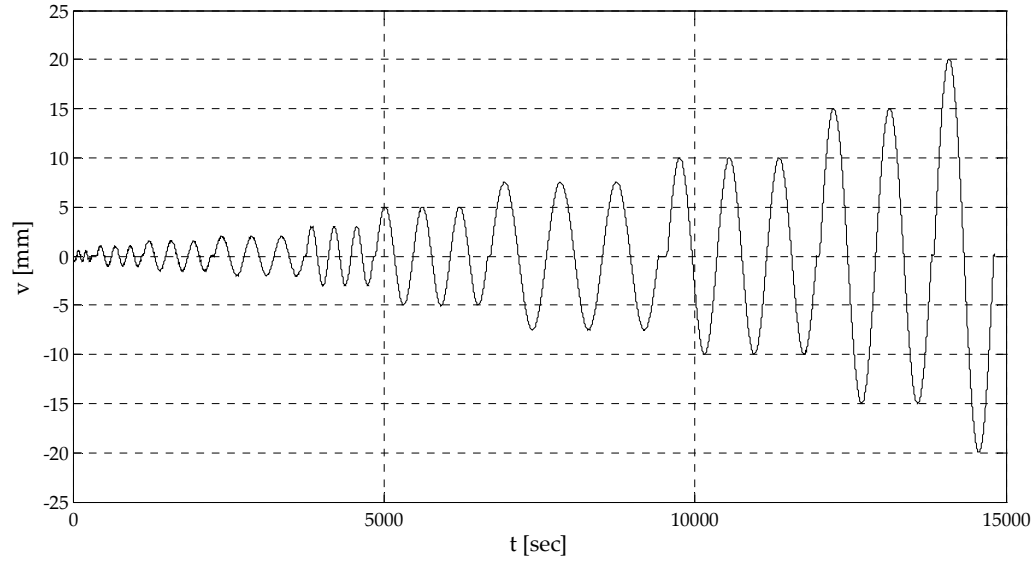
v [mm]
t [sec]
25
20
15
10
5
0
-5
-10
-15
-20
-25
0
5000
10000
15000

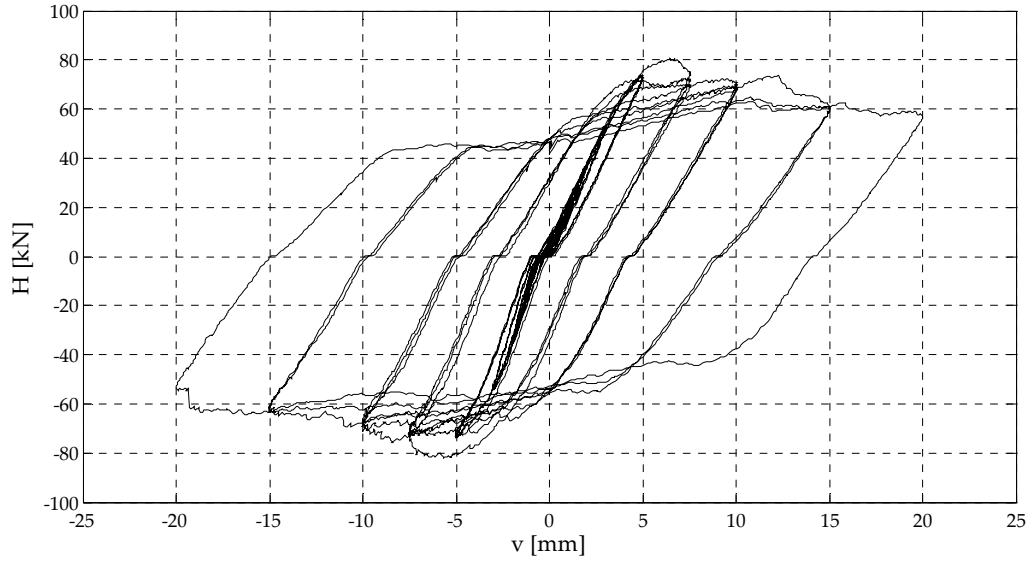
H [kN]
v [mm]
100
80
60
40
20
0
-20
-40
-60
-80
-100
-25
-20
-15
-10
-5
0
5
10
15
20
25

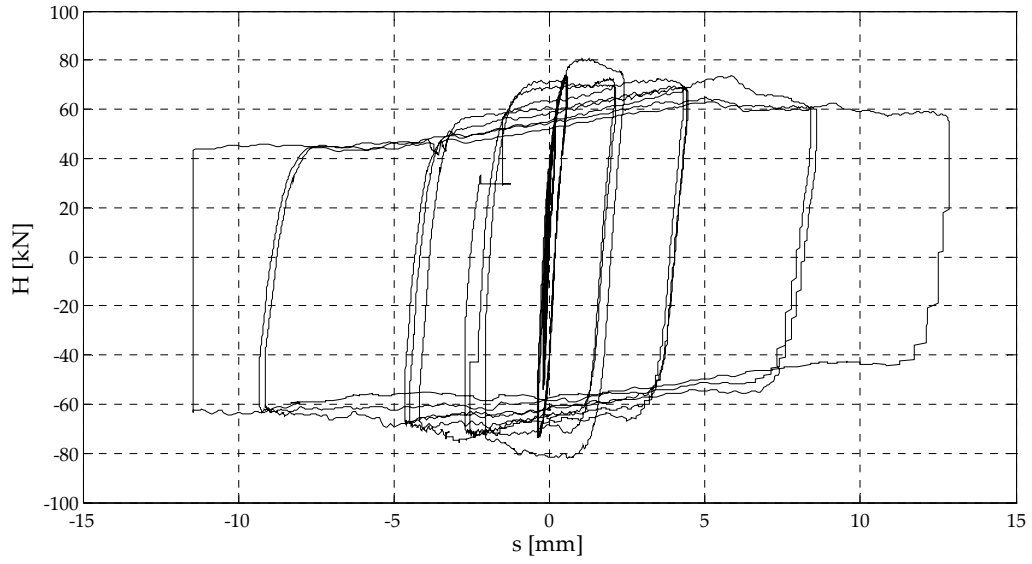
H [kN]
s [mm]
100
80
60
40
20
0
-20
-40
-60
-80
-100
-15
-10
-5
0
5
10
15

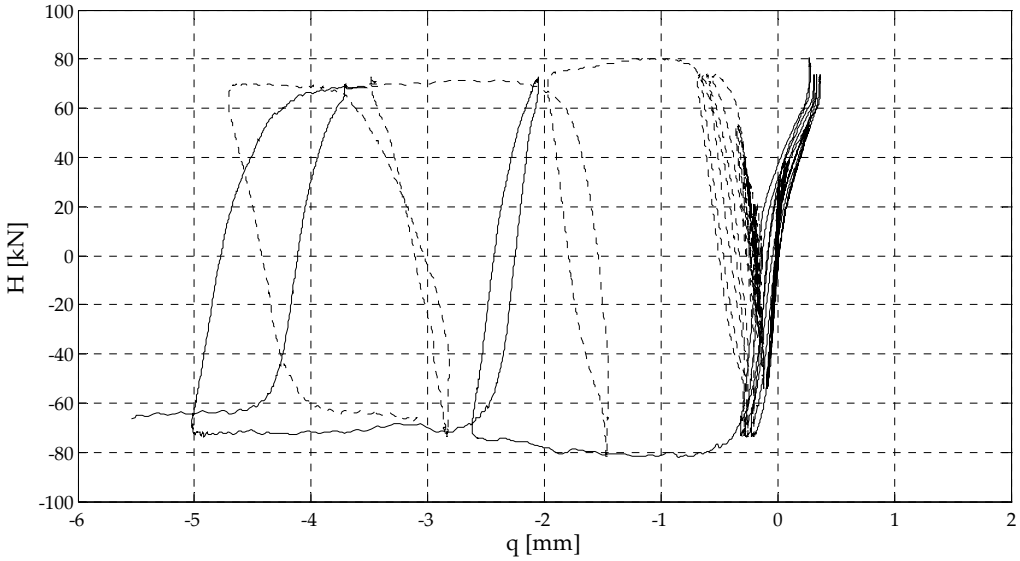
H [kN]
q [mm]

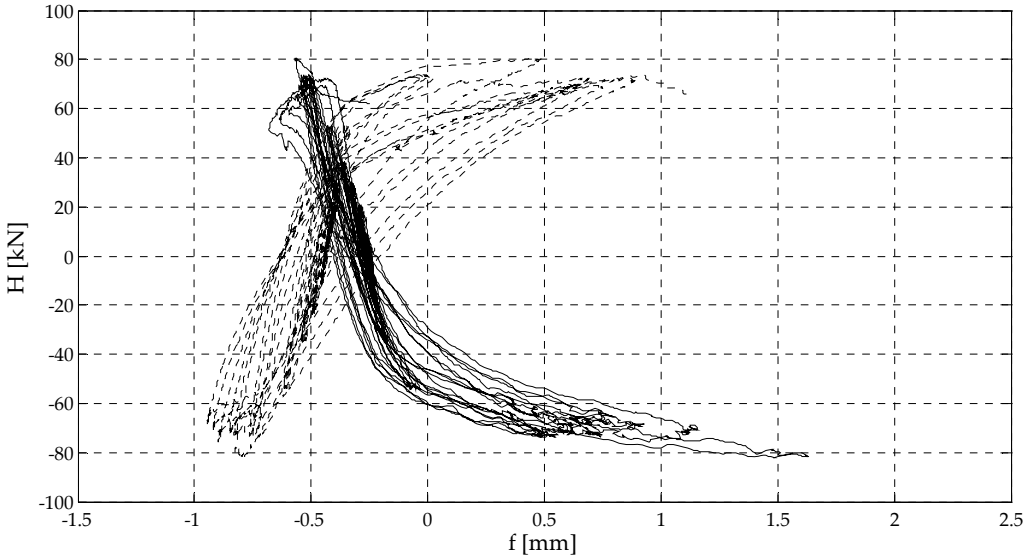
H [kN]
f [mm]

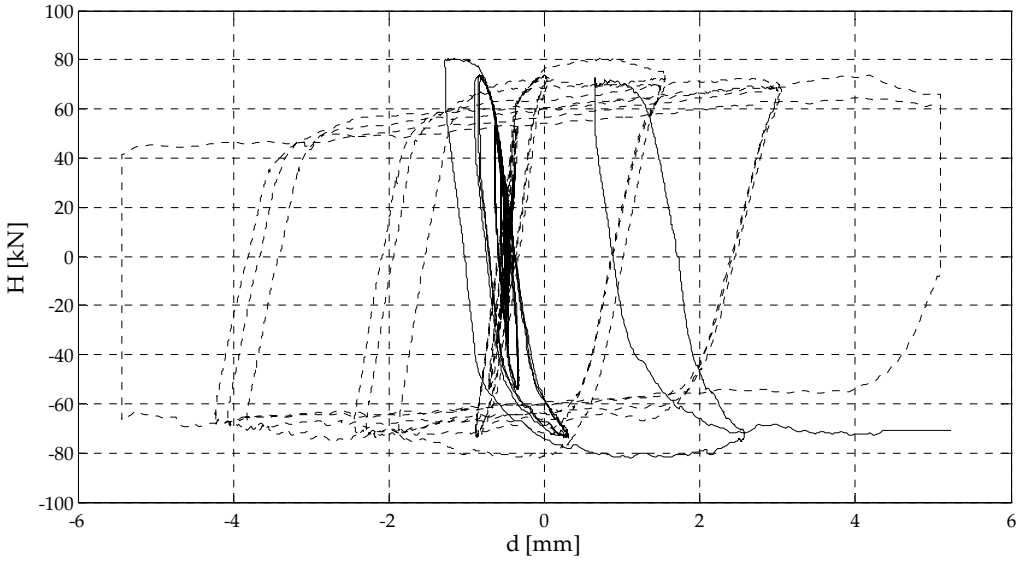
H [kN]
d [mm]

Test A1_3

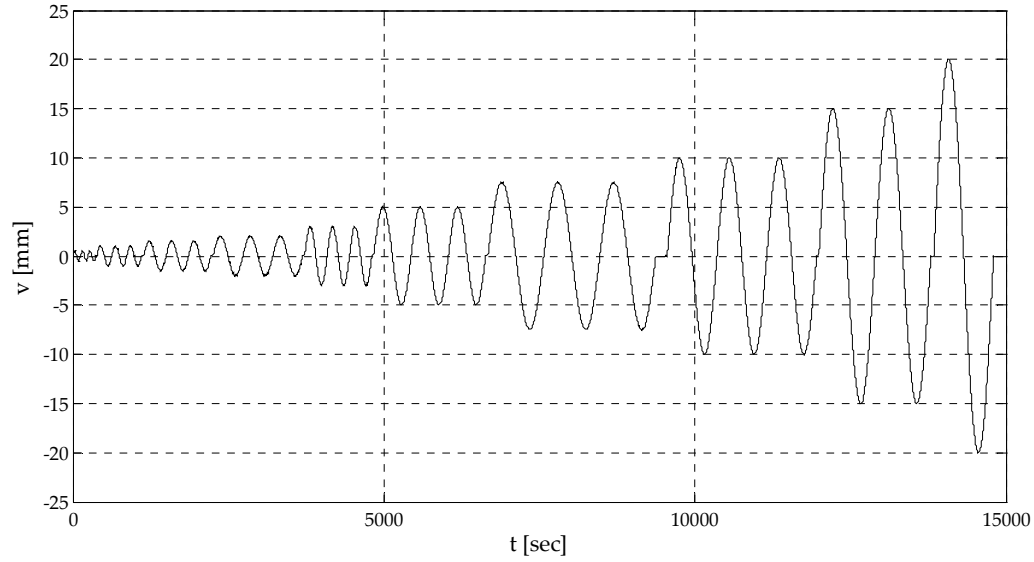
v [mm]
t [sec]
25
20
15
10
5
0
-5
-10
-15
-20
-25
0
5000
10000
15000

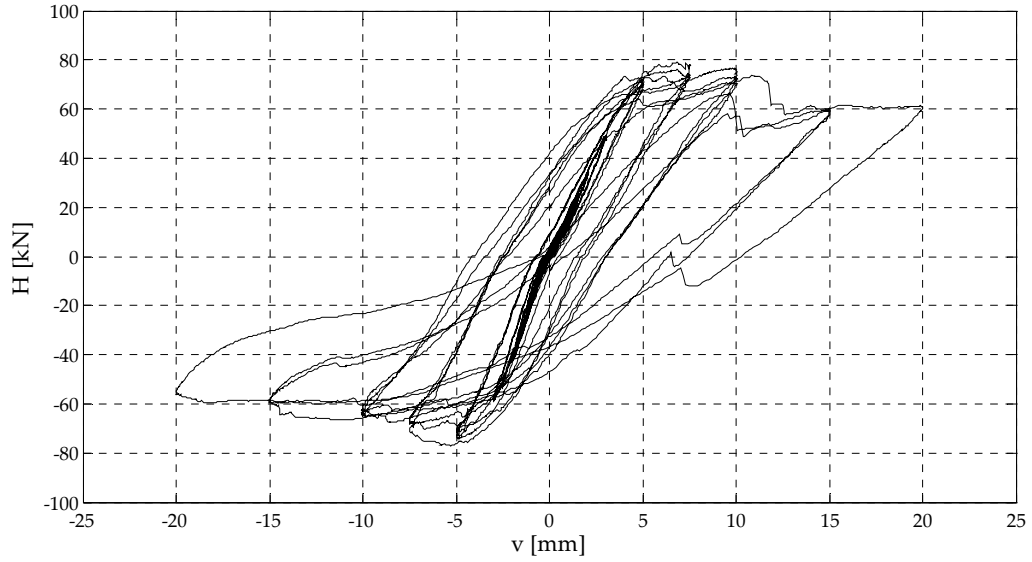
H [kN]
v [mm]
100
80
60
40
20
0
-20
-40
-60
-80
-100
-25
-20
-15
-10
-5
0
5
10
15
20
25

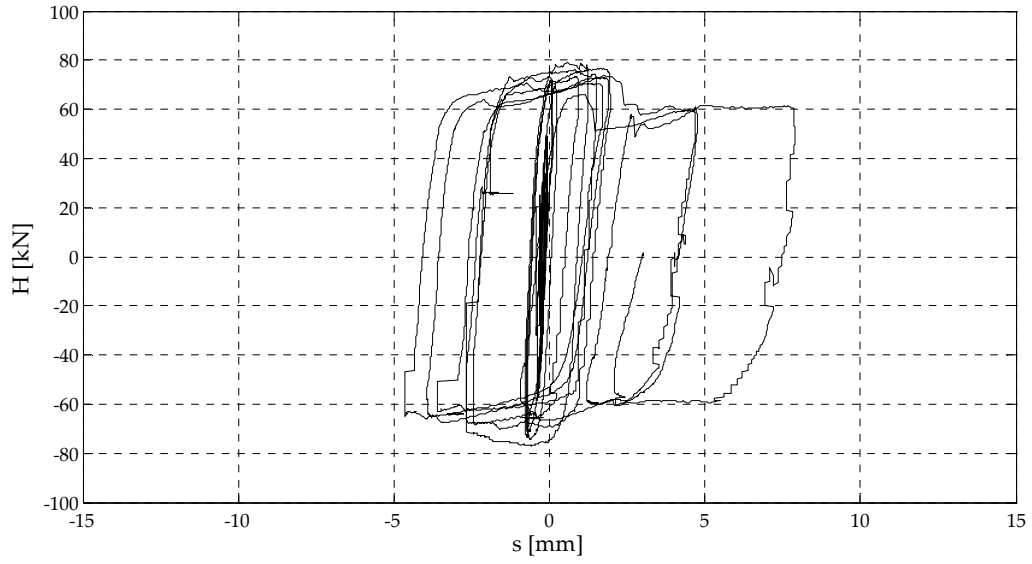
H [kN]
s [mm]
100
80
60
40
20
0
-20
-40
-60
-80
-100
-15
-10
-5
0
5
10
15

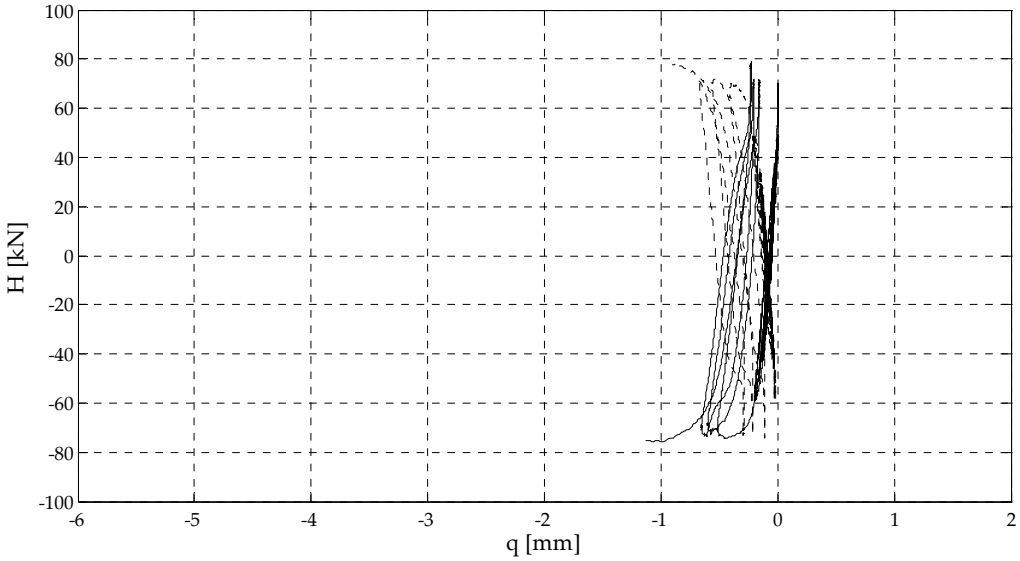
H [kN]
q [mm]

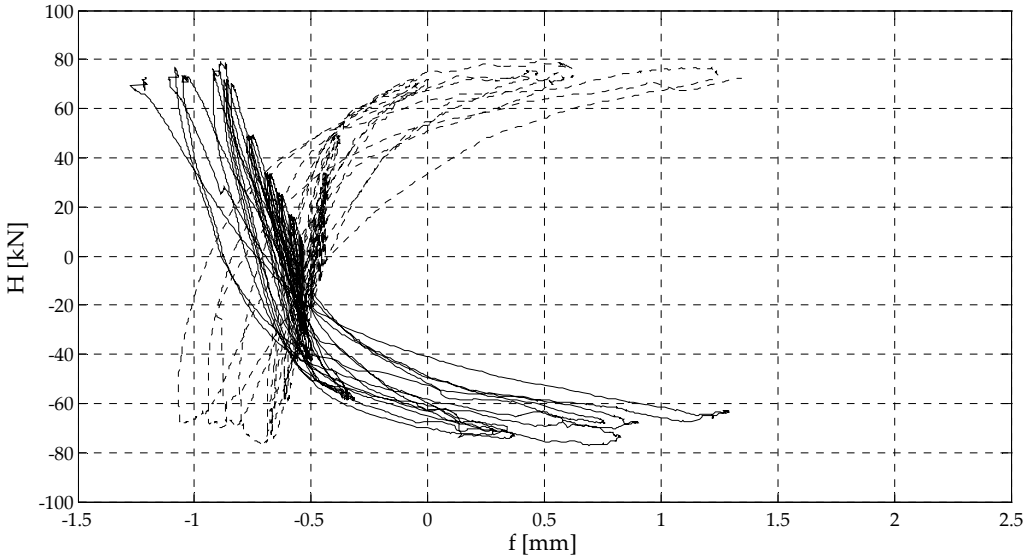
H [kN]
f [mm]

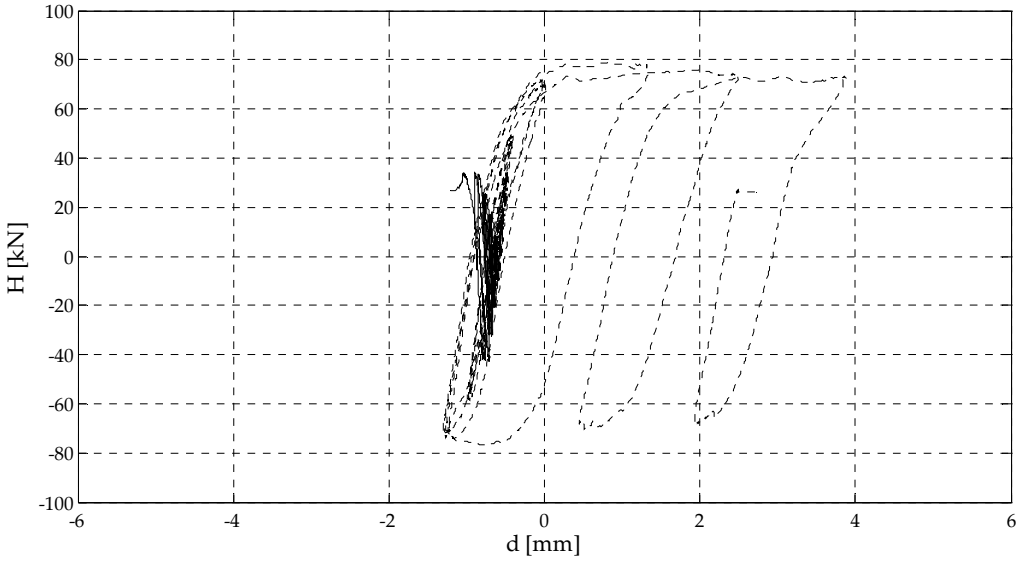
H [kN]
d [mm]

Test A2_1

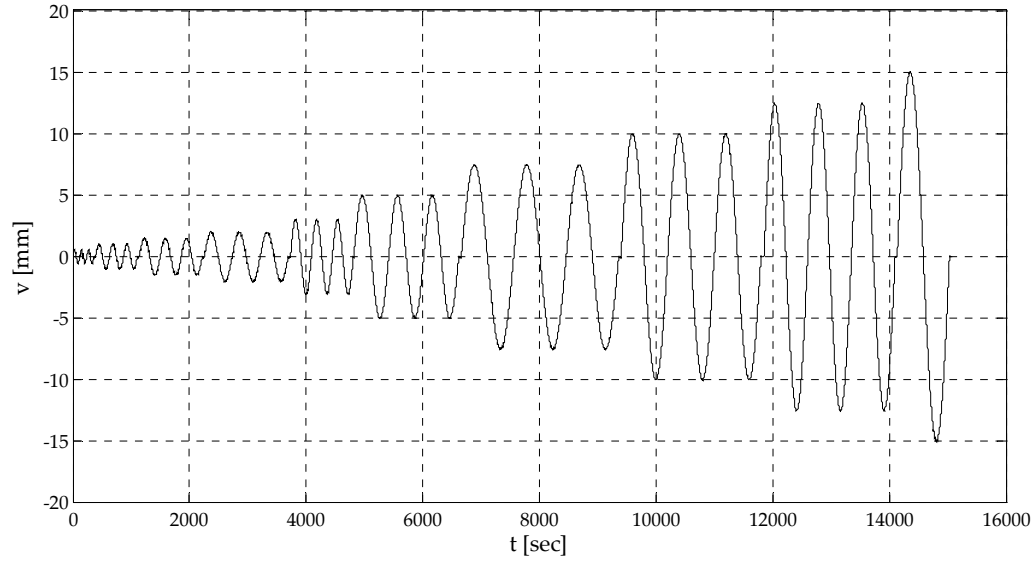

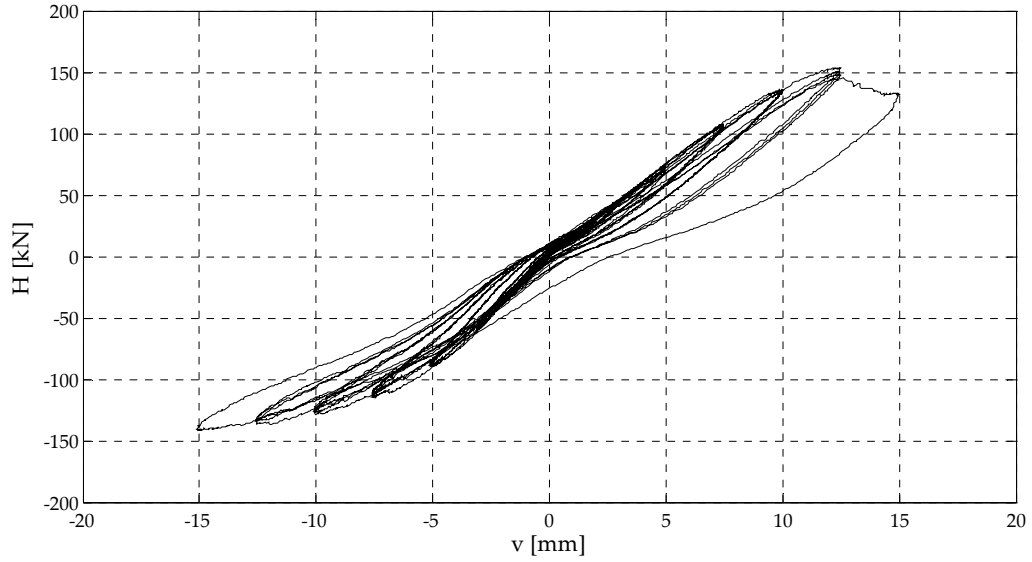

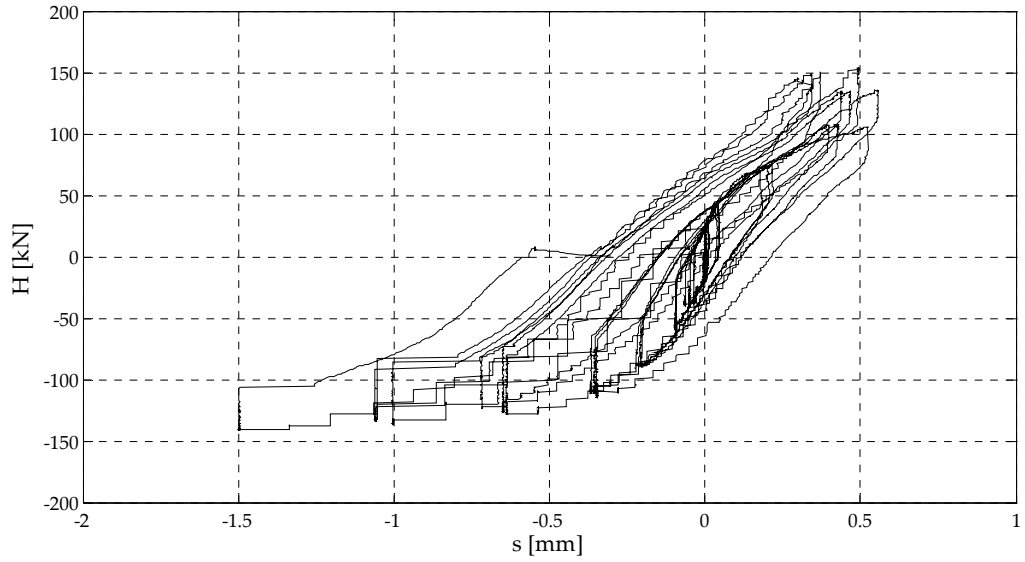

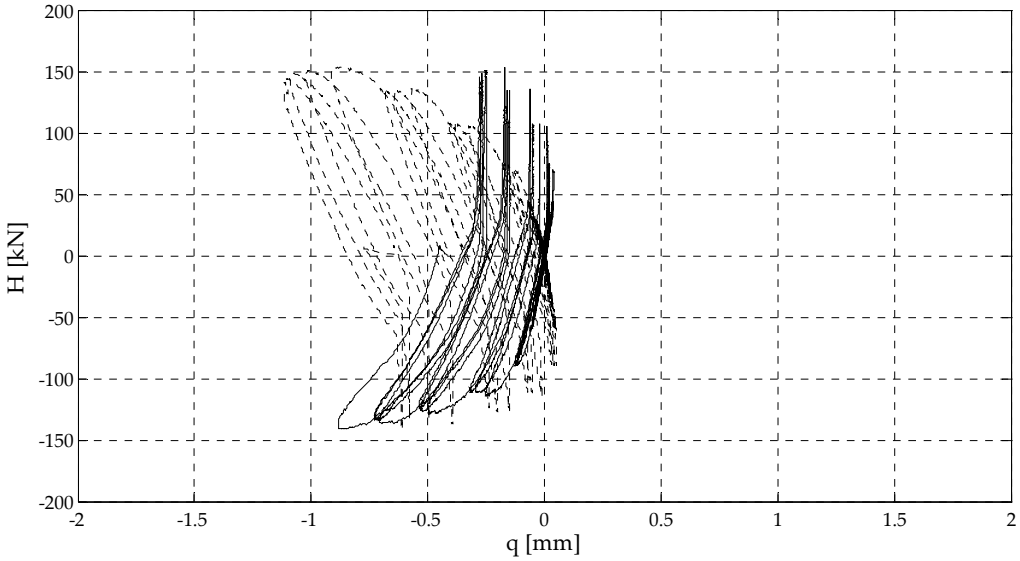
H [kN]
q [mm]

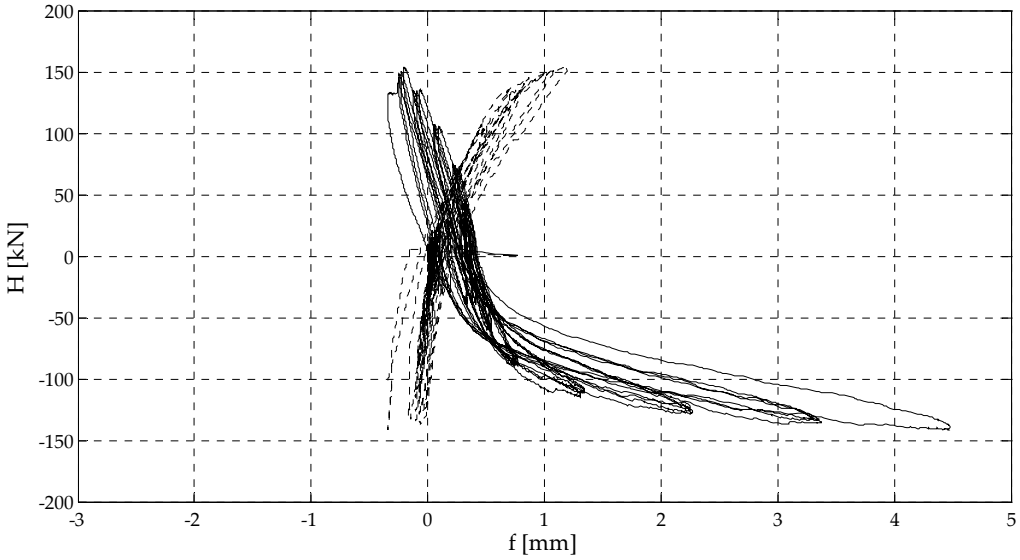
H [kN]
f [mm]

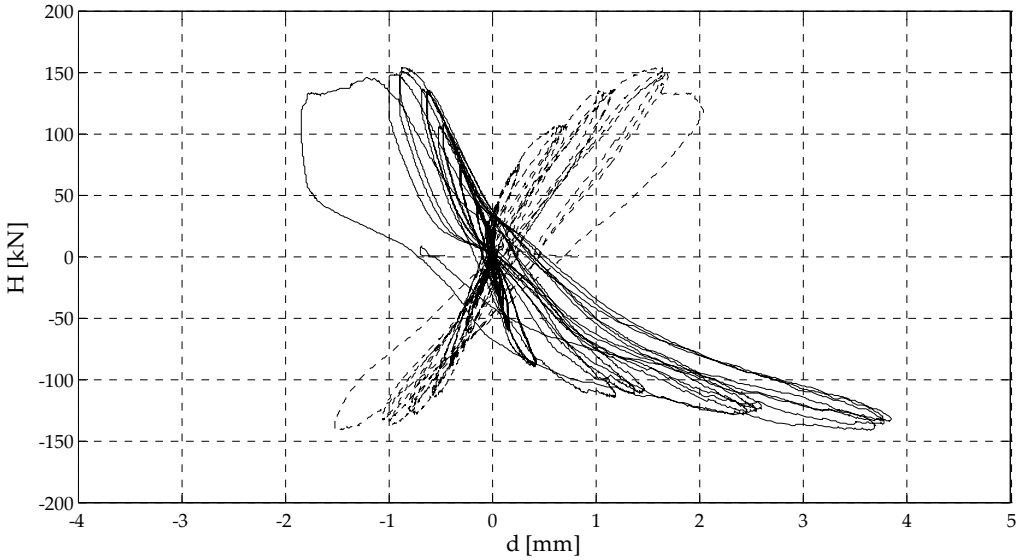
H [kN]
d [mm]

Test A2_2

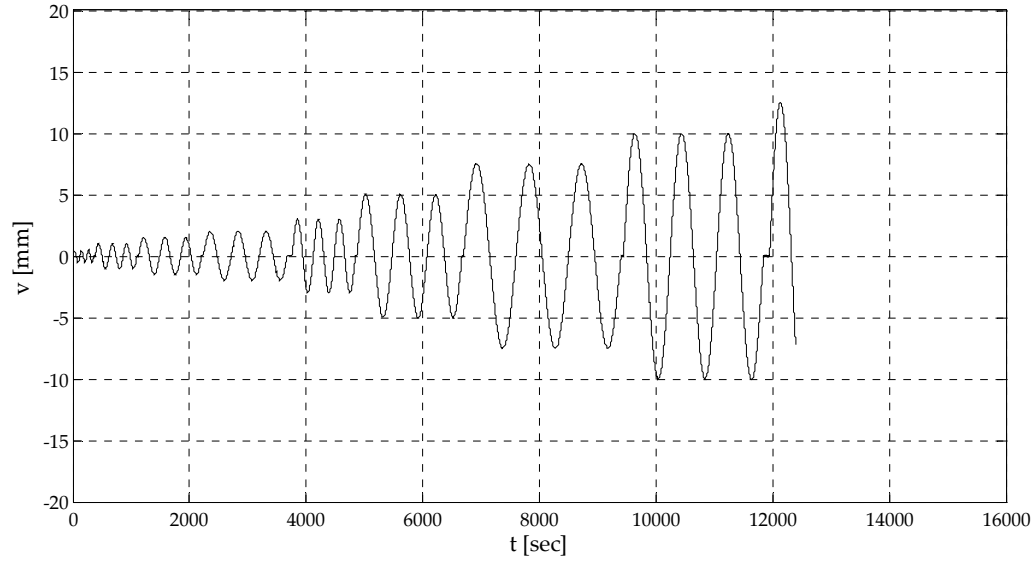

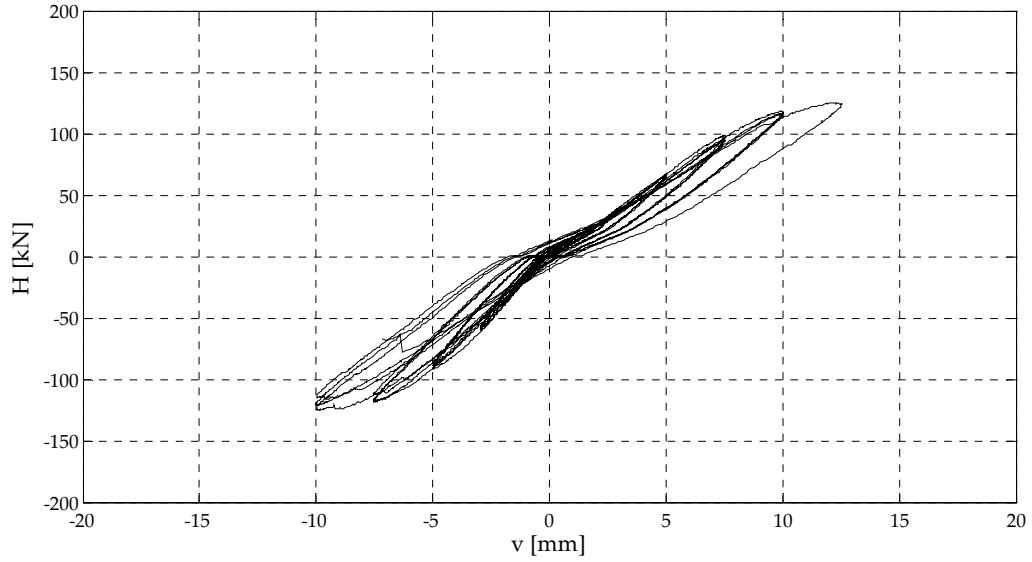

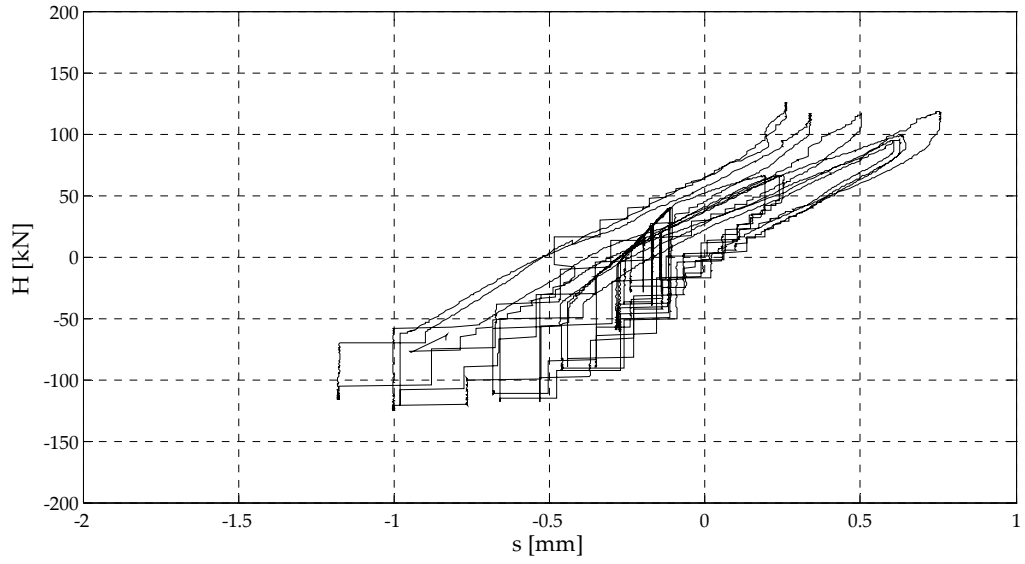

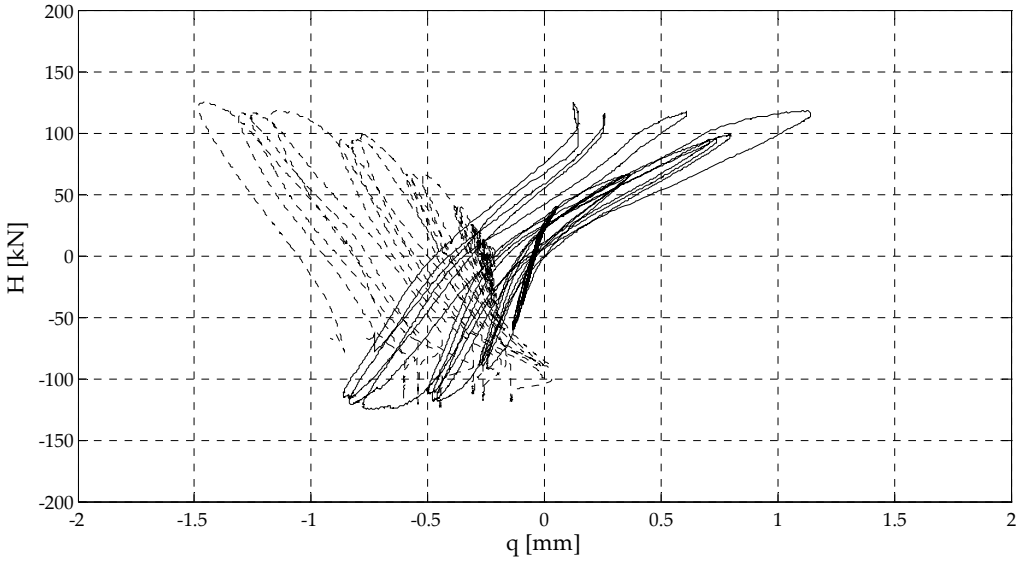
H [kN]
q [mm]

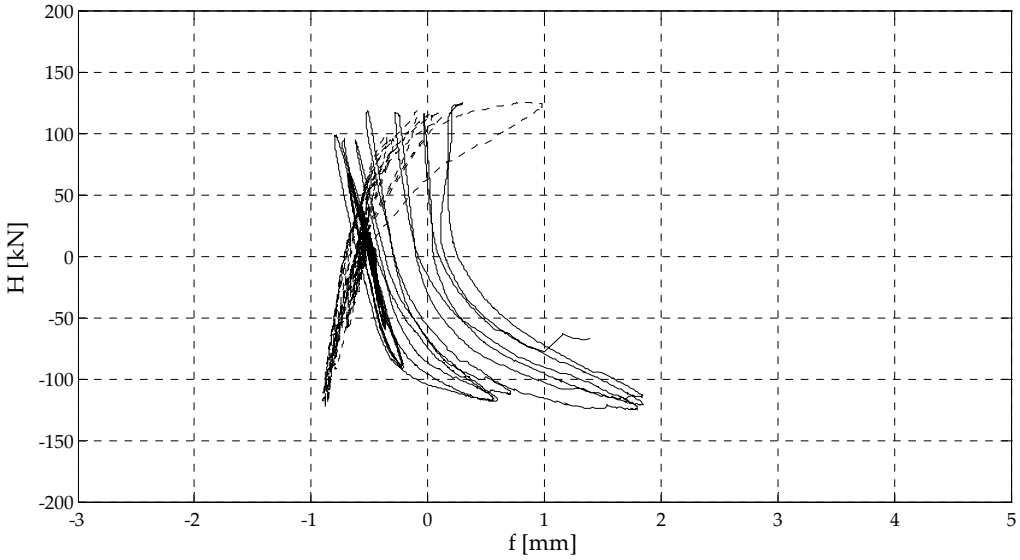
H [kN]
f [mm]

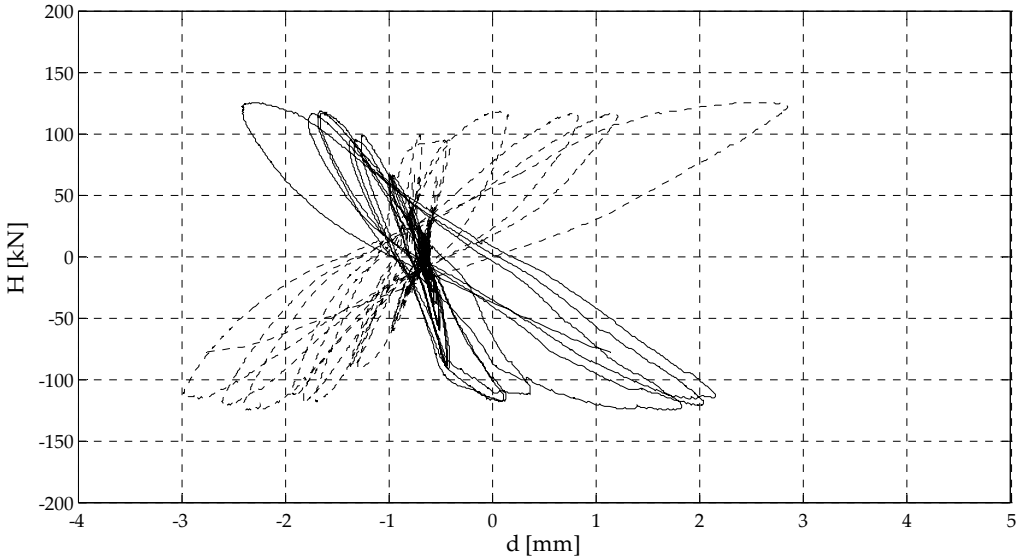
H [kN]
d [mm]

Test A2_3

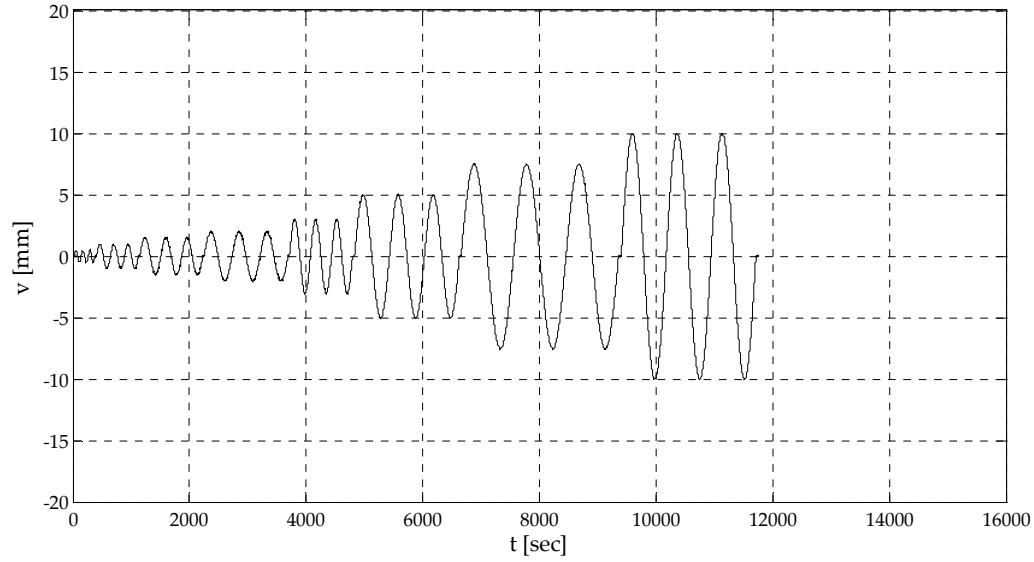

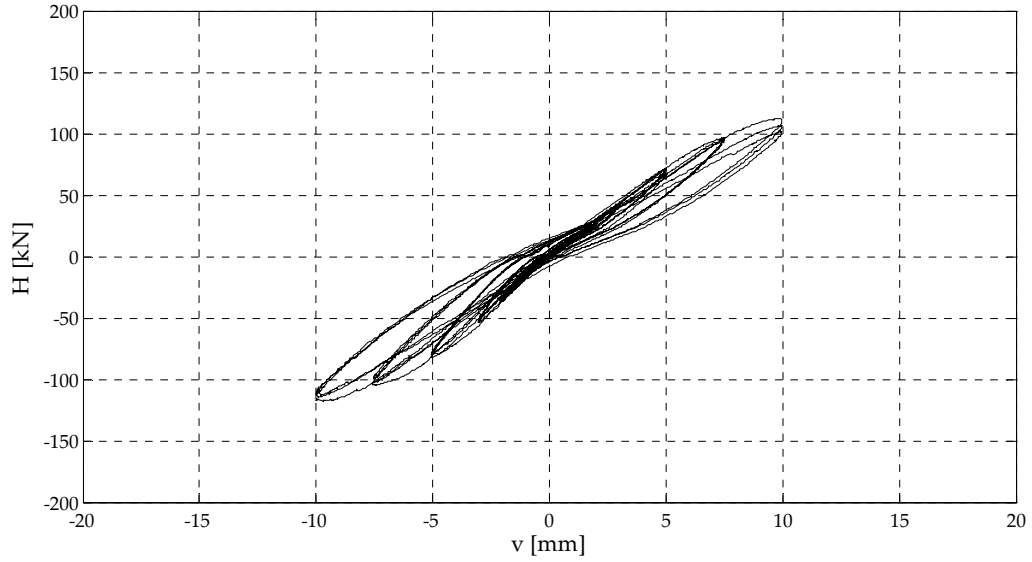

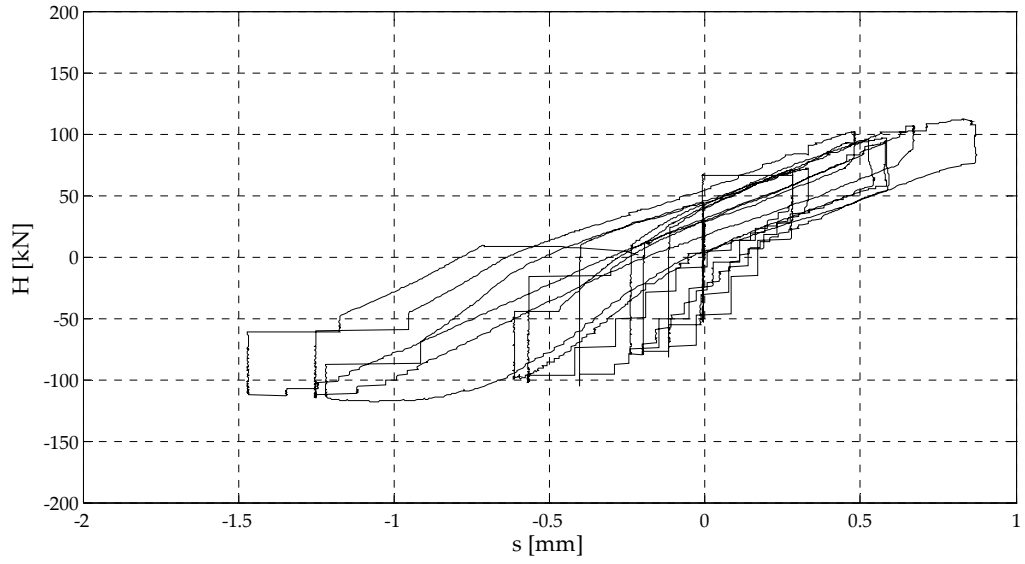

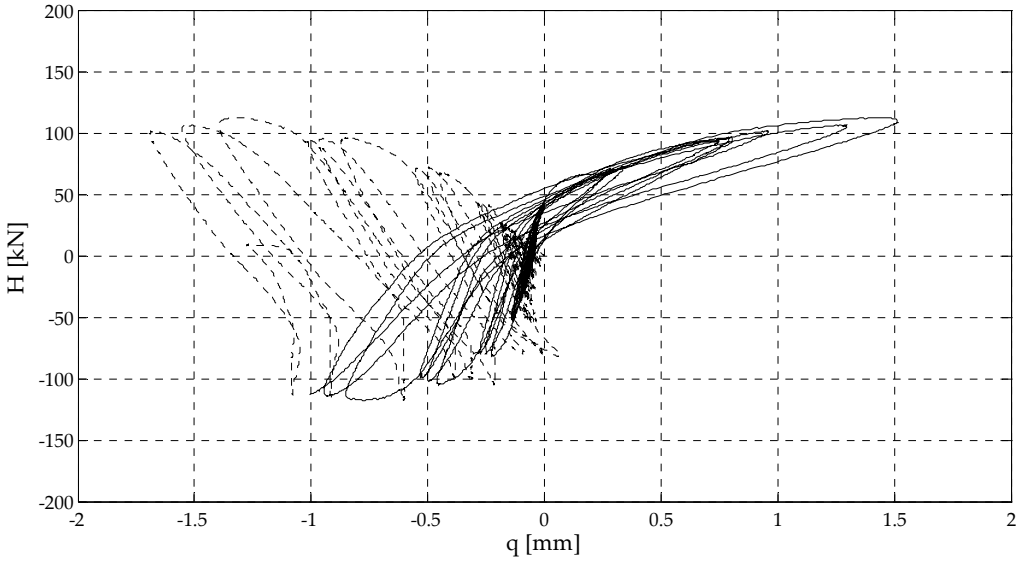
H [kN]
q [mm]

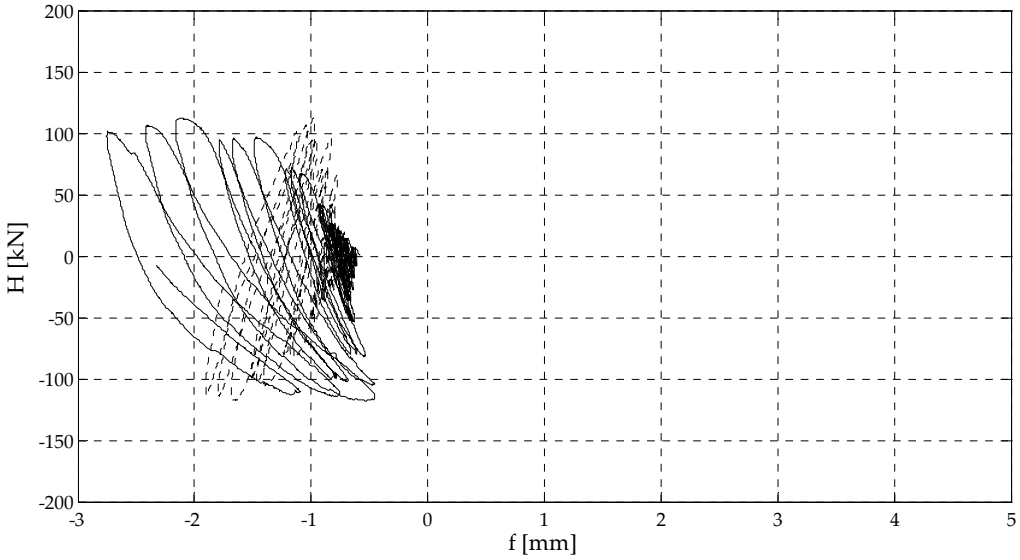
H [kN]
f [mm]

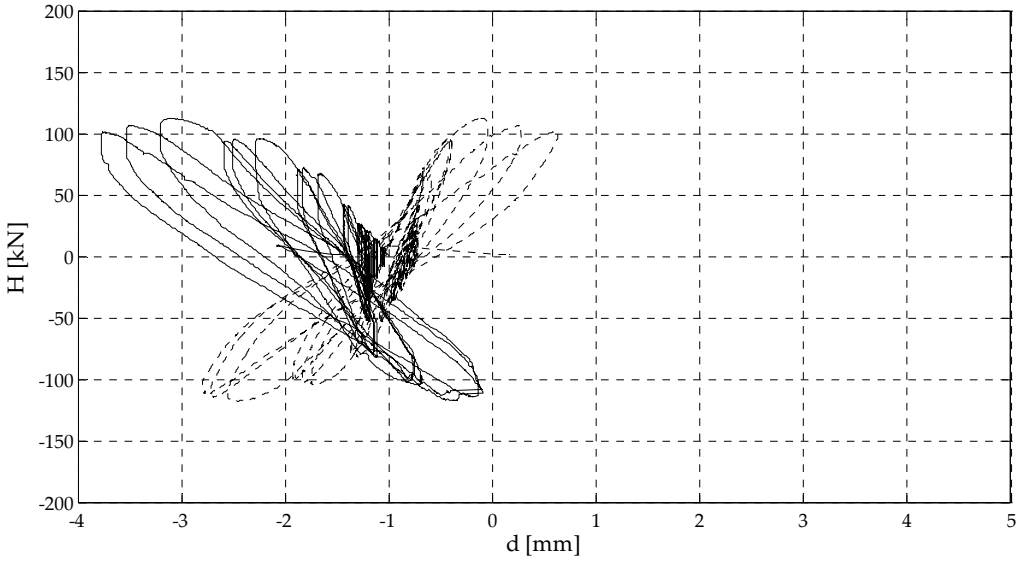
H [kN]
d [mm]

Test A3_1

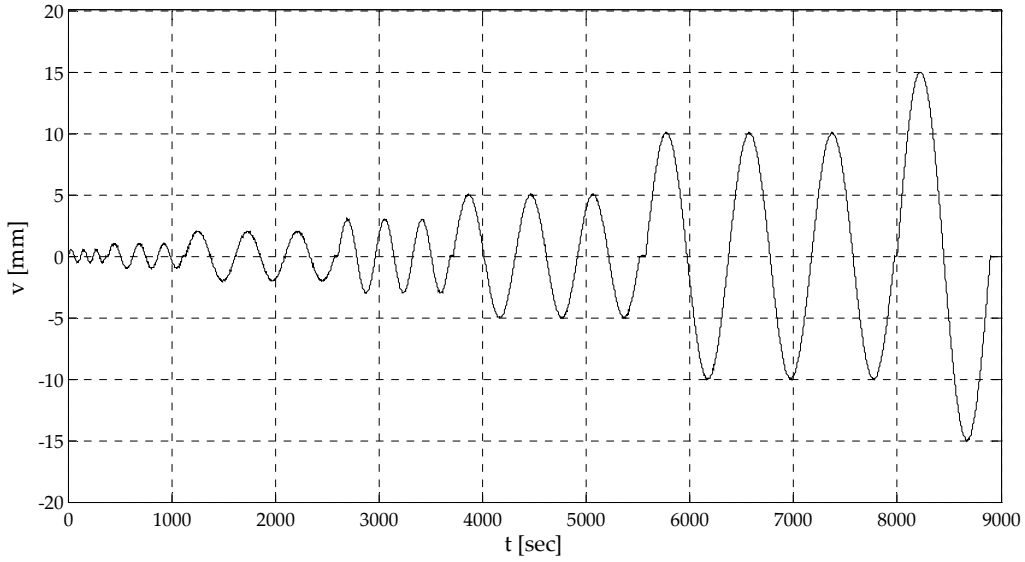

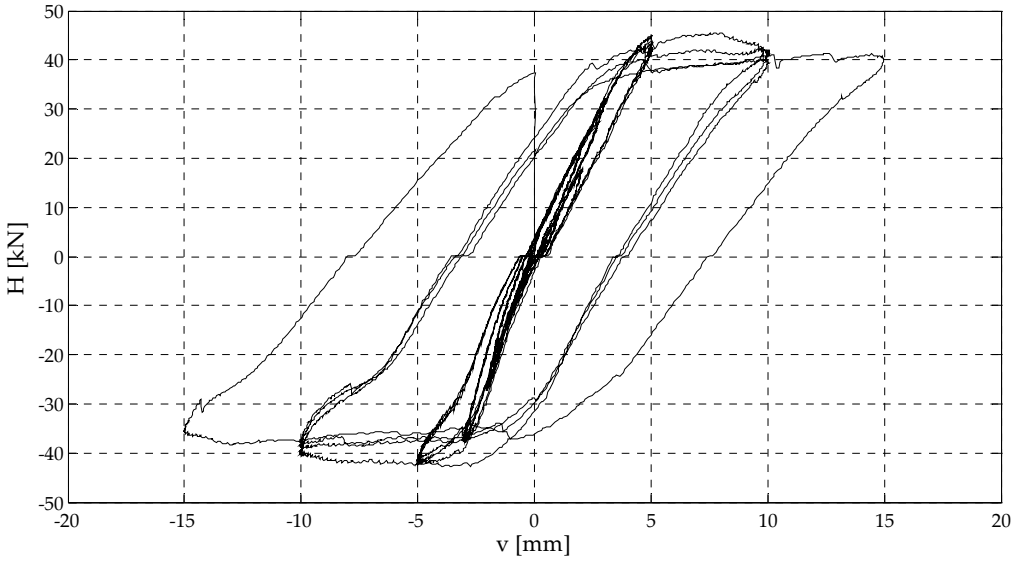

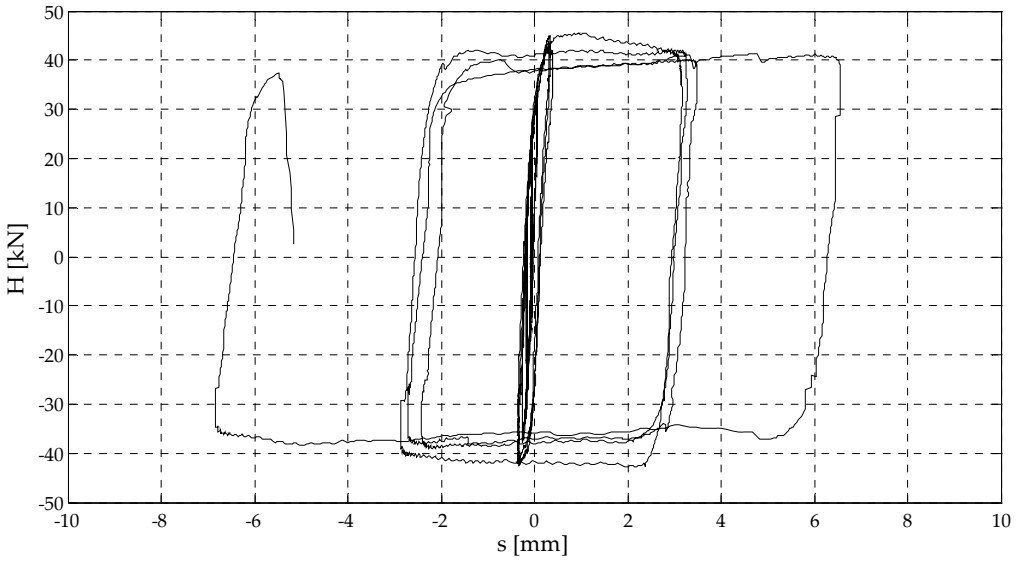

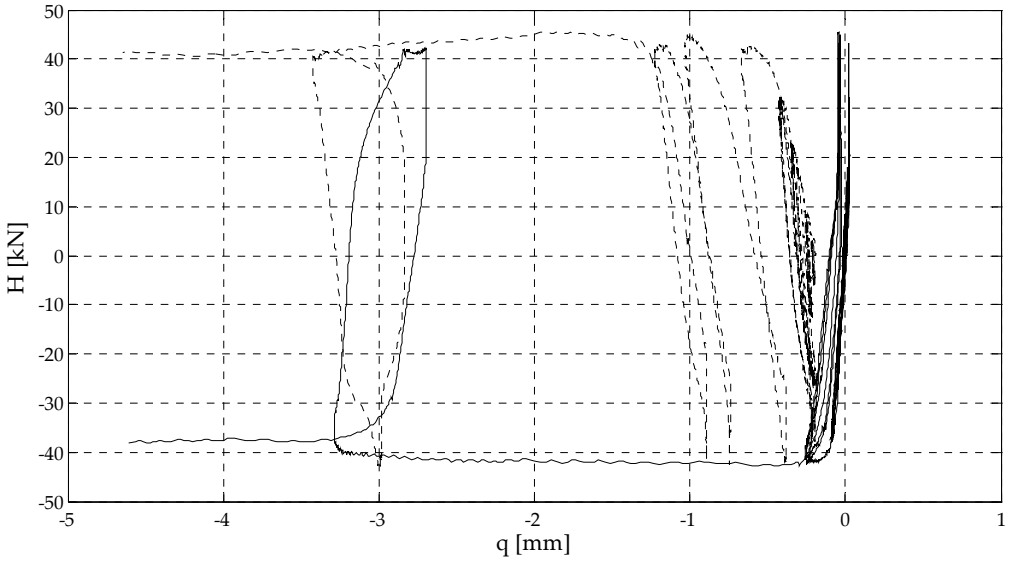
H [kN]
q [mm]

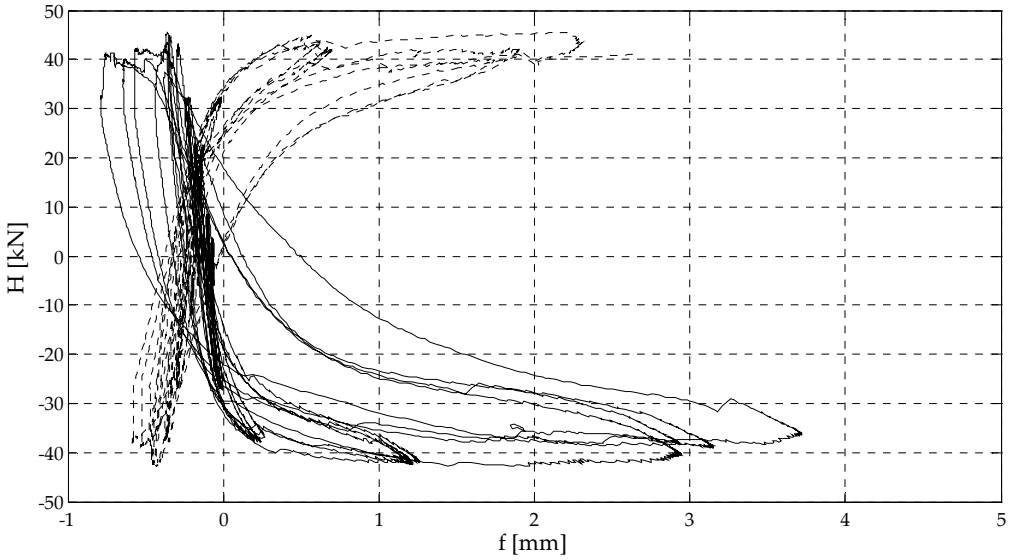
H [kN]
f [mm]

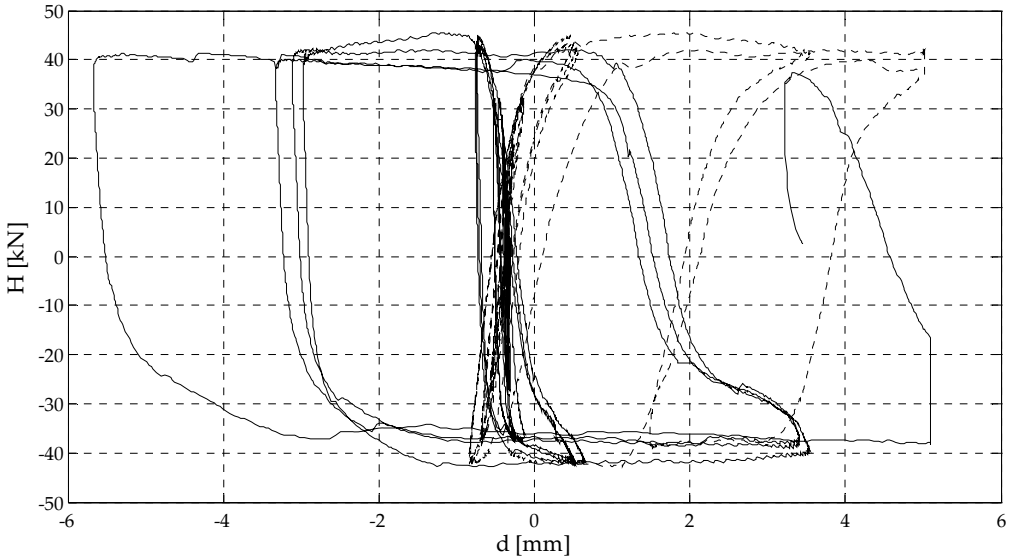
H [kN]
d [mm]

Test A3_2

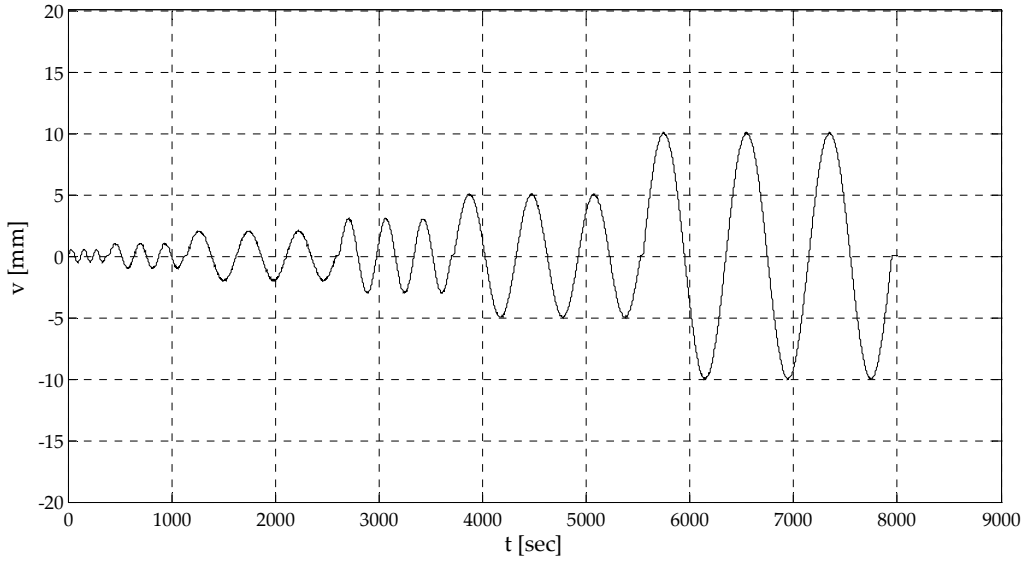

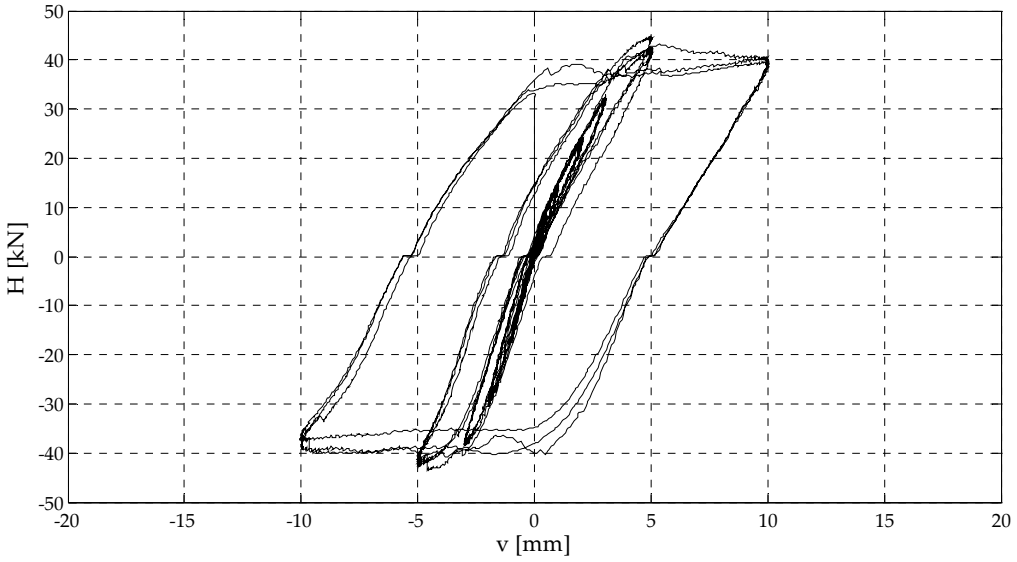

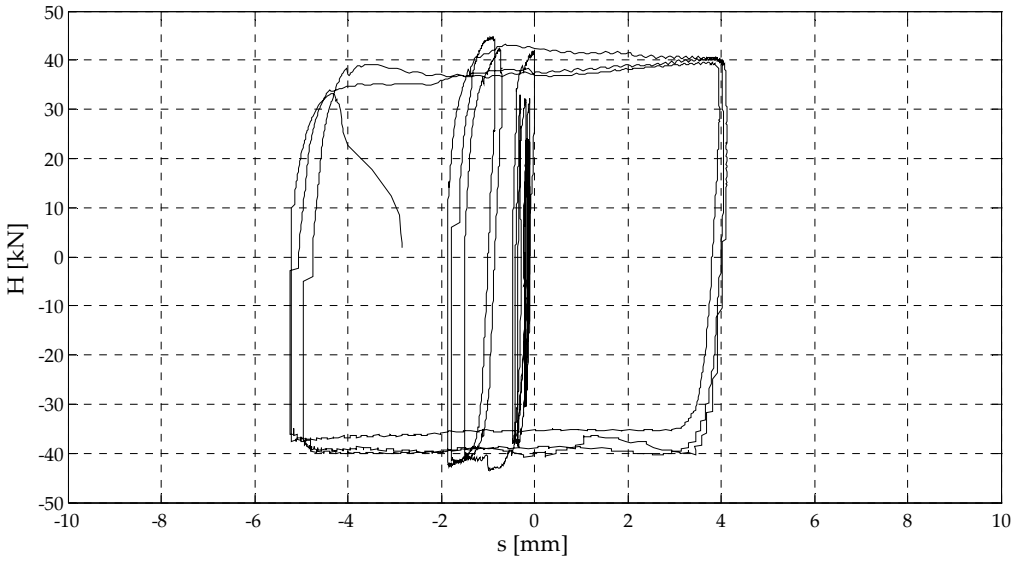

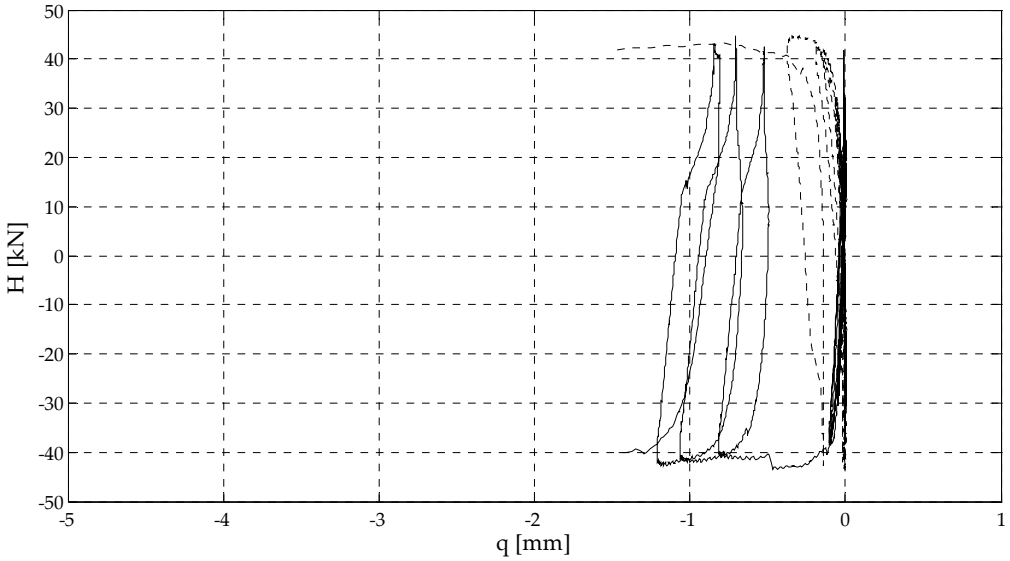
H [kN]
q [mm]

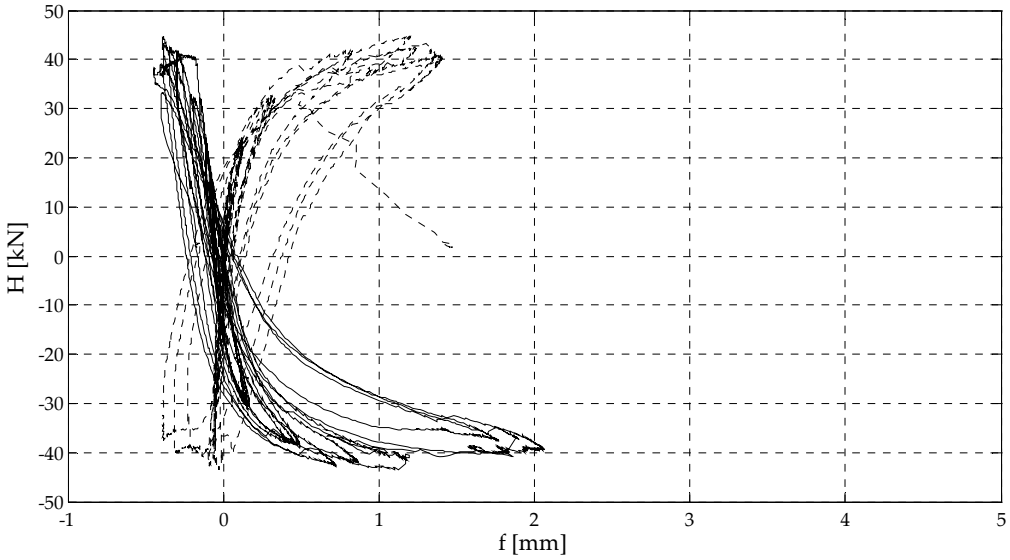
H [kN]
f [mm]

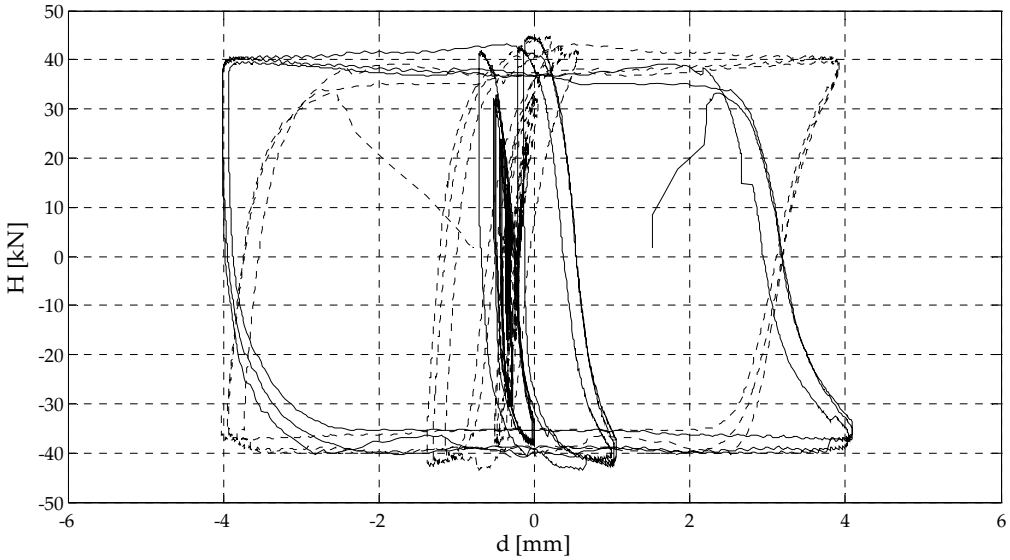
H [kN]
d [mm]

Test A3_3

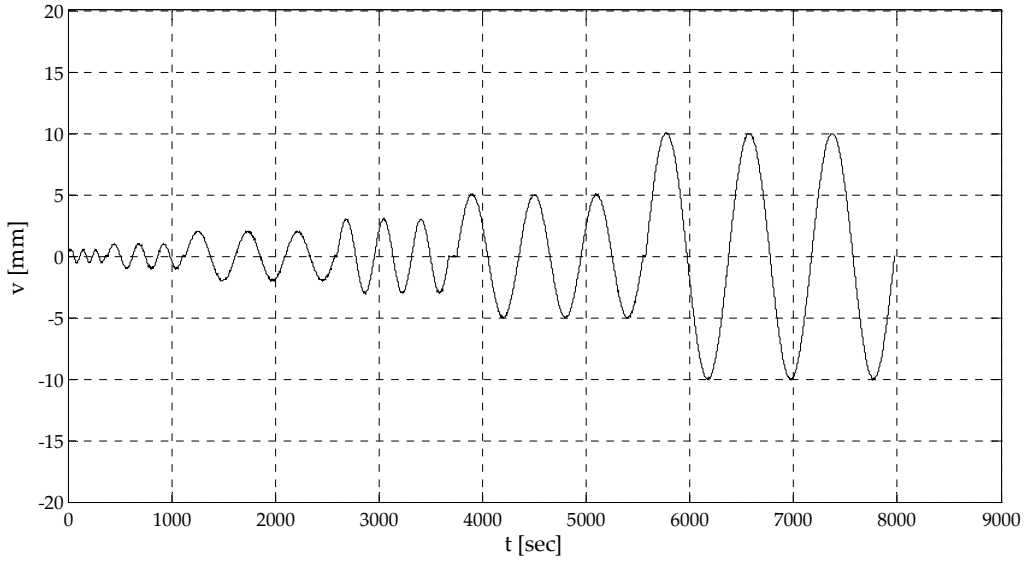

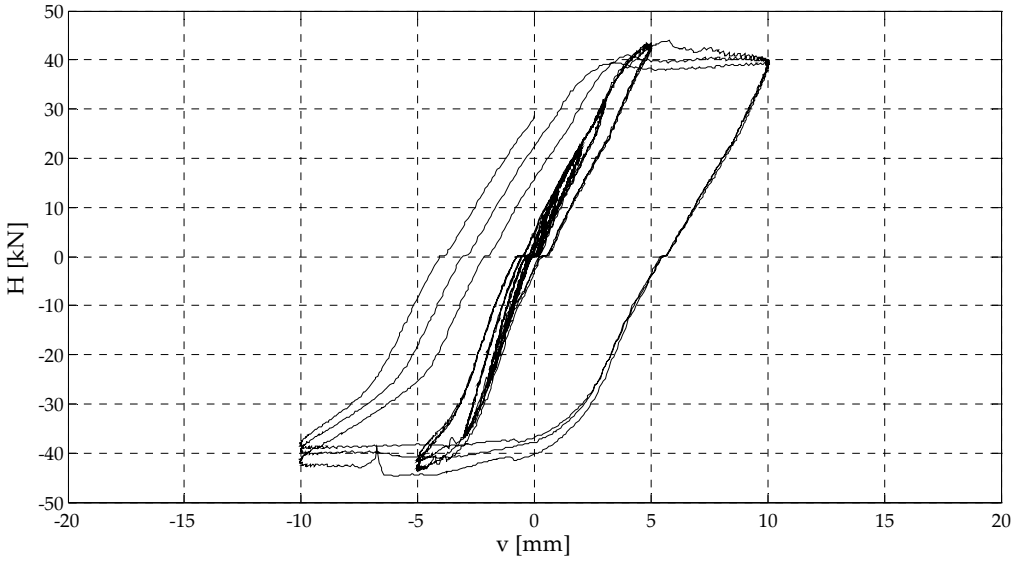

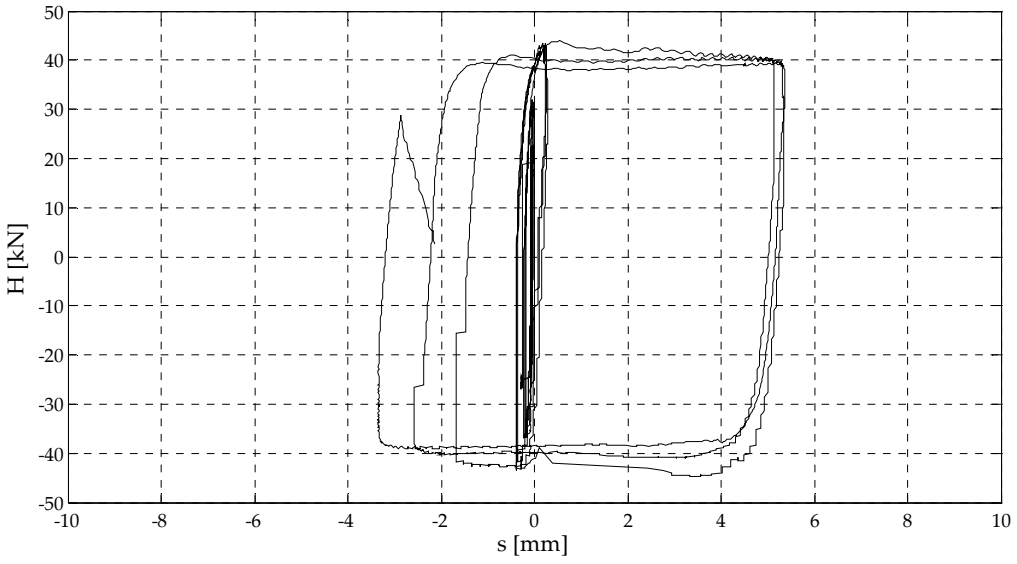

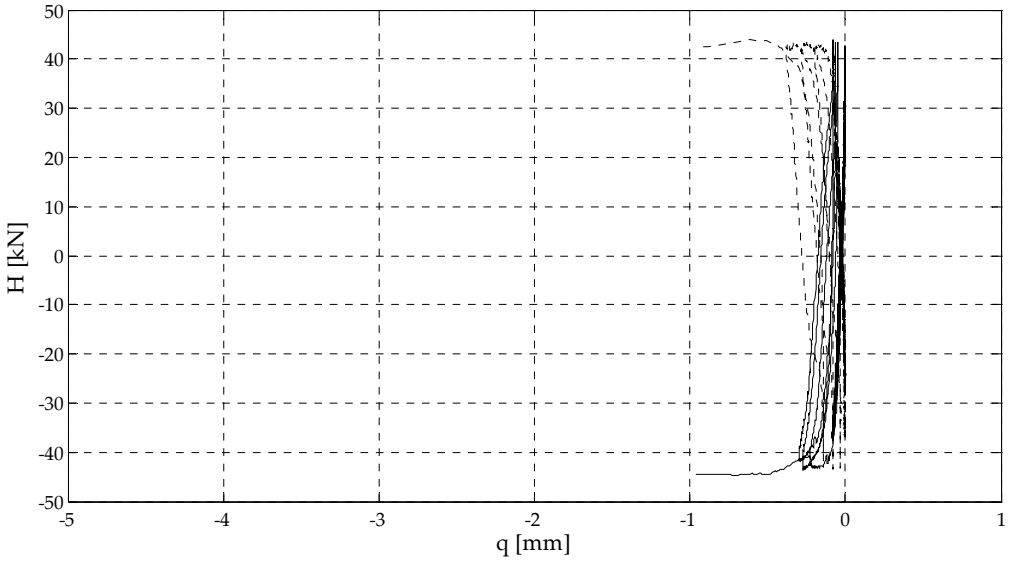
H [kN]
q [mm]

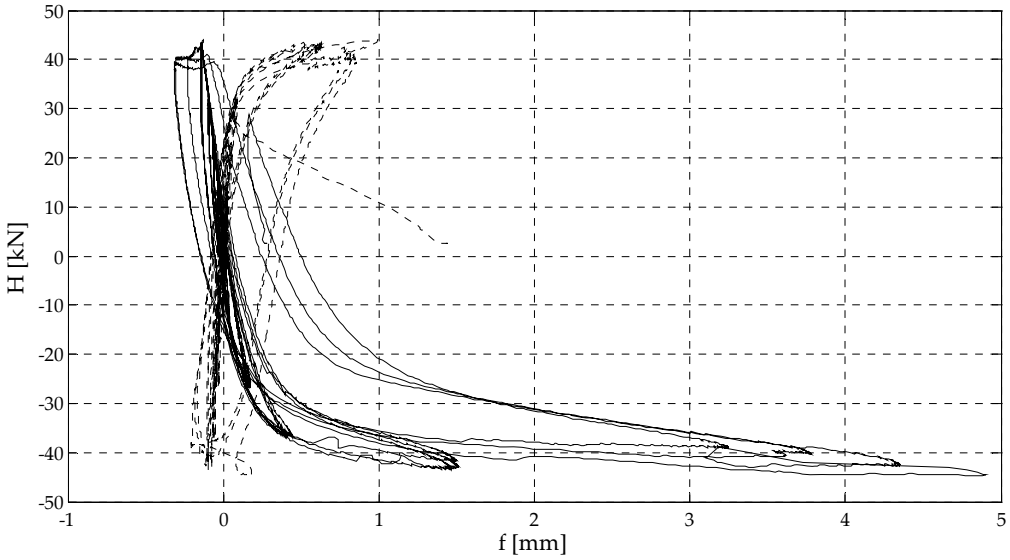
H [kN]
f [mm]

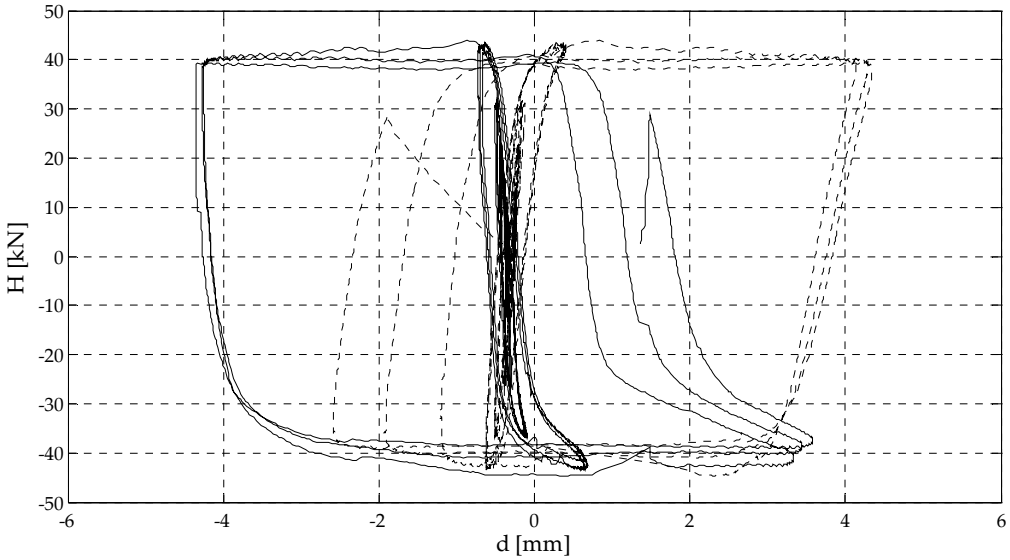
H [kN]
d [mm]

Test B1_1

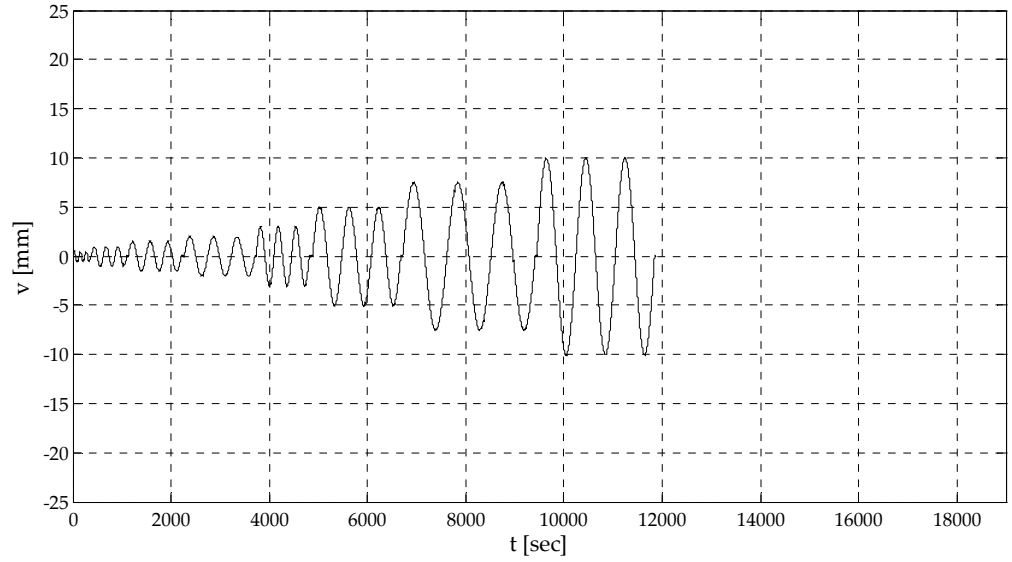

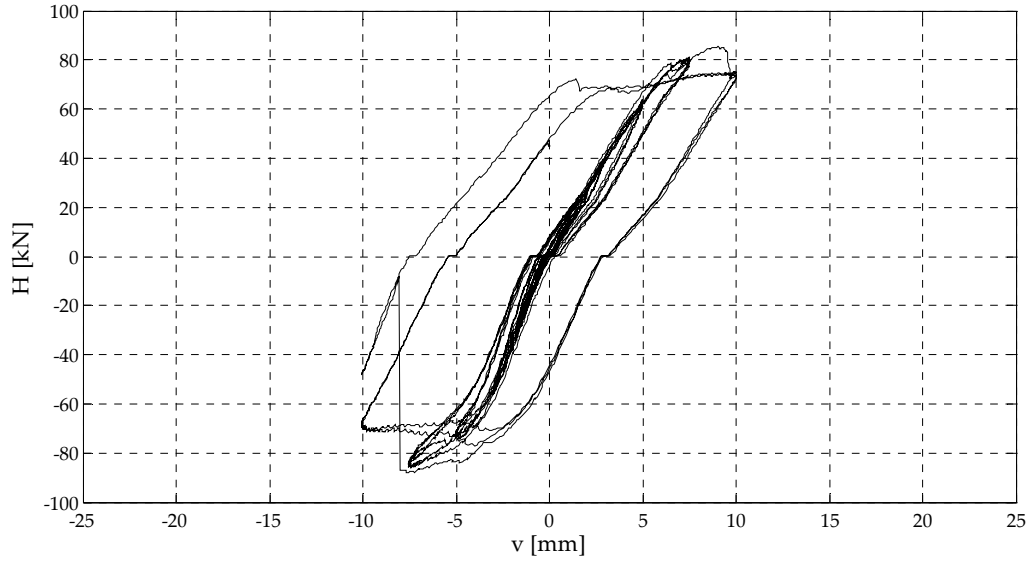

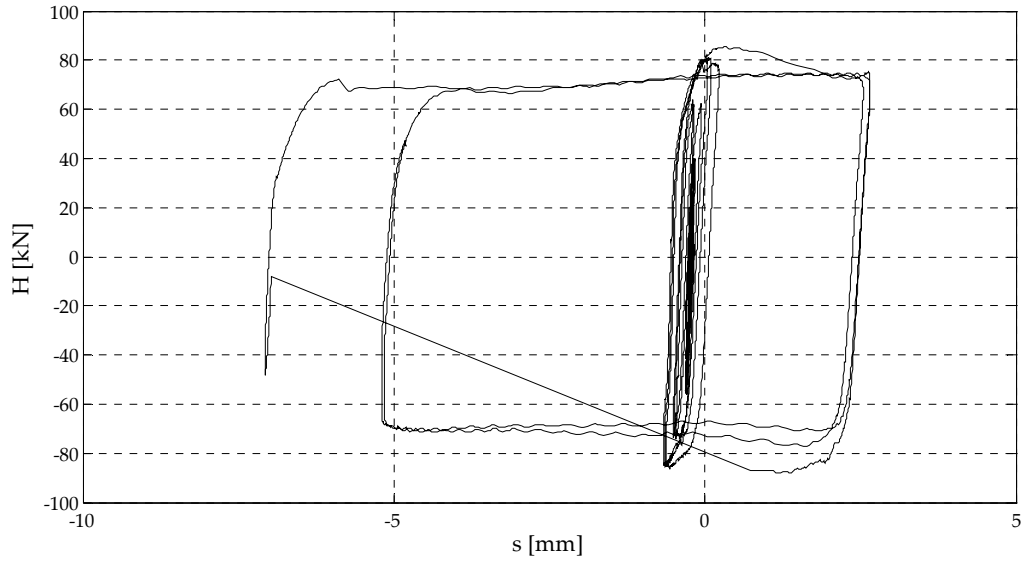

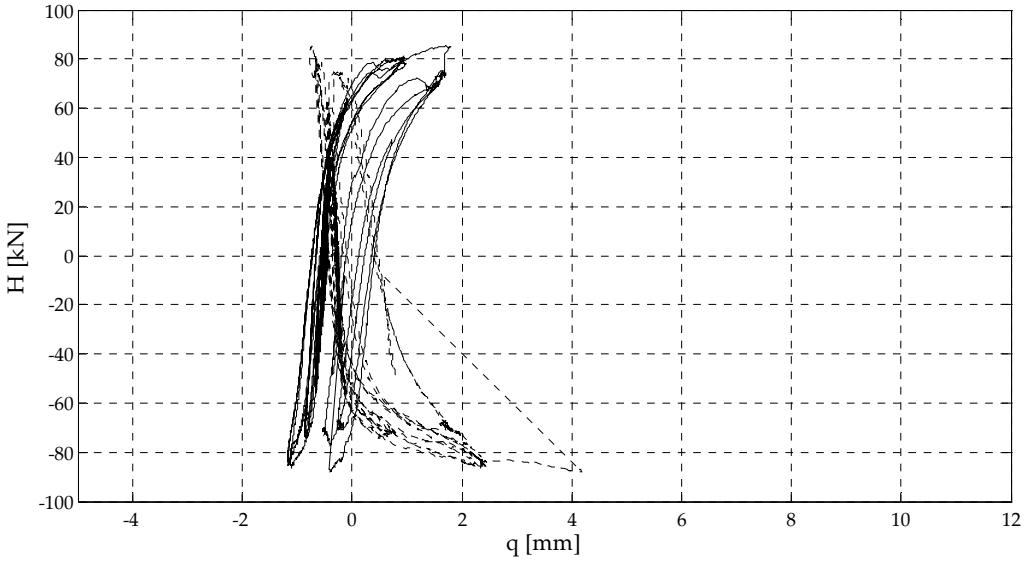
H [kN]
q [mm]

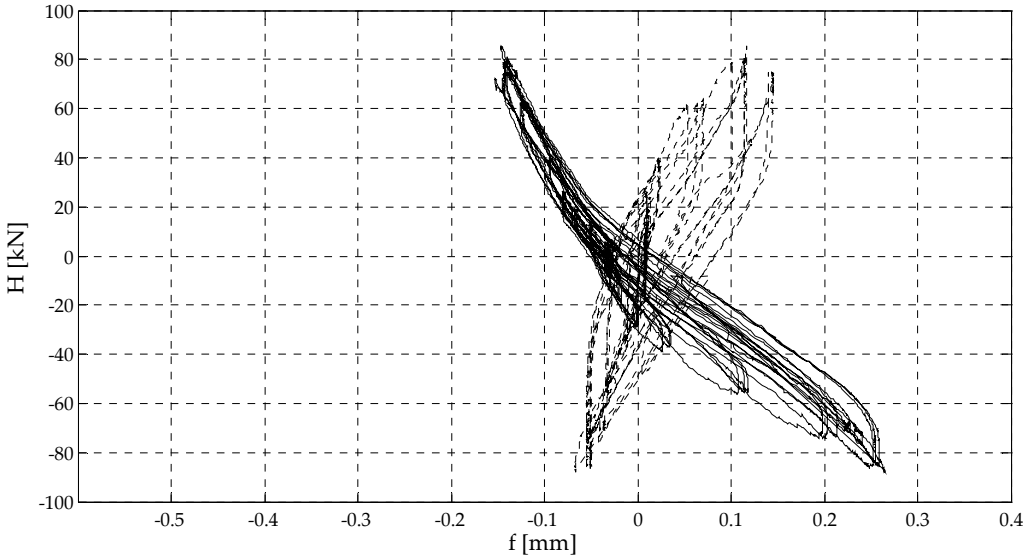
H [kN]
f [mm]

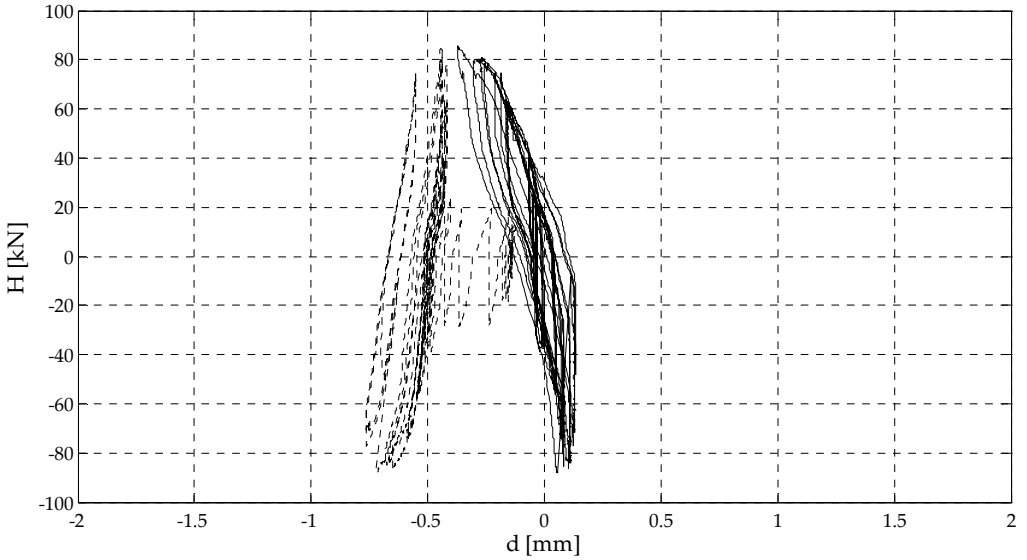
H [kN]
d [mm]

Test B1_2

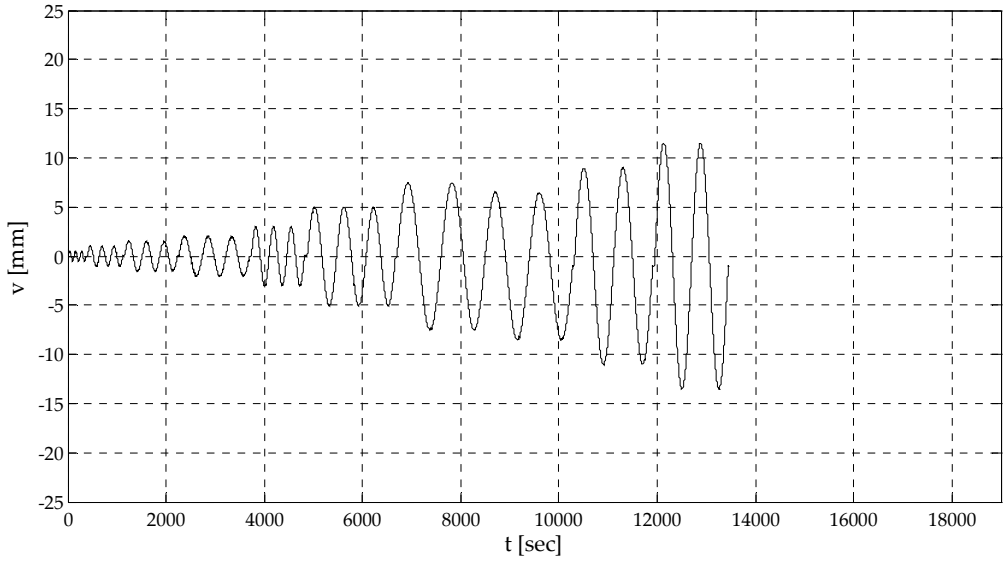

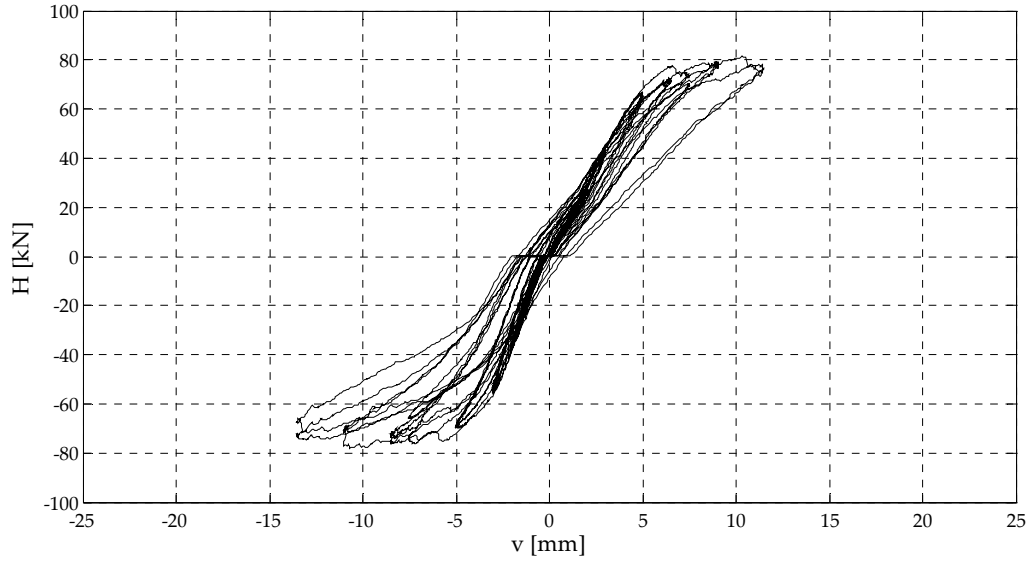

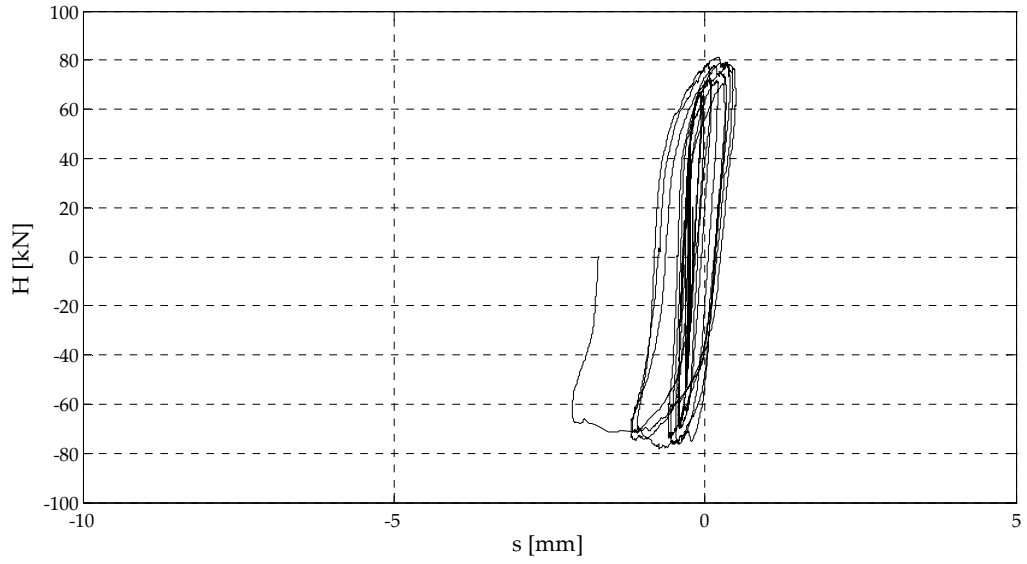

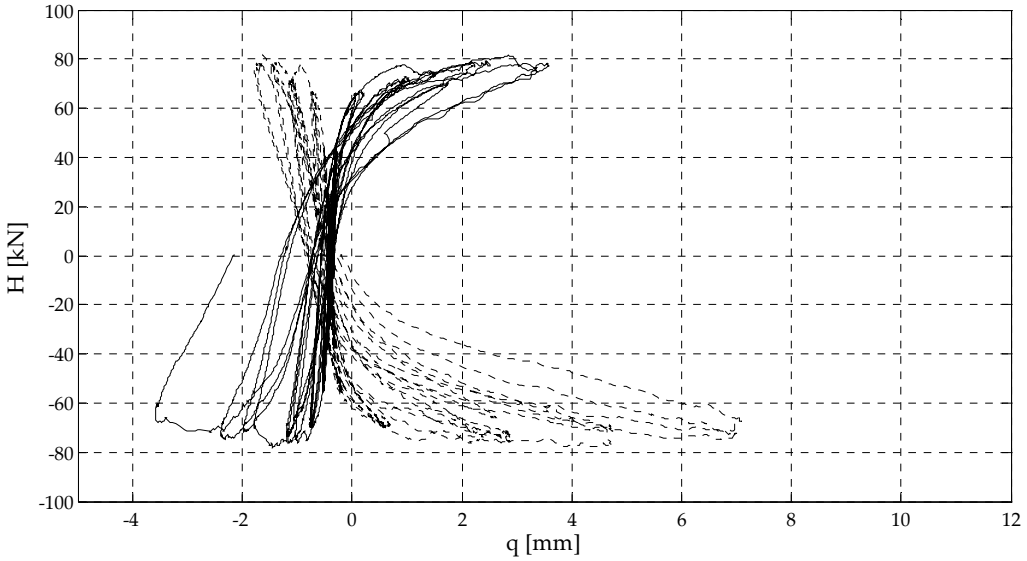
H [kN]
q [mm]

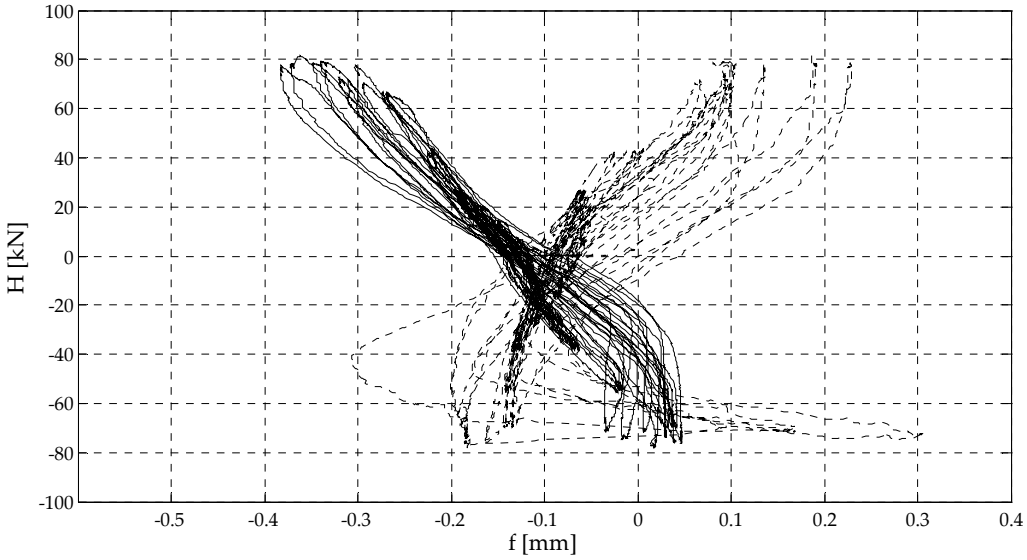
H [kN]
f [mm]

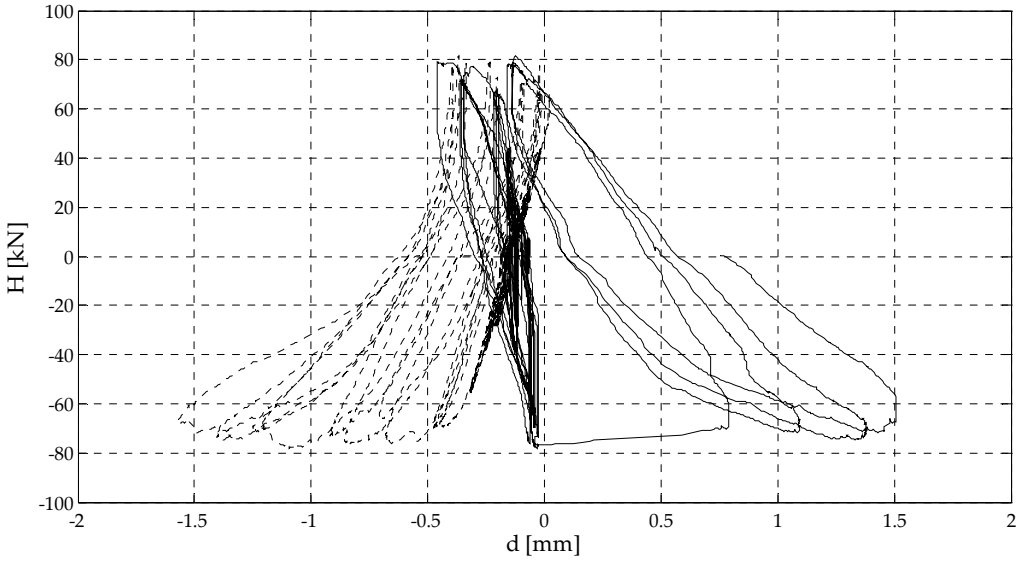
H [kN]
d [mm]

Test B1_3

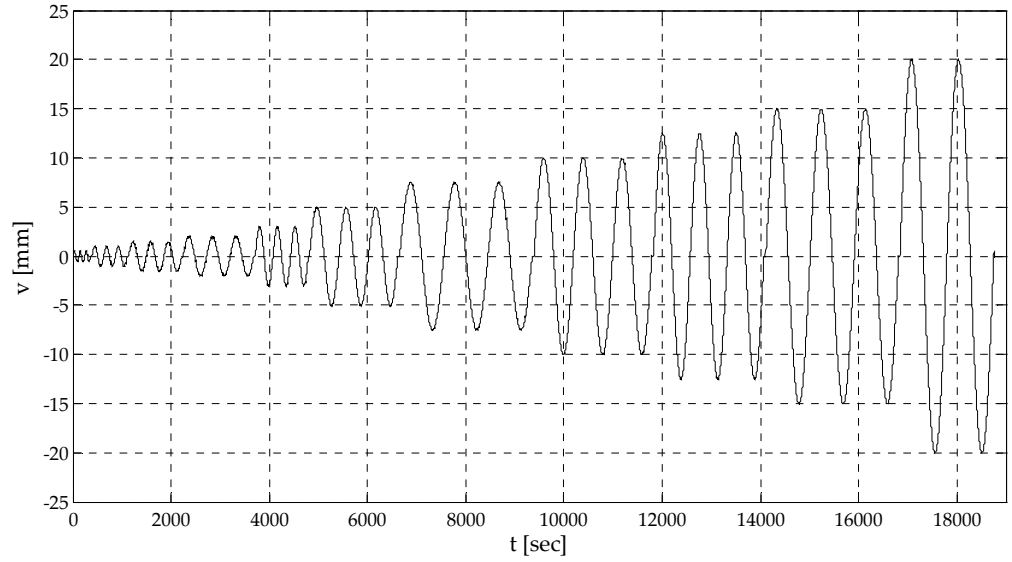

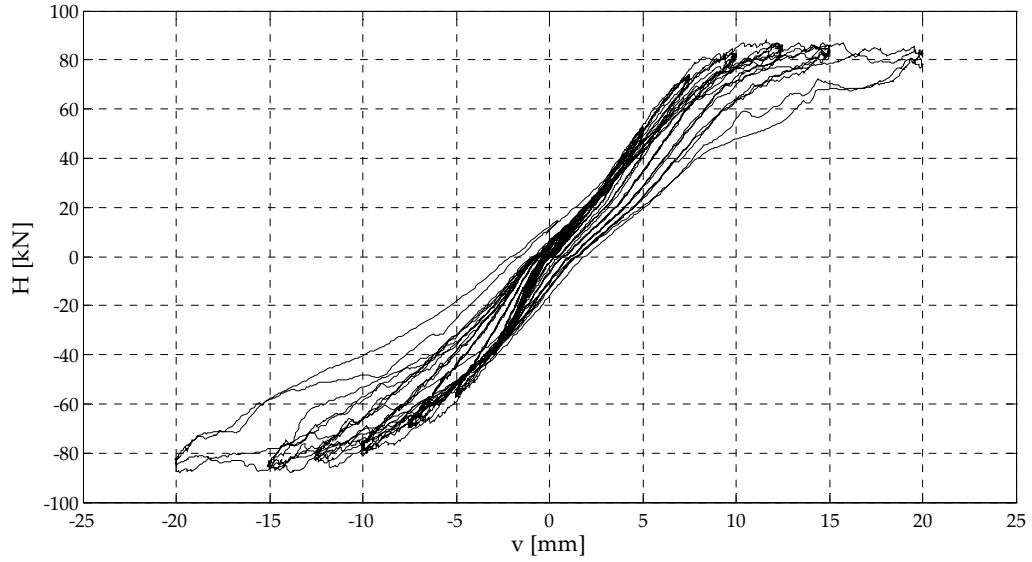

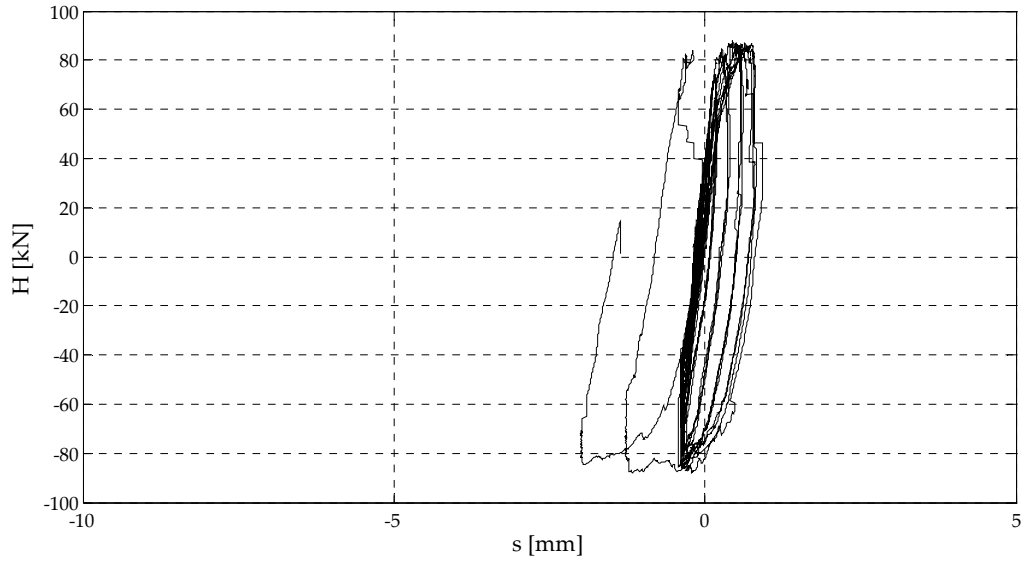

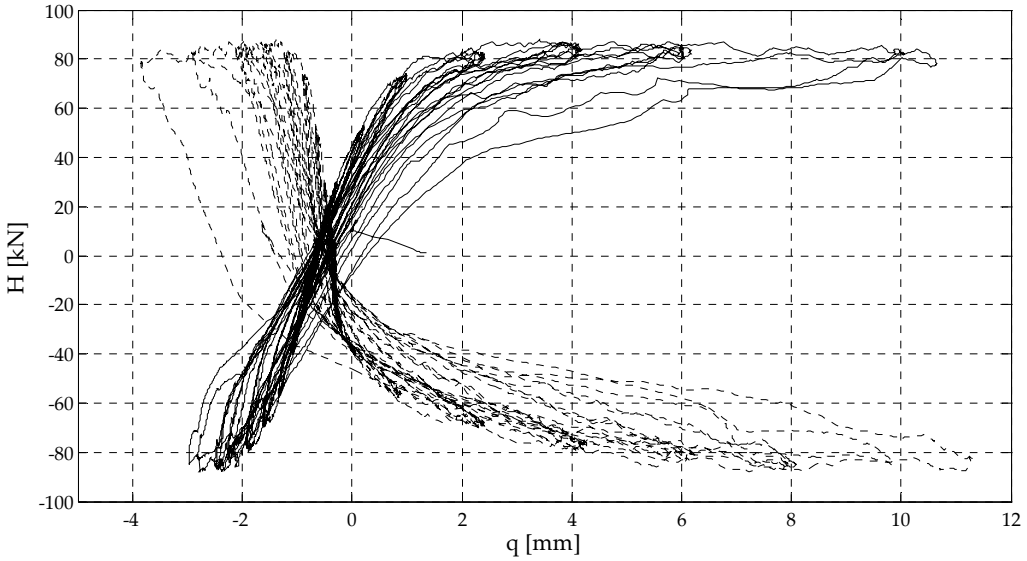
H [kN]
q [mm]

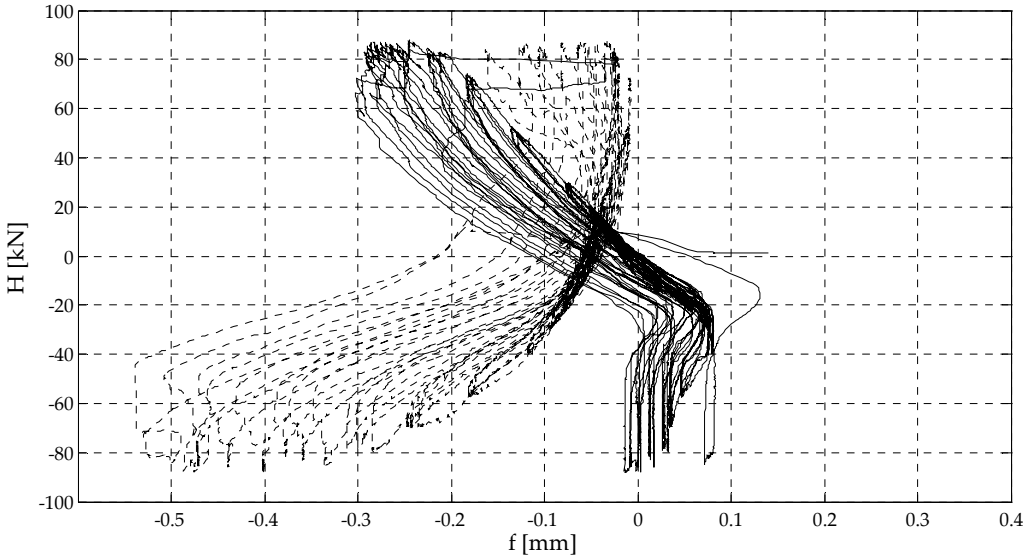
H [kN]
f [mm]

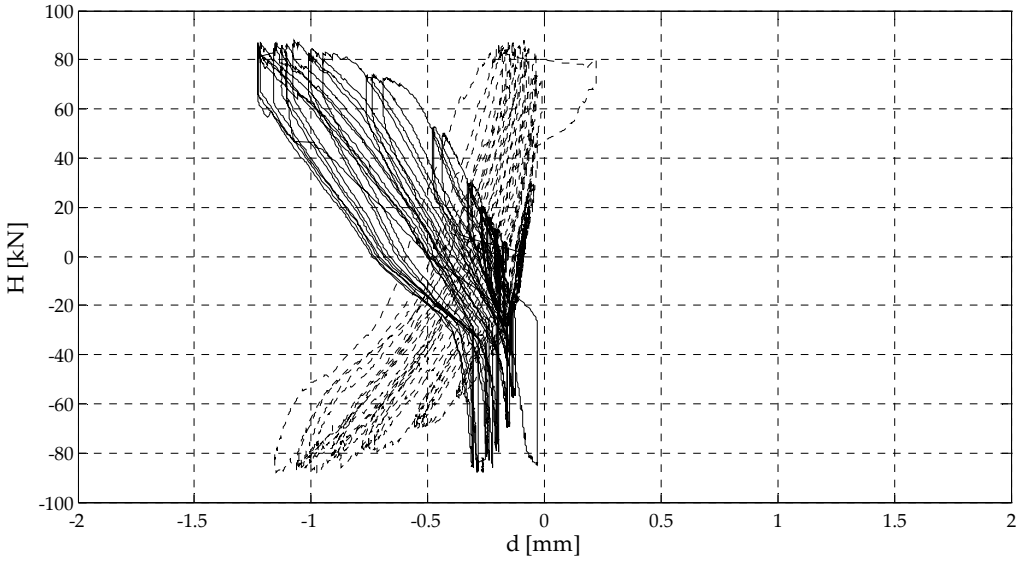
H [kN]
d [mm]

Test B2_1

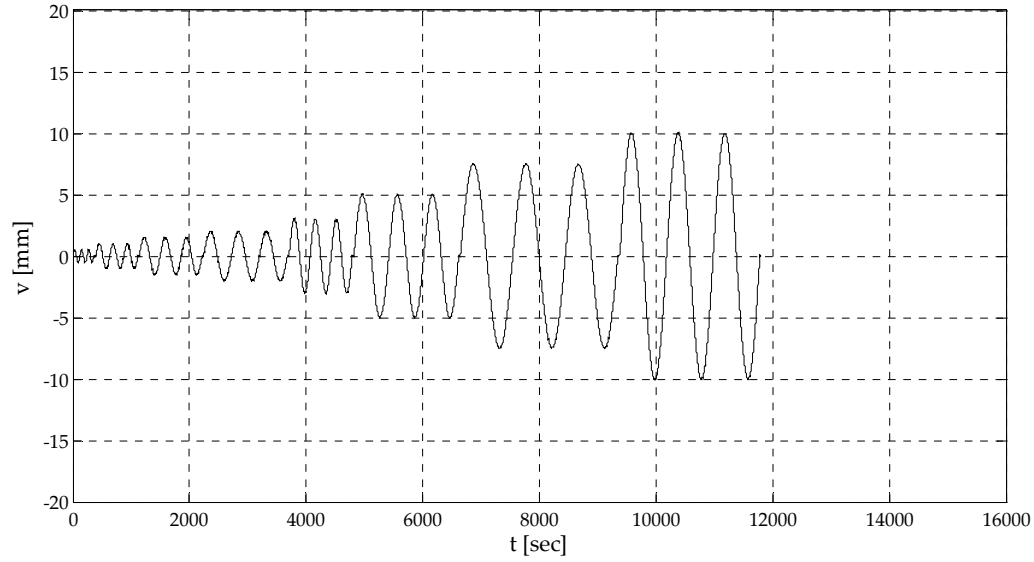

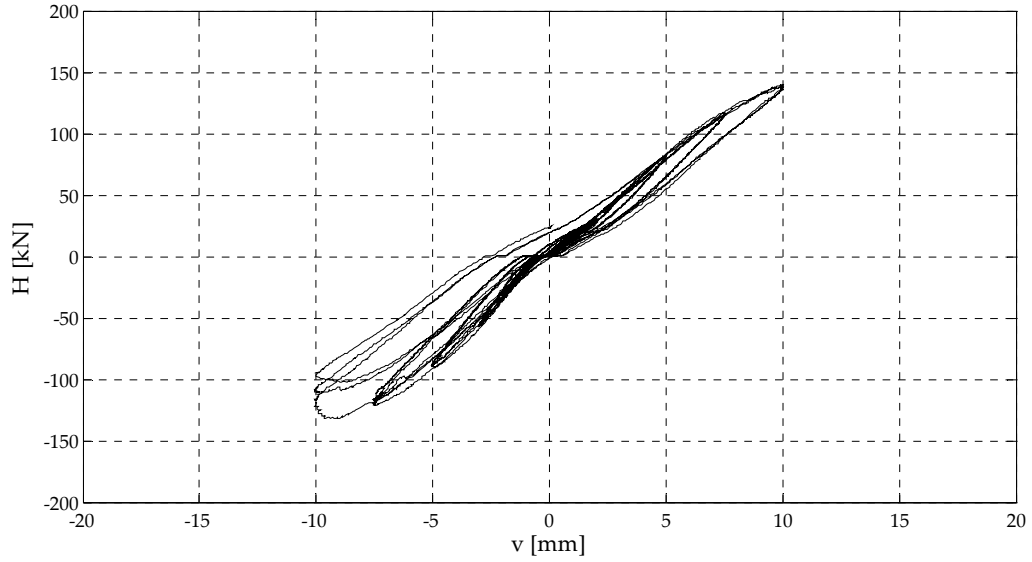

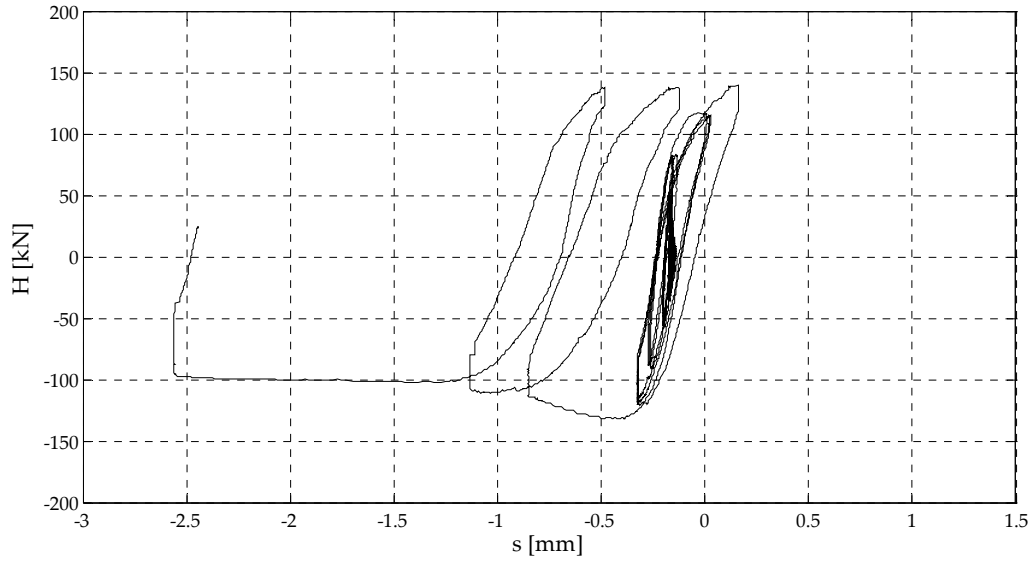

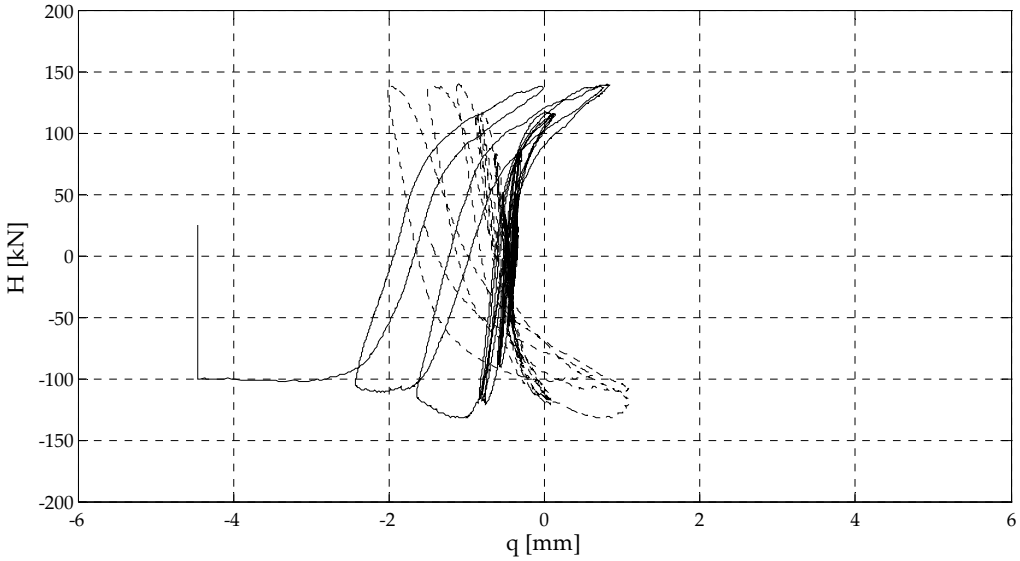
H [kN]
q [mm]

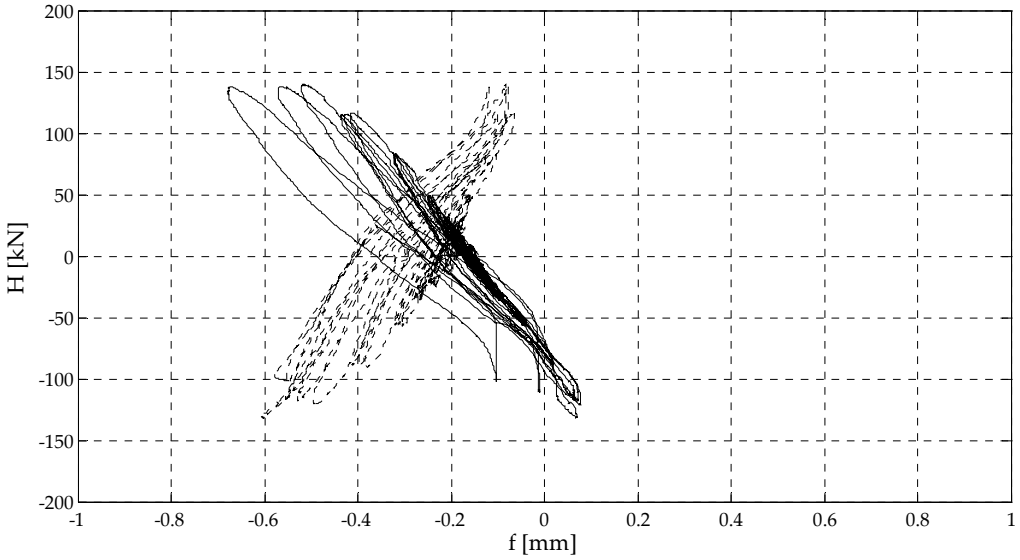
H [kN]
f [mm]

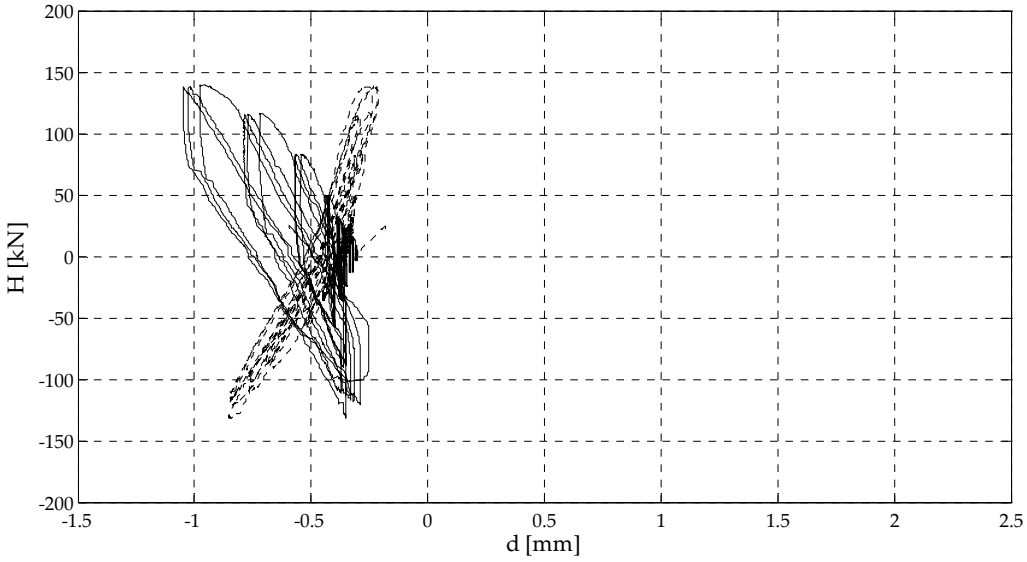
H [kN]
d [mm]

Test B2_2

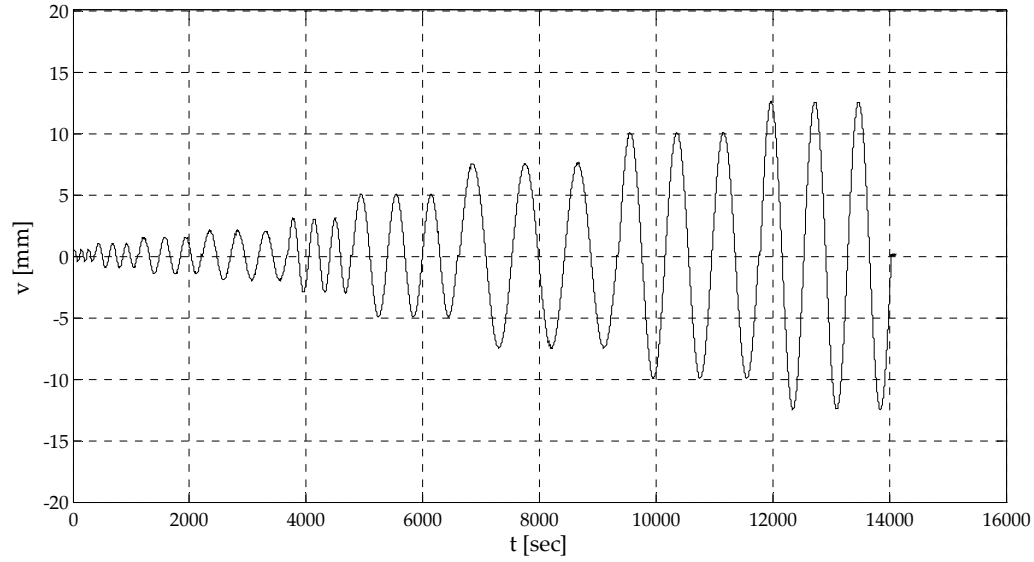

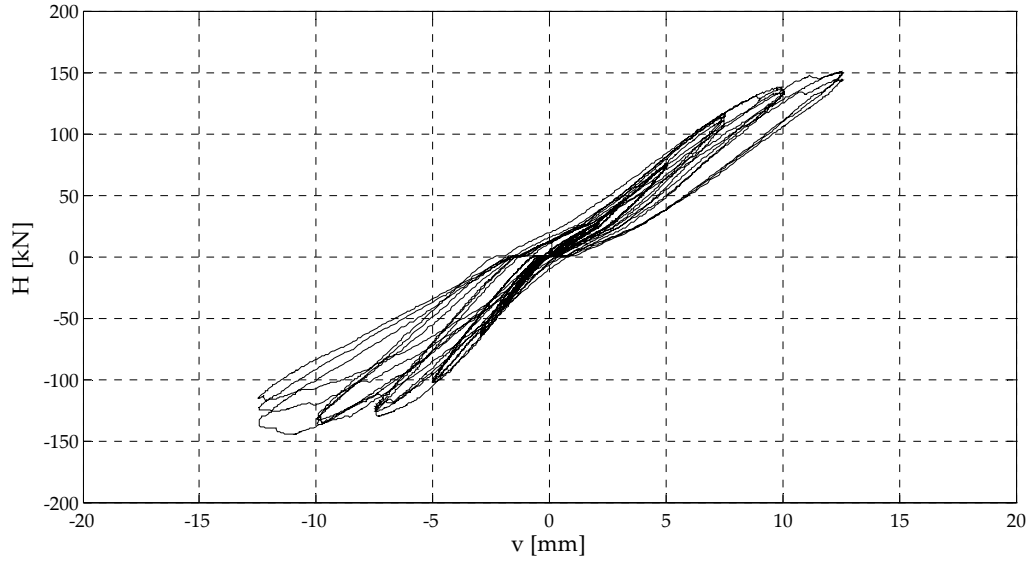

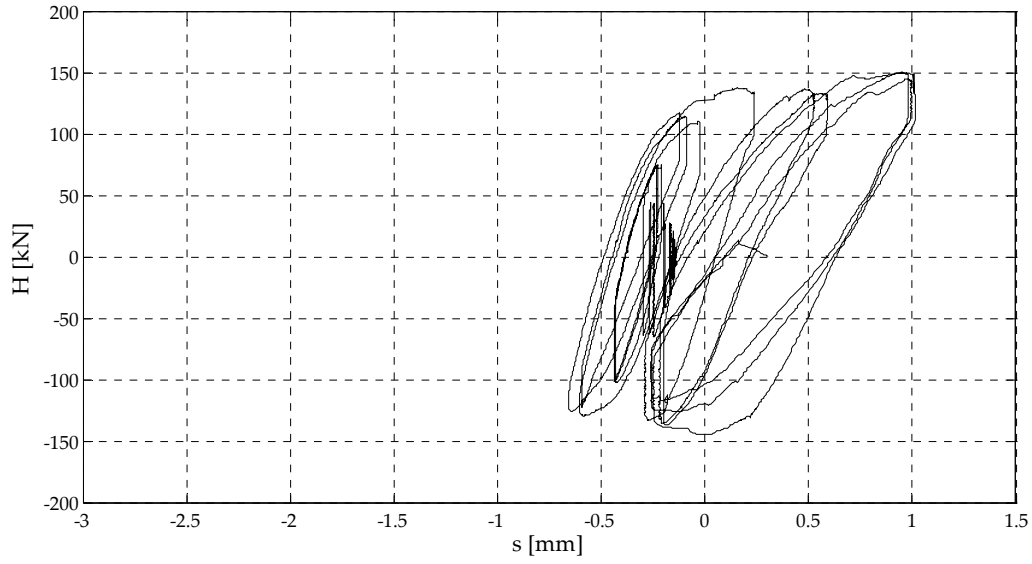

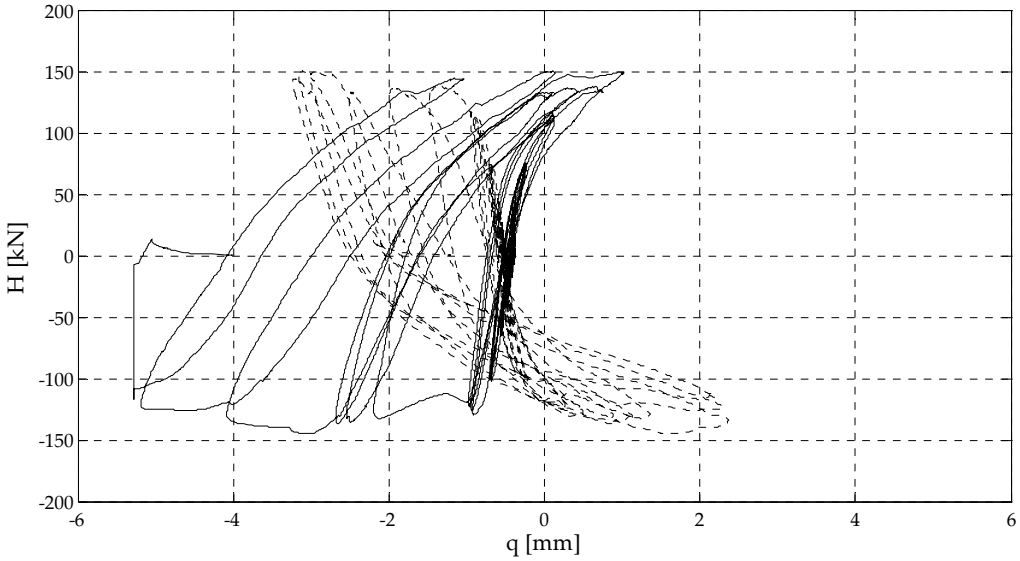
H [kN]
q [mm]

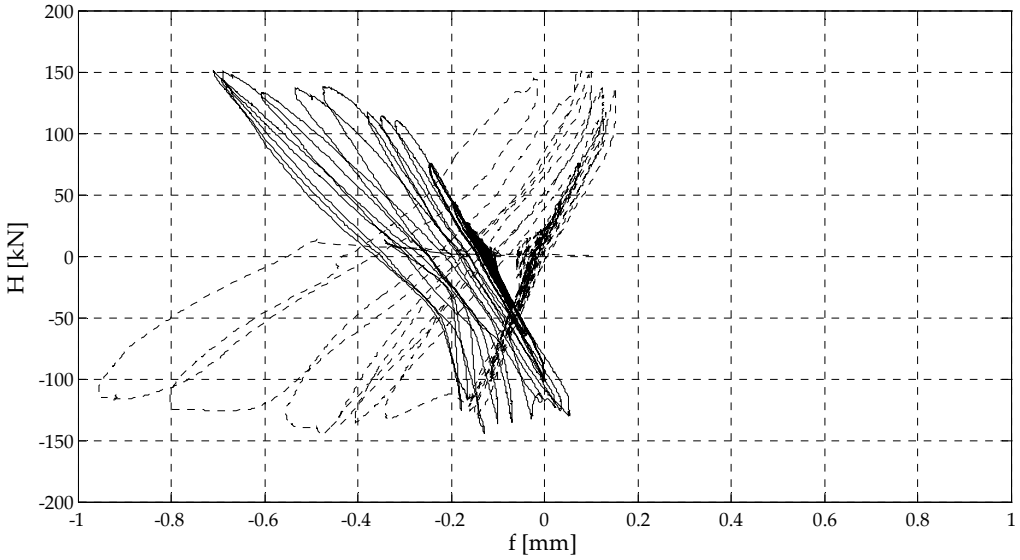
H [kN]
f [mm]

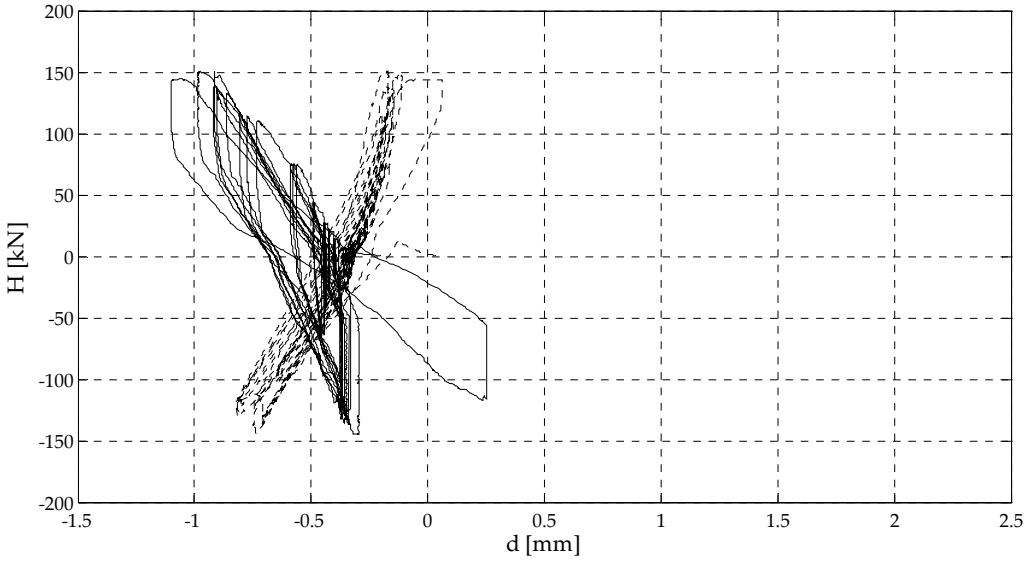
H [kN]
d [mm]

Test B2_3

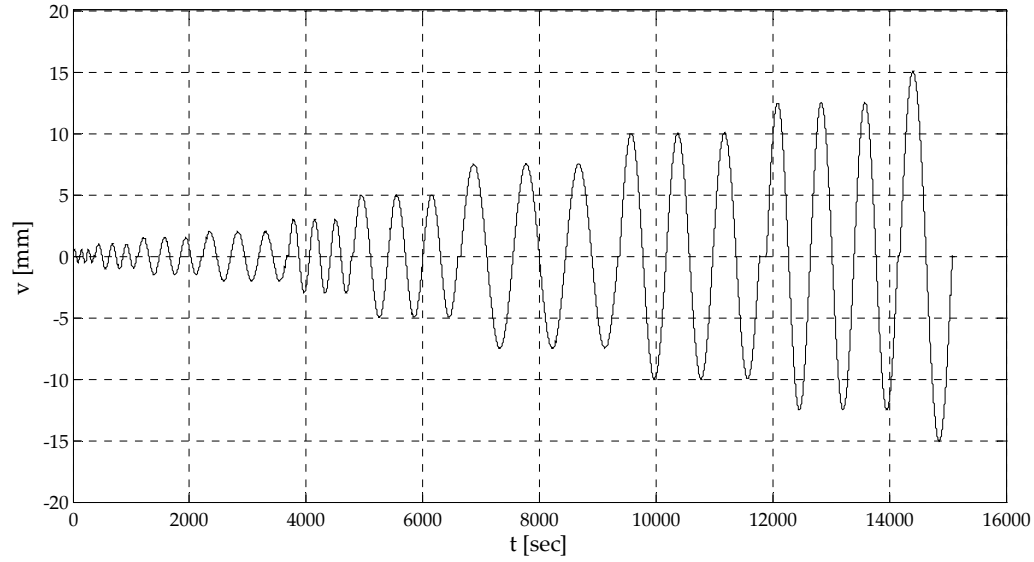

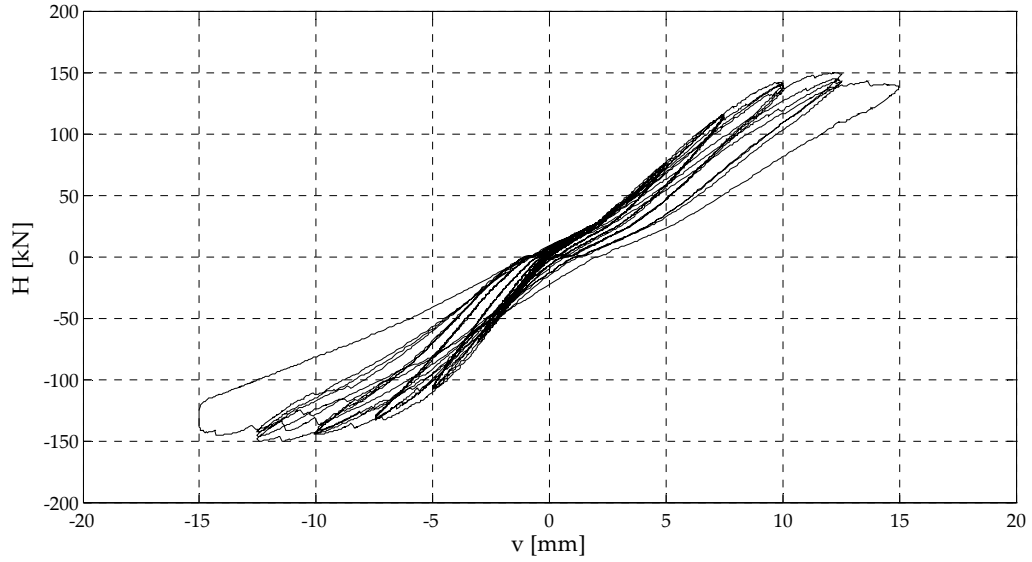

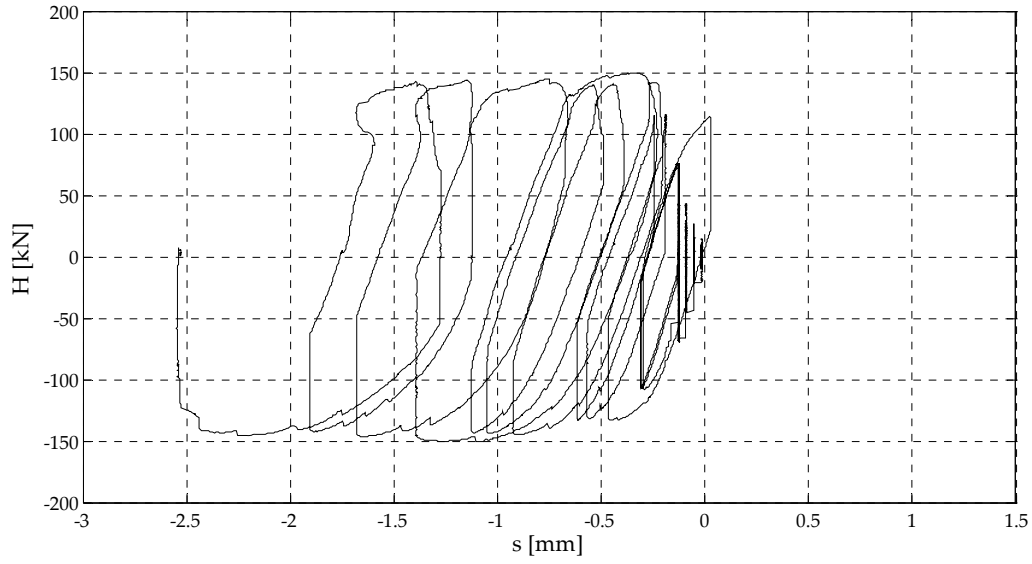

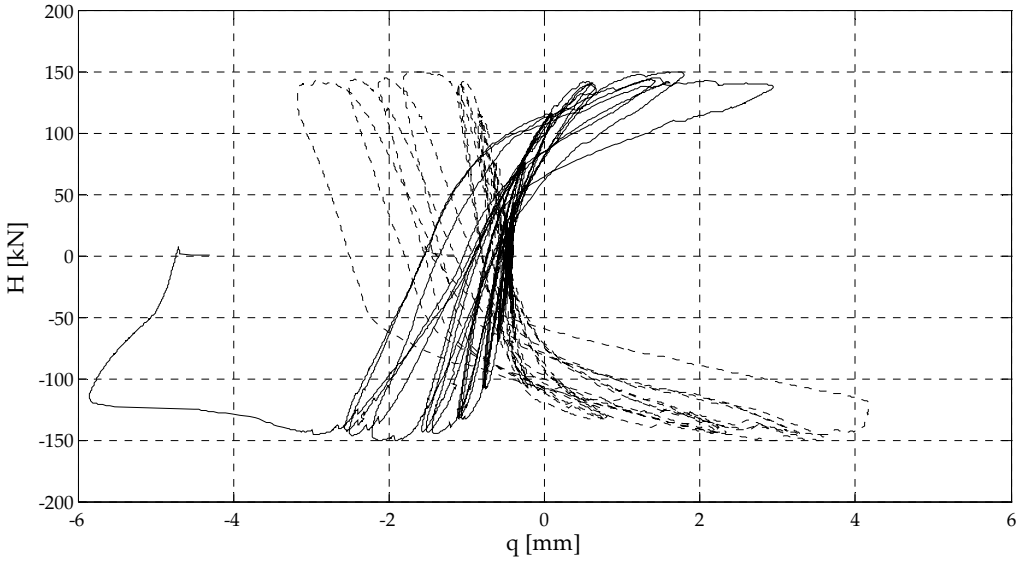
H [kN]
q [mm]

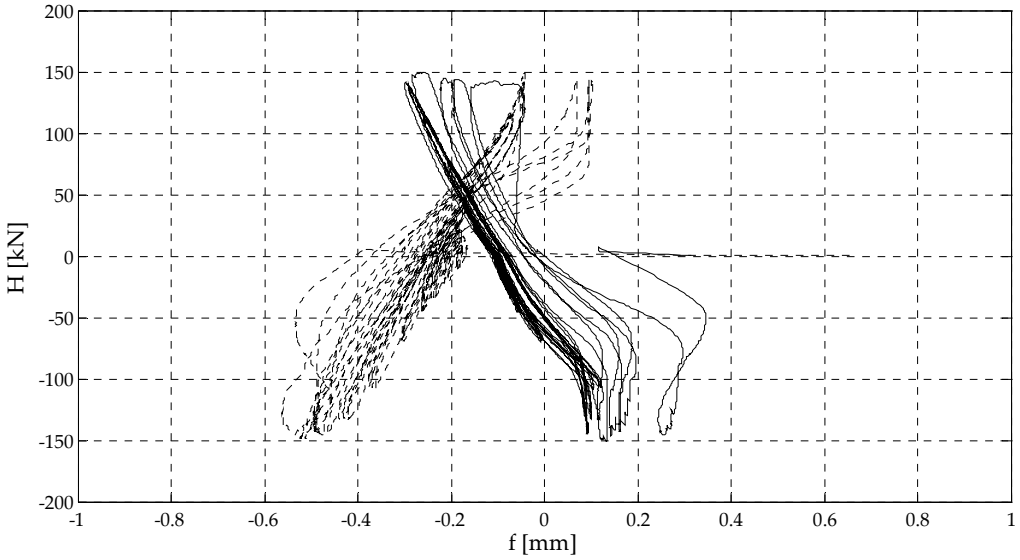
H [kN]
f [mm]

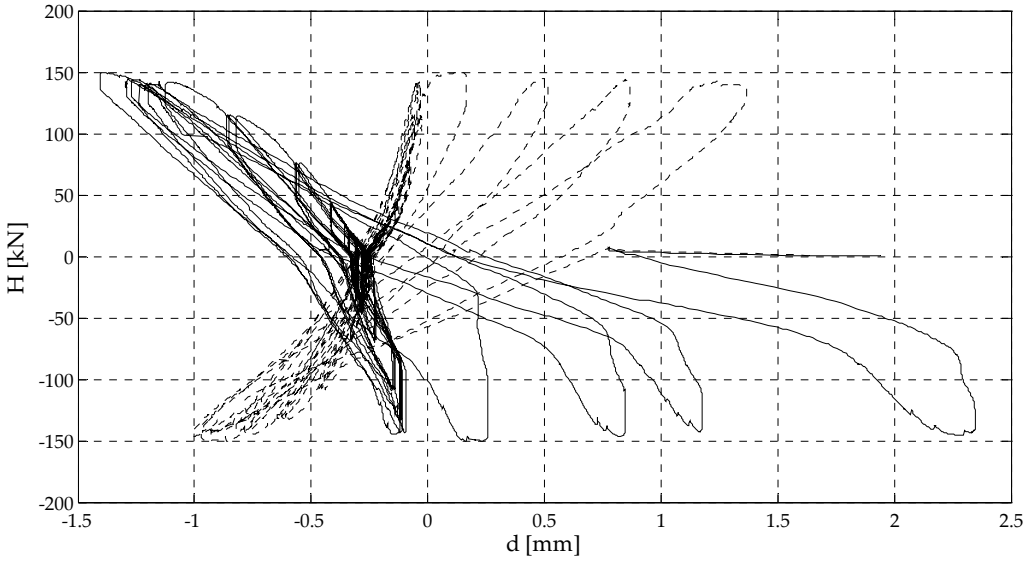
H [kN]
d [mm]

Test B3_1

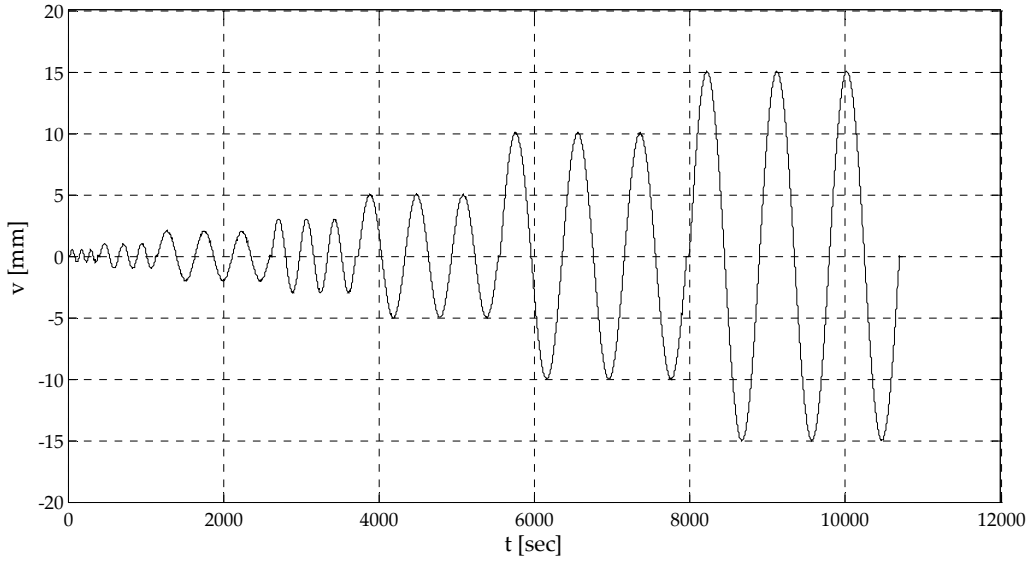
v [mm]
t [sec]
20
15
10
5
0
-5
-10
-15
-20
0
2000
4000
6000
8000
10000
12000

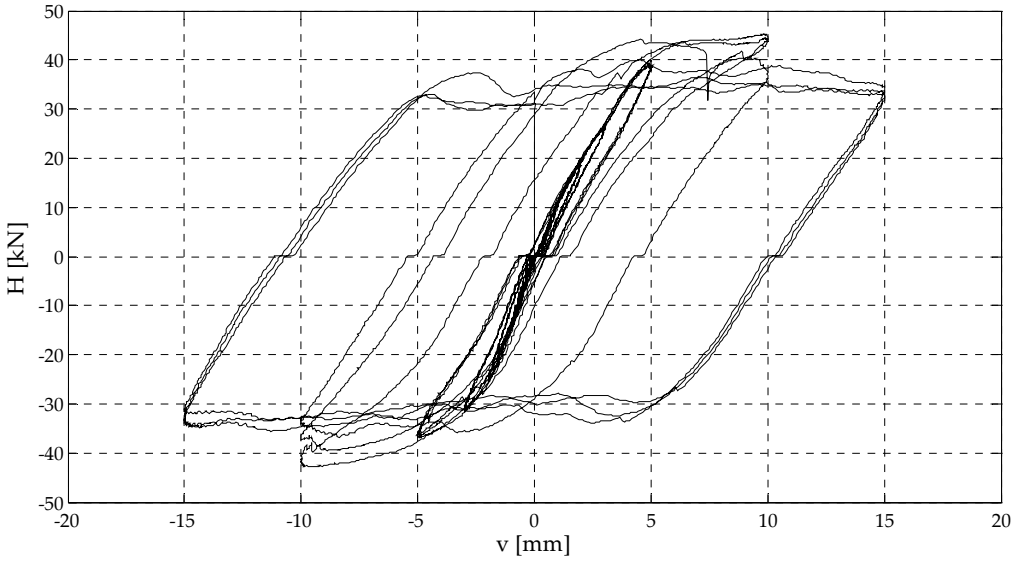
H [kN]
v [mm]
50
40
30
20
10
0
-10
-20
-30
-40
-50
-20
-15
-10
-5
0
5
10
15
20

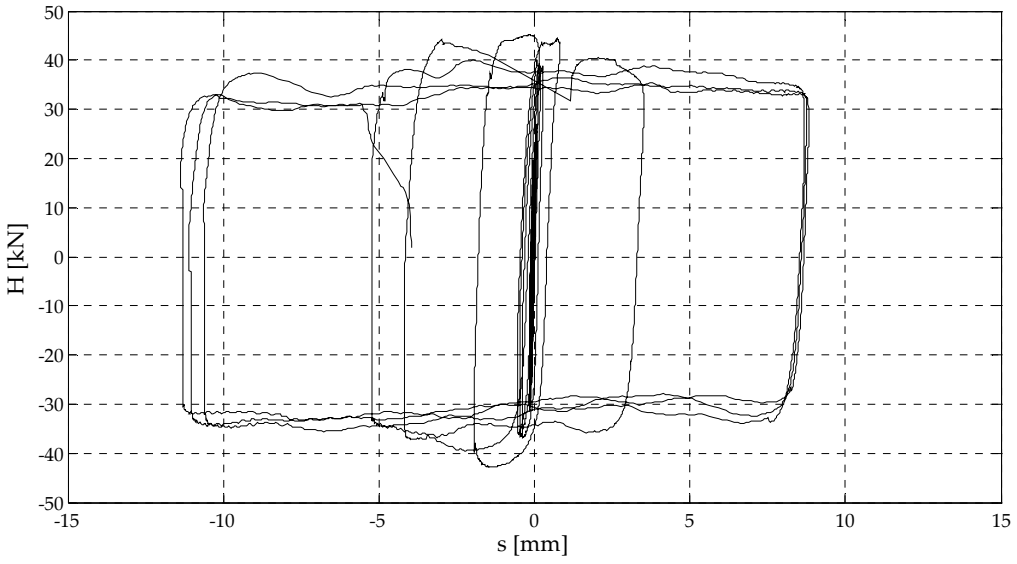
H [kN]
s [mm]
50
40
30
20
10
0
-10
-20
-30
-40
-50
-15
-10
-5
0
5
10
15

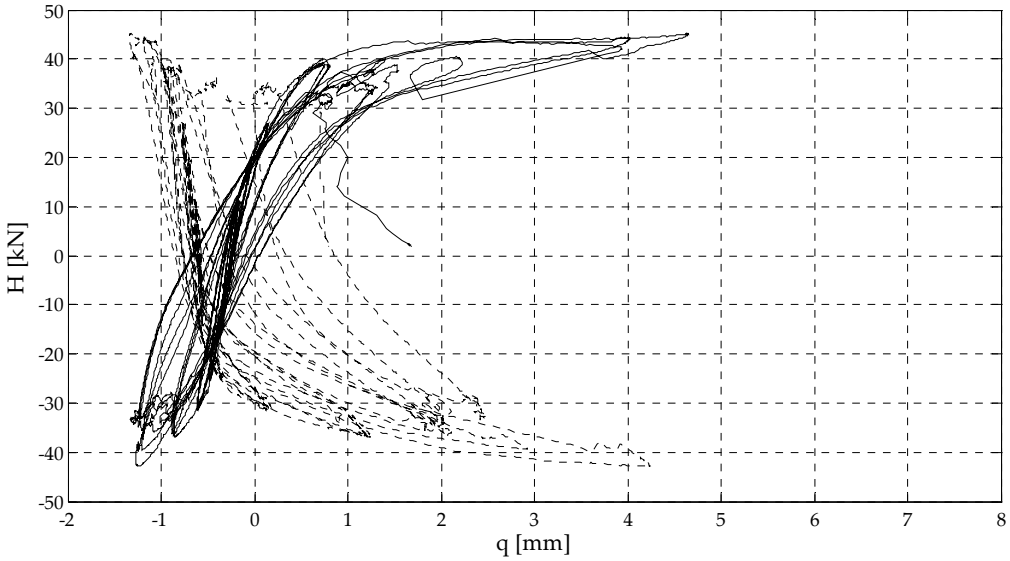
H [kN]
q [mm]

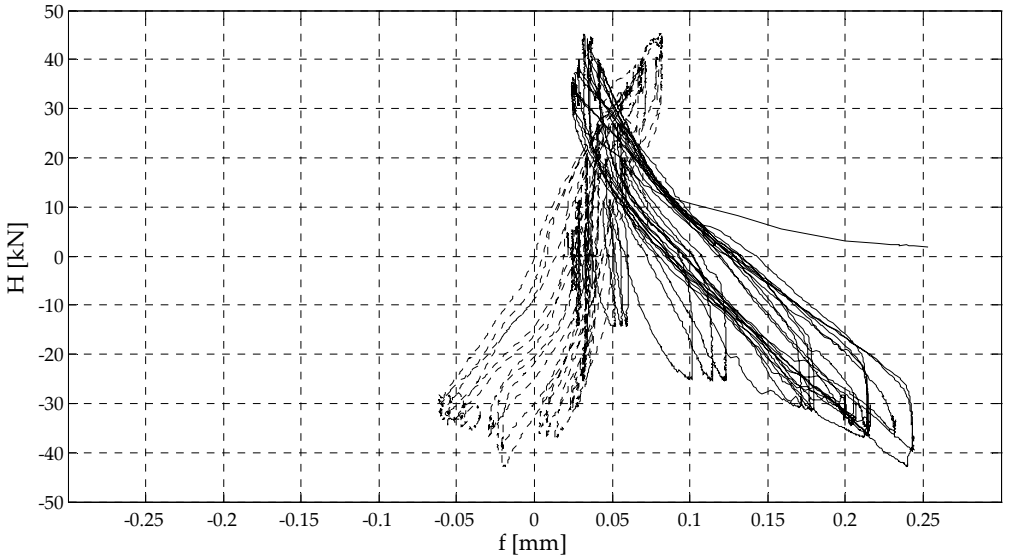
H [kN]
f [mm]

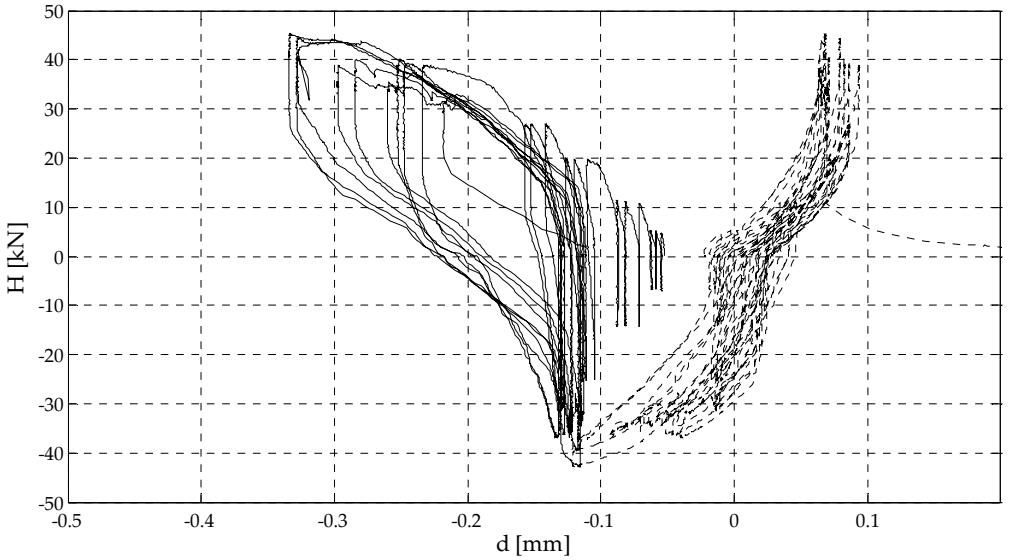
H [kN]
d [mm]

Test B3_2

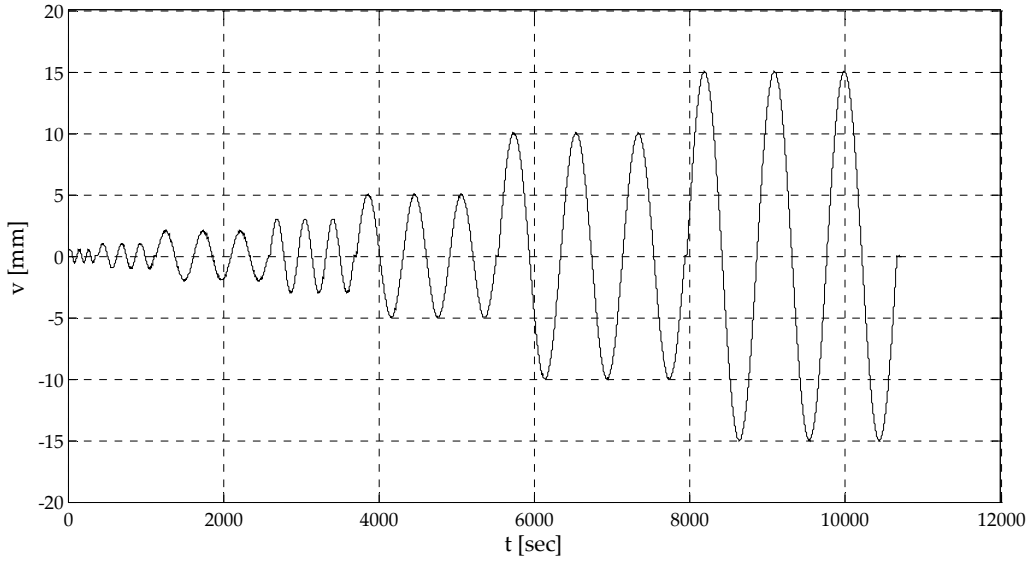
v [mm]
t [sec]
20
15
10
5
0
-5
-10
-15
-20
0
2000
4000
6000
8000
10000
12000

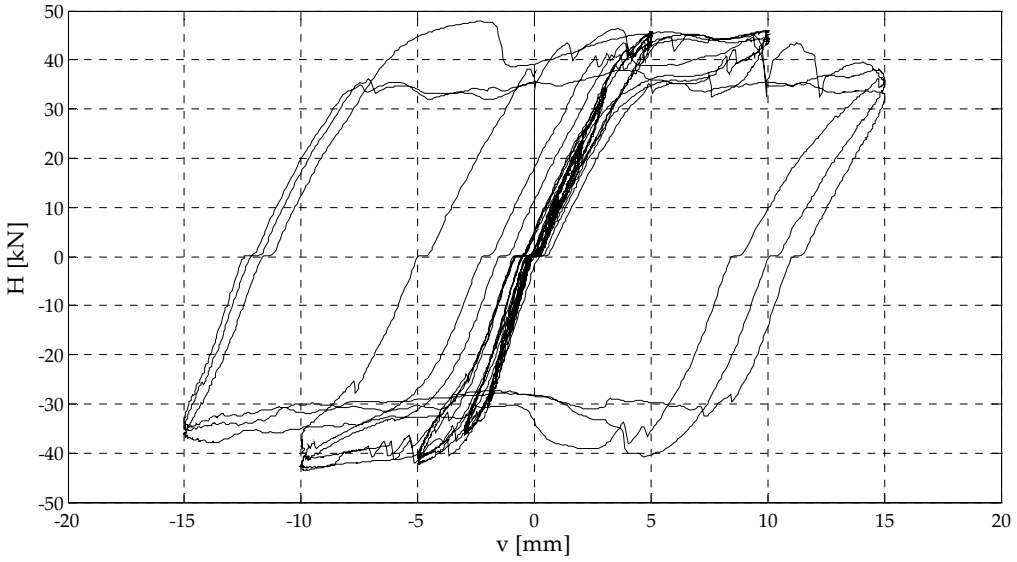
H [kN]
v [mm]
50
40
30
20
10
0
-10
-20
-30
-40
-50
-20
-15
-10
-5
0
5
10
15
20

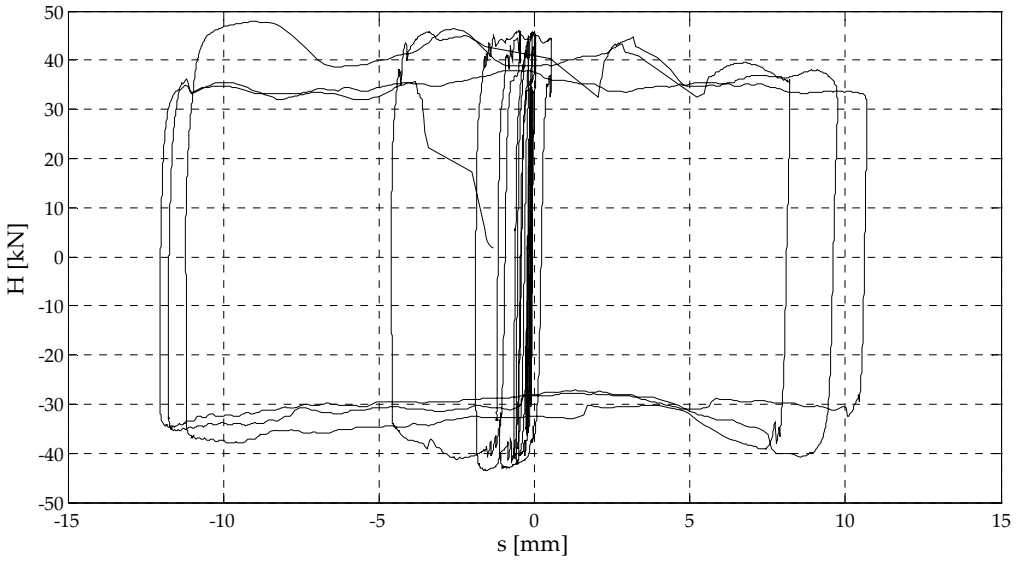
H [kN]
s [mm]
50
40
30
20
10
0
-10
-20
-30
-40
-50
-15
-10
-5
0
5
10
15

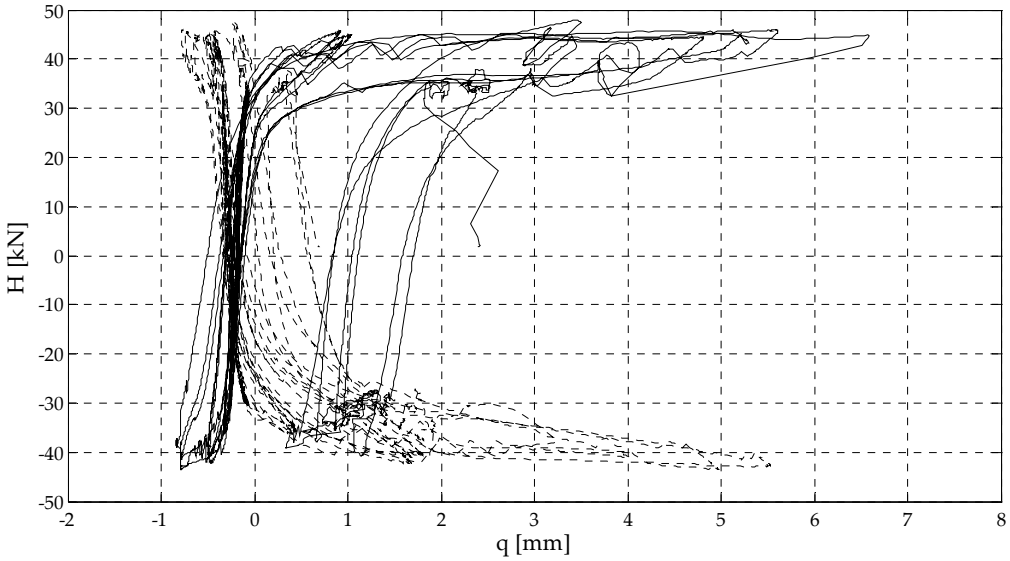
H [kN]
q [mm]

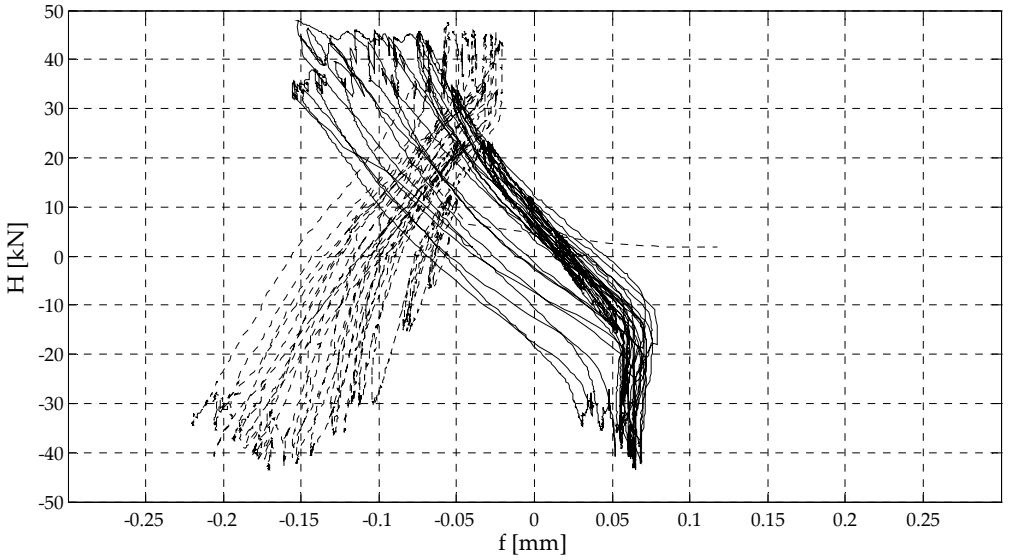
H [kN]
f [mm]

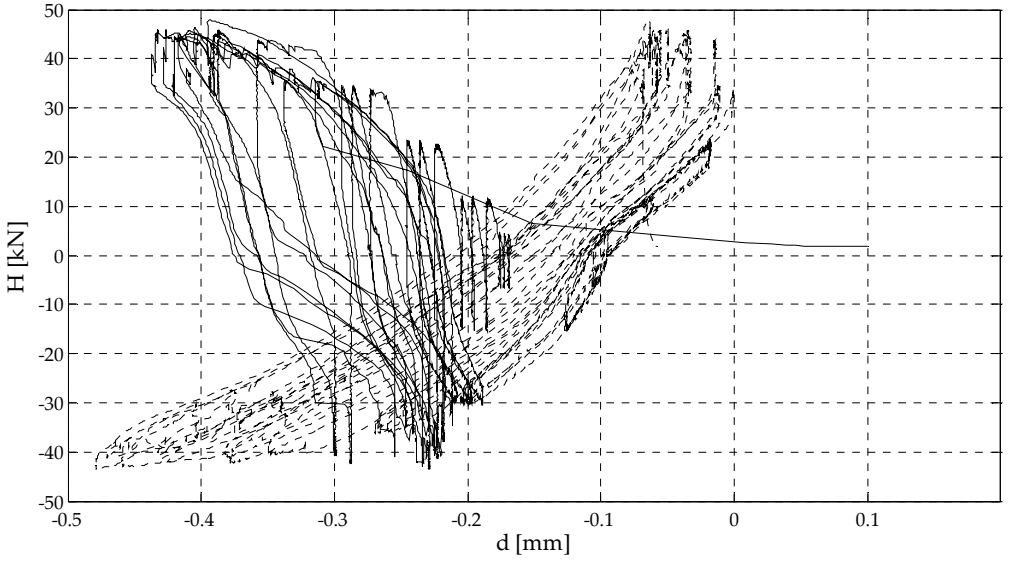
H [kN]
d [mm]

Test B3_3

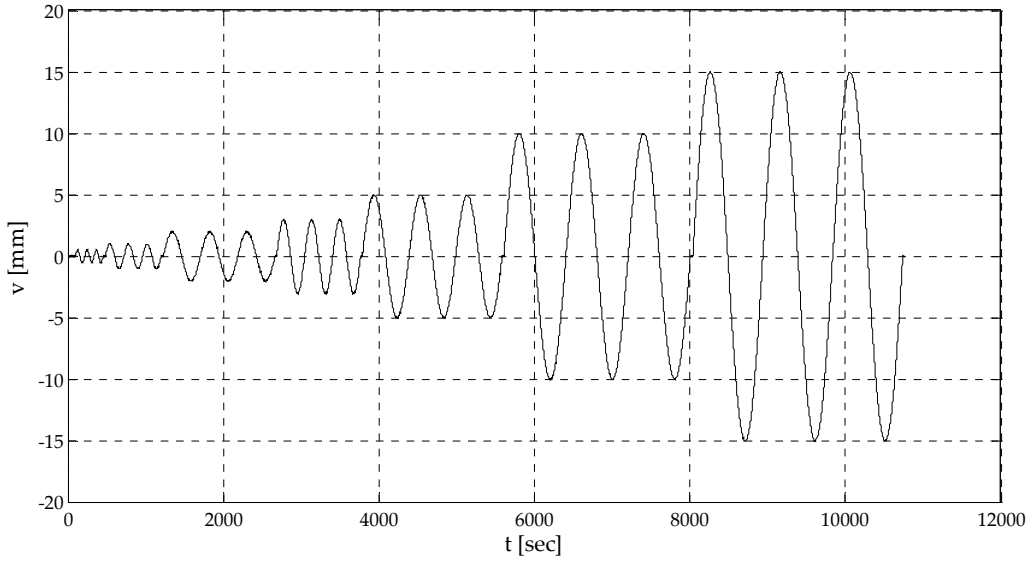
v [mm]
t [sec]
20
15
10
5
0
-5
-10
-15
-20
0
2000
4000
6000
8000
10000
12000

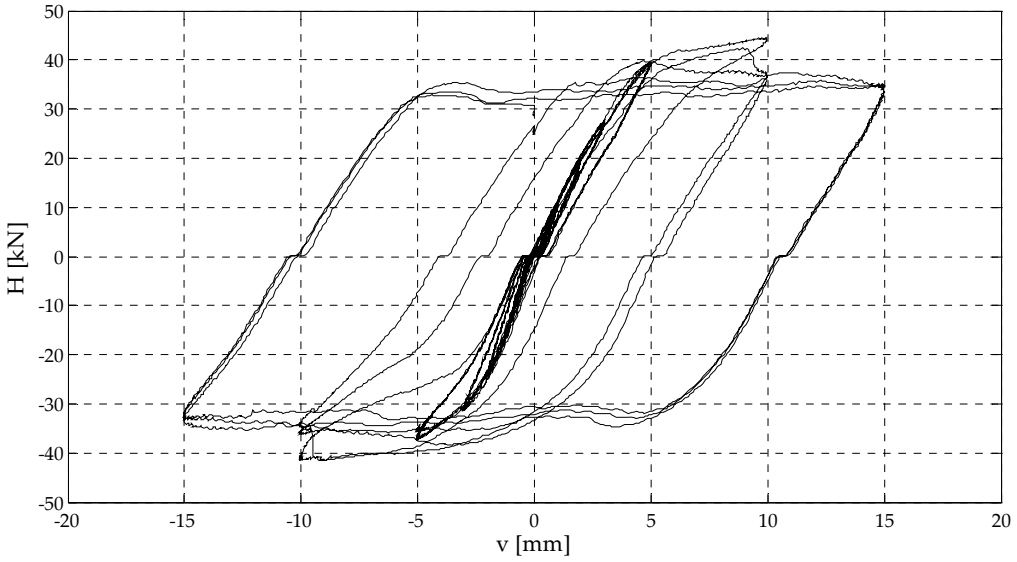
H [kN]
v [mm]
50
40
30
20
10
0
-10
-20
-30
-40
-50
-20
-15
-10
-5
0
5
10
15
20

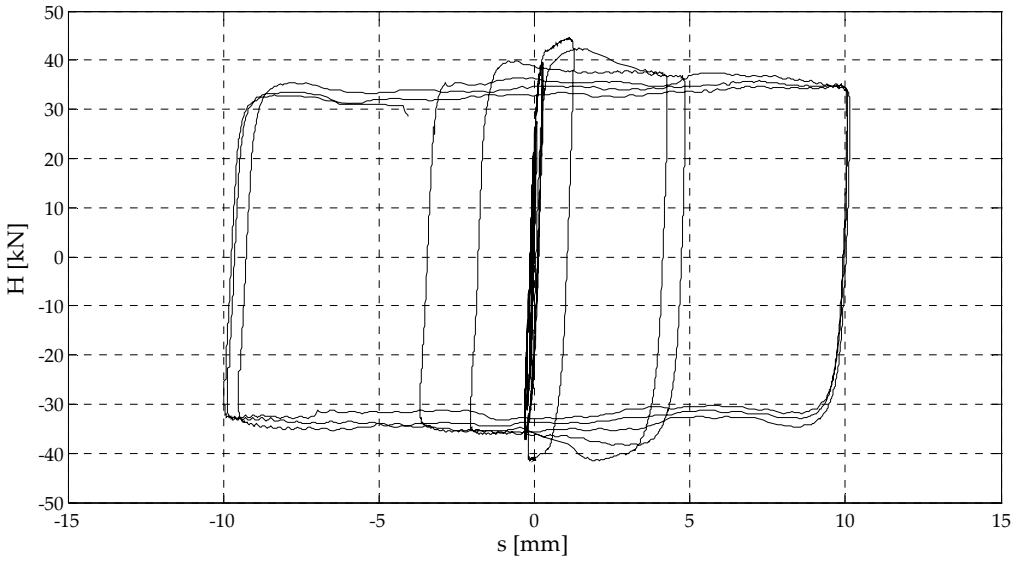
H [kN]
s [mm]
50
40
30
20
10
0
-10
-20
-30
-40
-50
-15
-10
-5
0
5
10
15

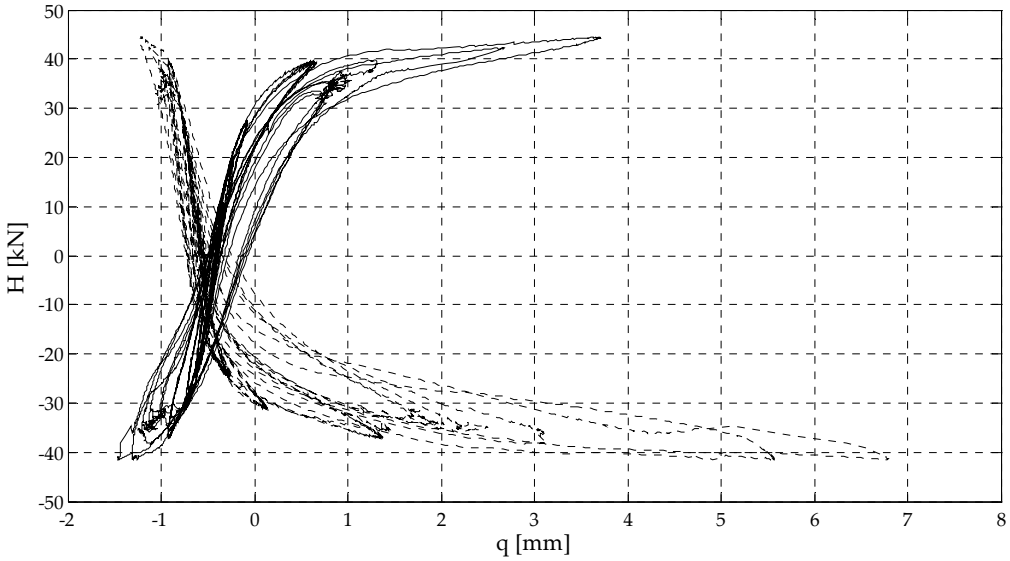
H [kN]
q [mm]

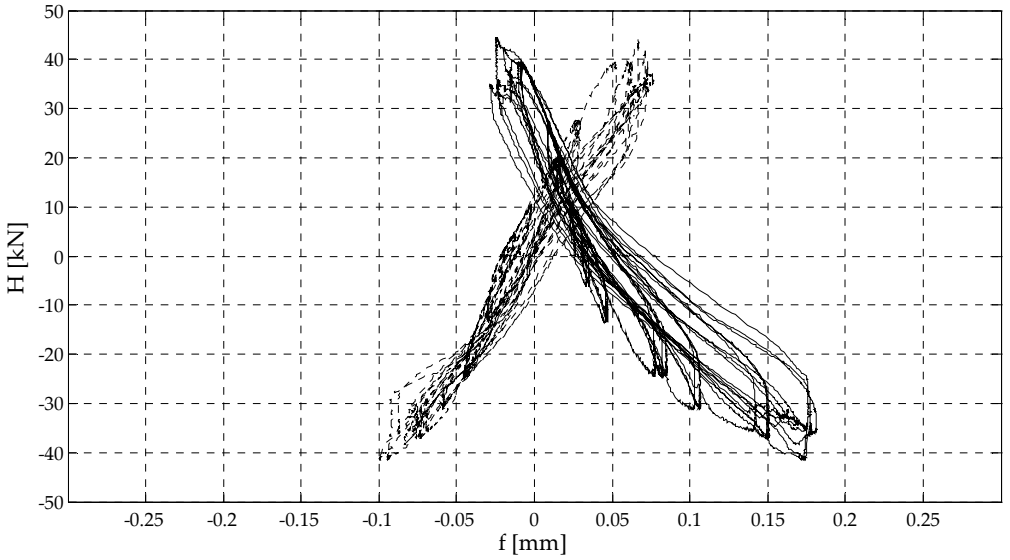
H [kN]
f [mm]

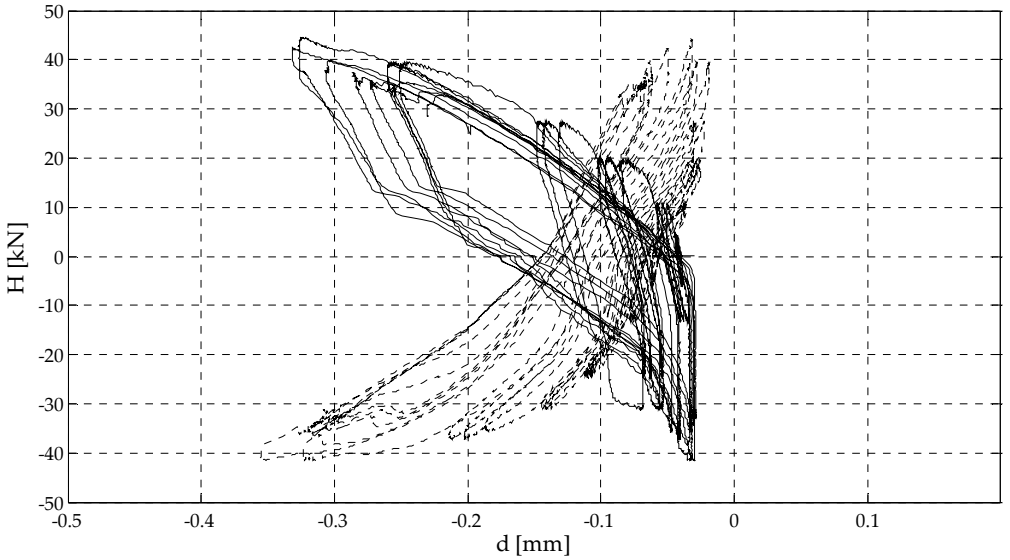
H [kN]
d [mm]

Test C1

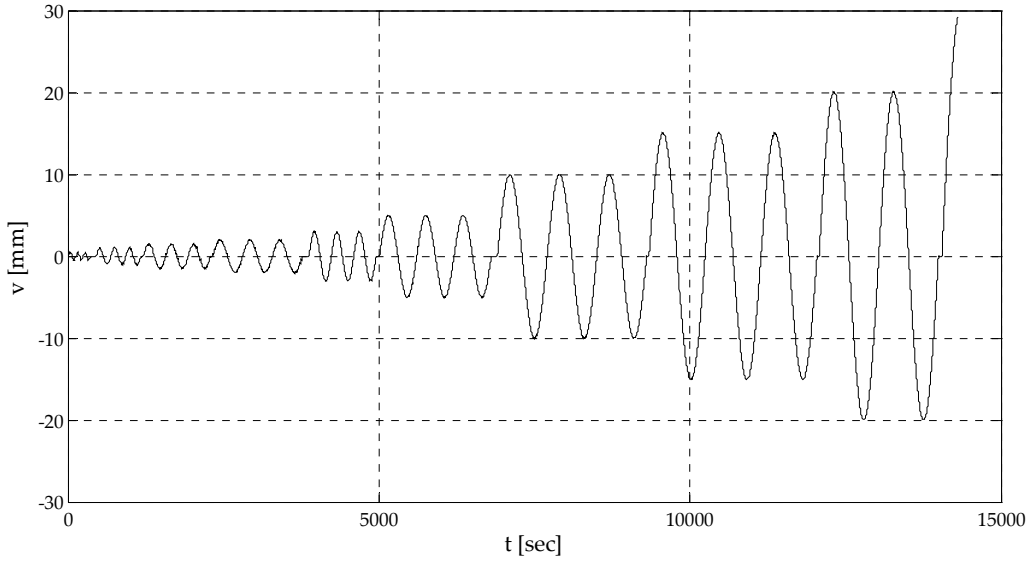

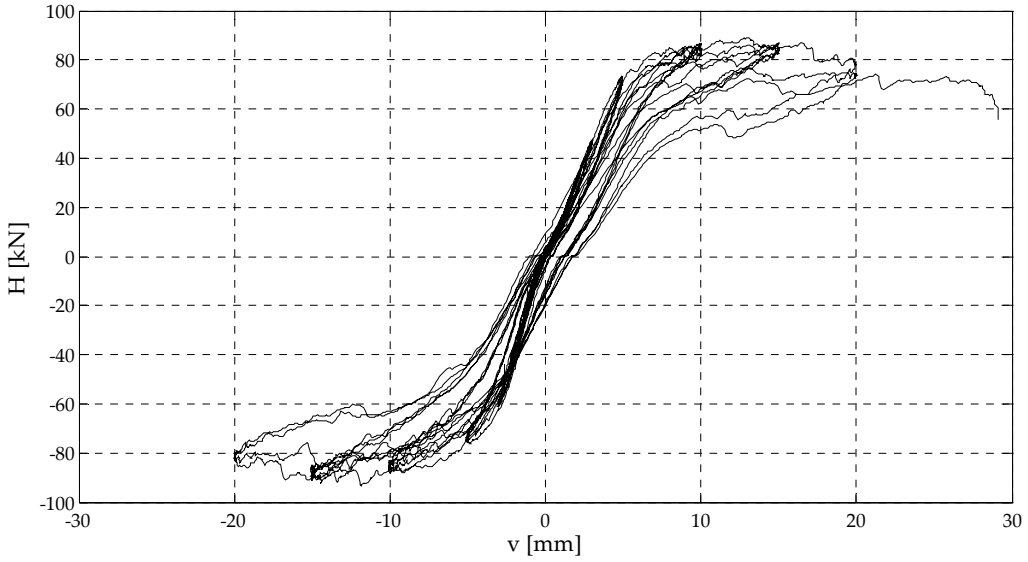

This space is intentionally left blank.

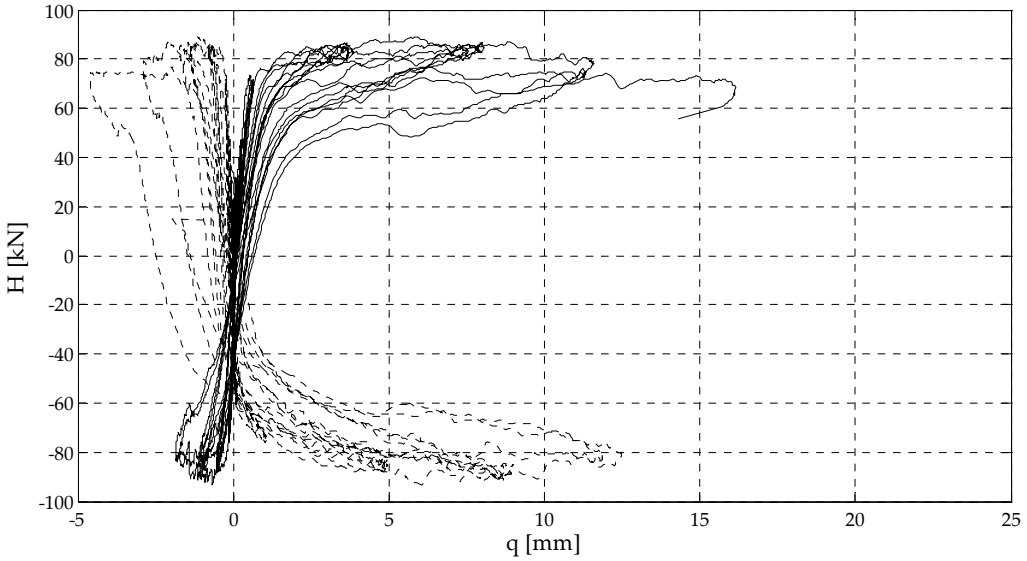
H [kN]
q [mm]
100
80
60
40
20
0
-20
-40
-60
-80
-100
-5
0
5
10
15
20
25

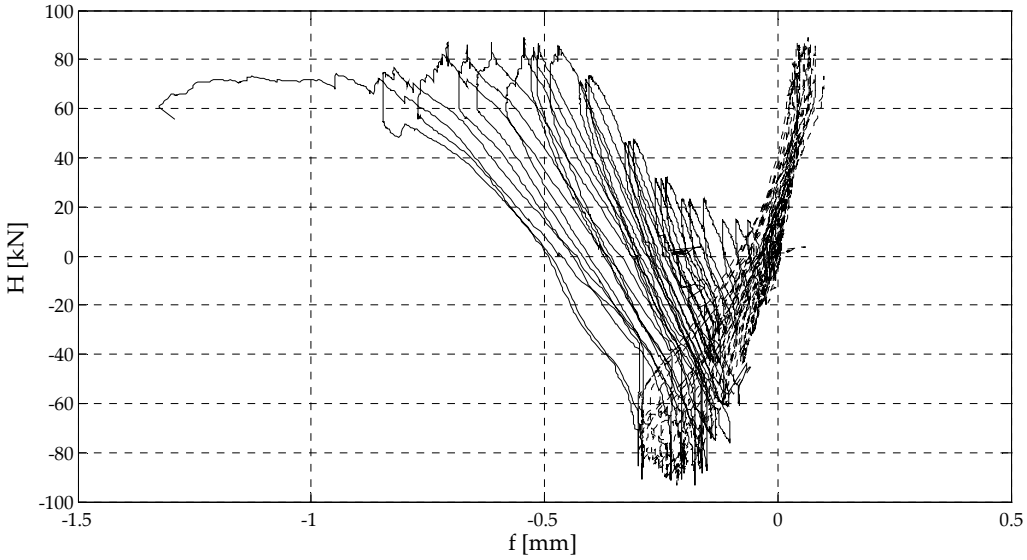
H [kN]
f [mm]
100
80
60
40
20
0
-20
-40
-60
-80
-100
-1.5
-1
-0.5
0
0.5

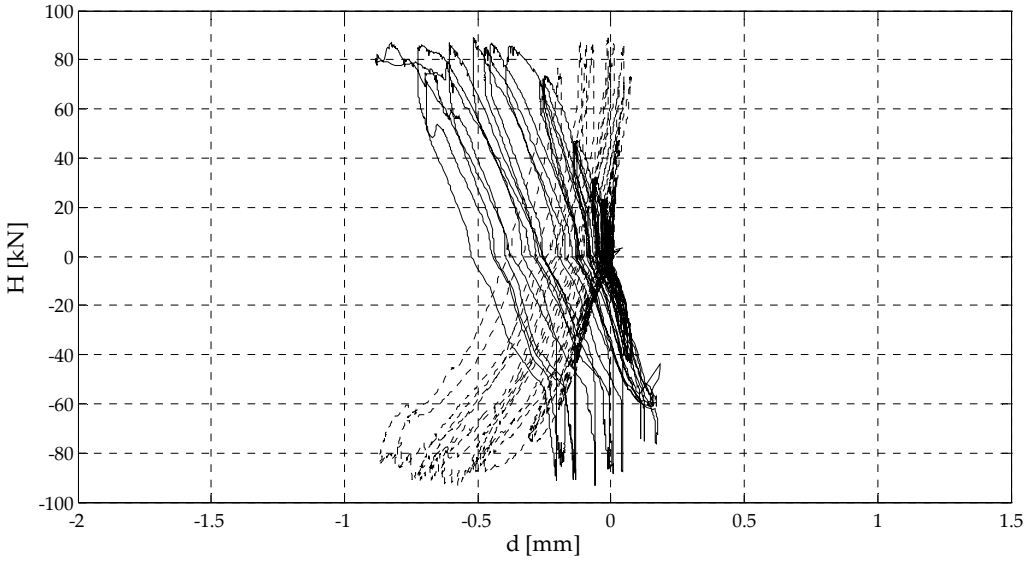
H [kN]
d [mm]
100
80
60
40
20
0
-20
-40
-60
-80
-100
-2
-1.5
-1
-0.5
0
0.5
1
1.5

Test C2

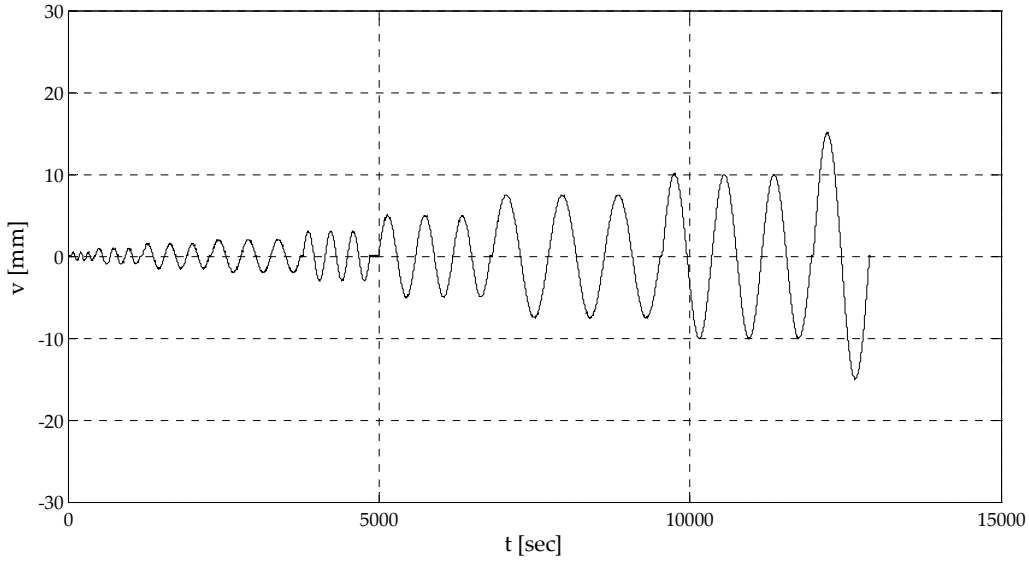
30
20
10
0
-10
-20
-30
v [mm]
0
5000
10000
15000
t [sec]

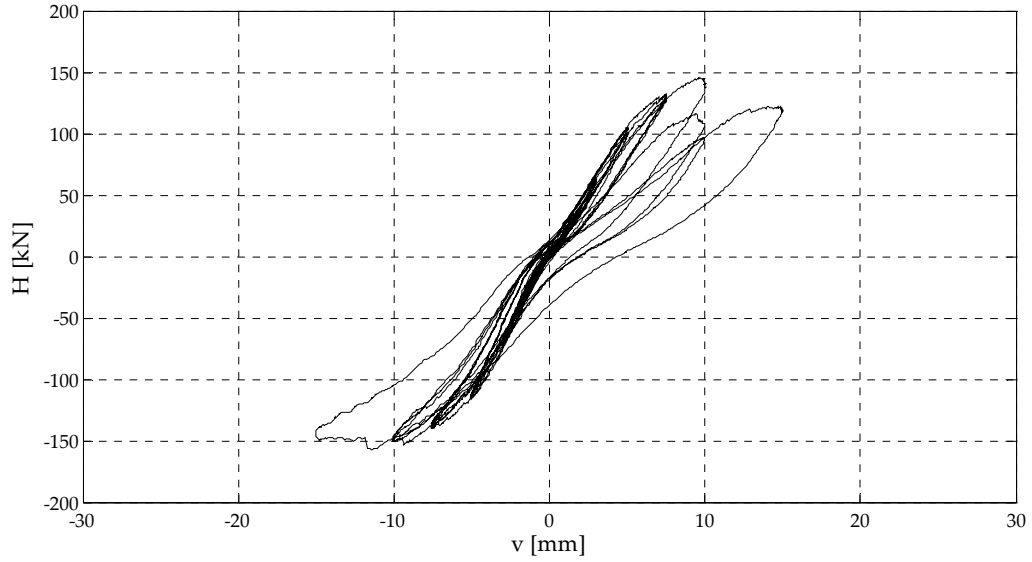
200
150
100
50
0
-50
-100
-150
-200
H [kN]
-30
-20
-10
0
10
20
30
v [mm]

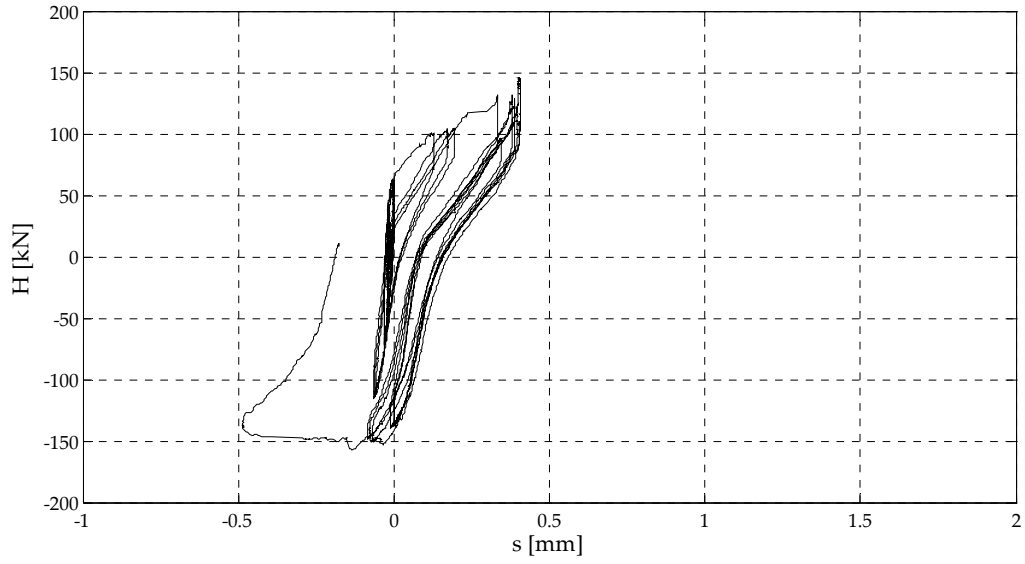
200
150
100
50
0
-50
-100
-150
-200
H [kN]
-1
-0.5
0
0.5
1
1.5
2
s [mm]

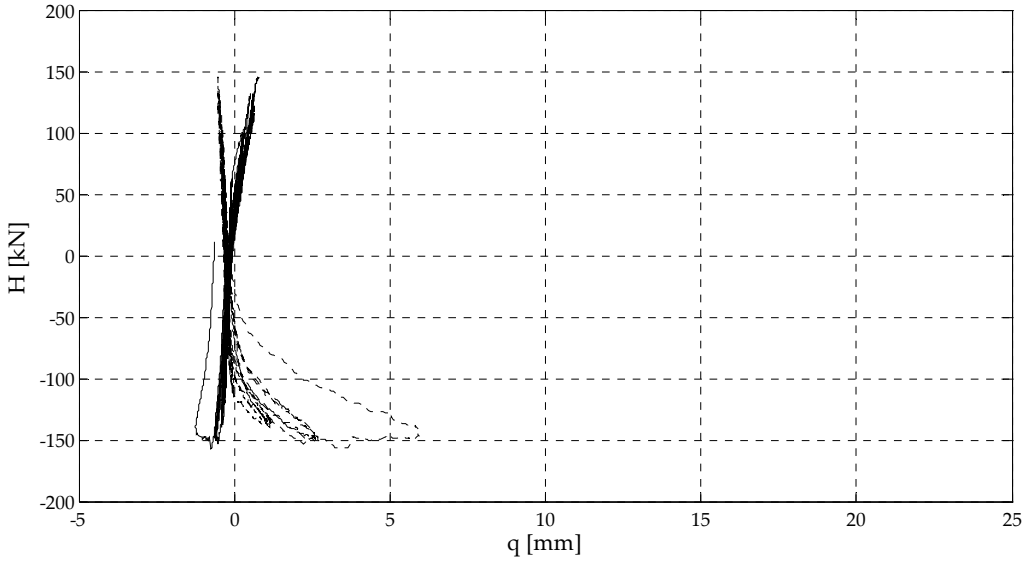
H [kN]
q [mm]

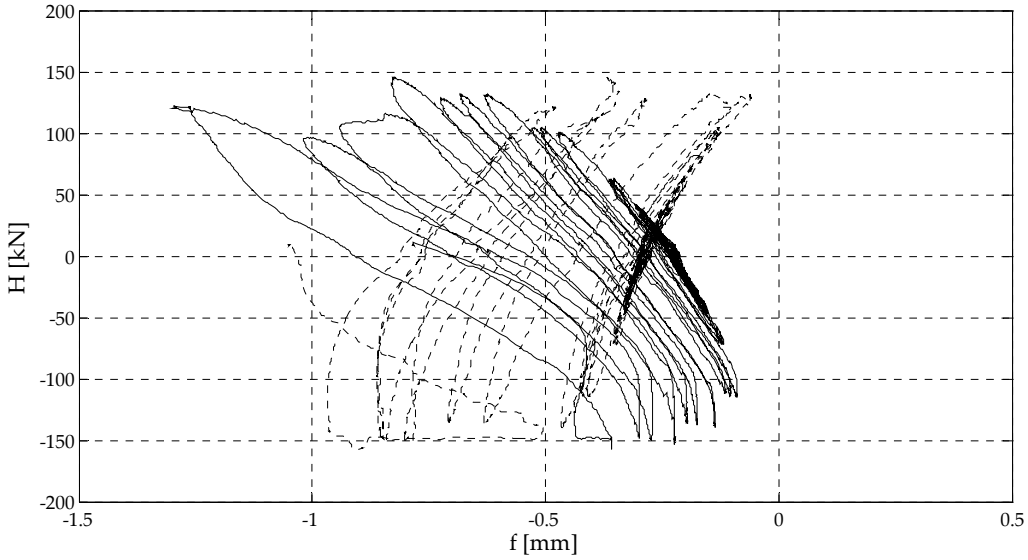
H [kN]
f [mm]

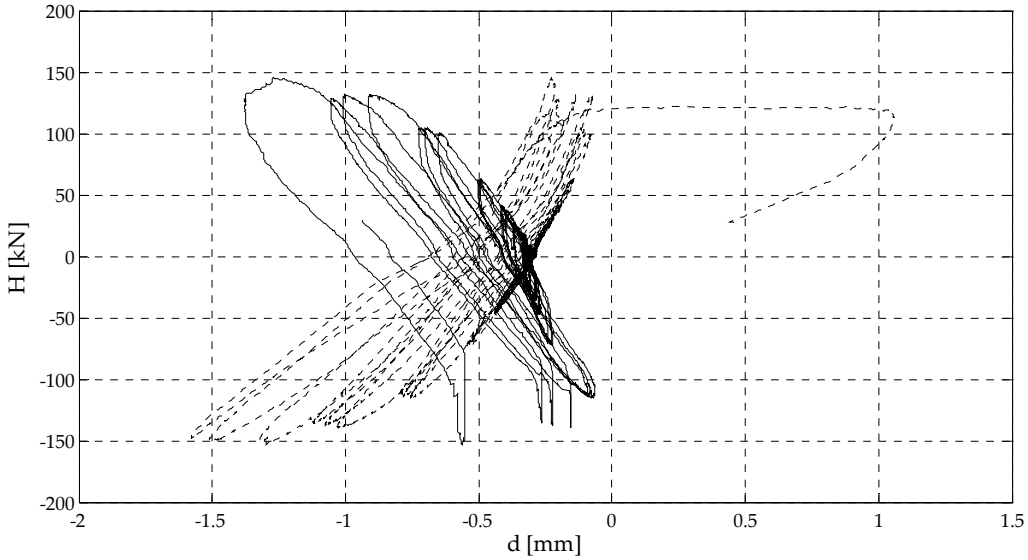
H [kN]
d [mm]

Test C3

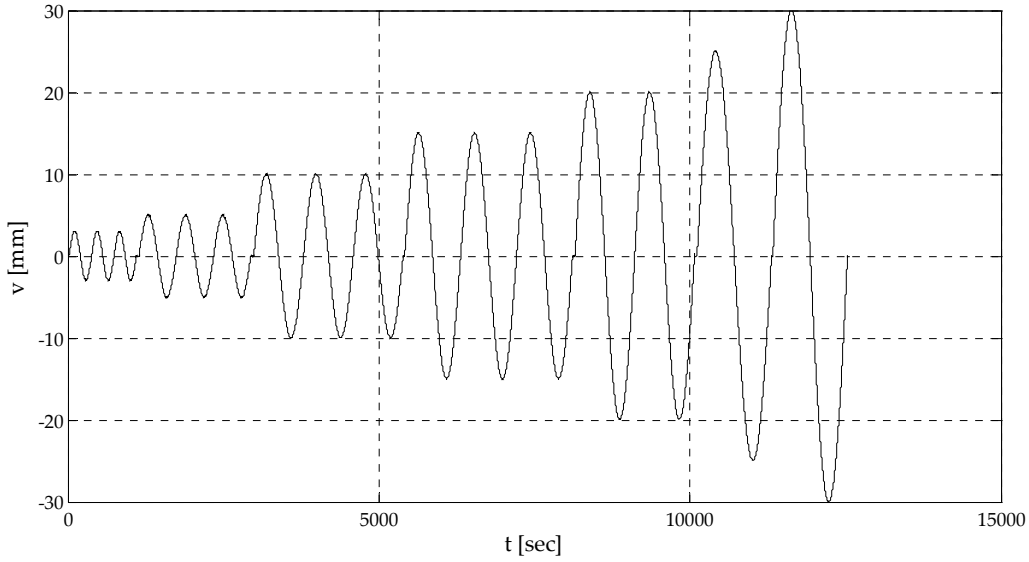
30
20
10
0
-10
-20
-30
v [mm]
0
5000
10000
15000
t [sec]

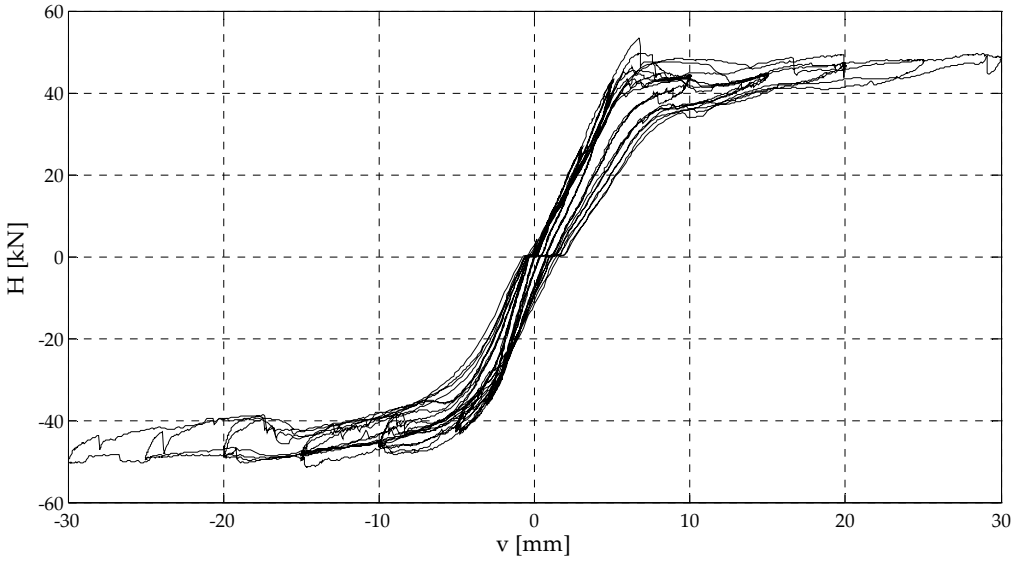
60
40
20
0
-20
-40
-60
H [kN]
-30
-20
-10
0
10
20
30
v [mm]

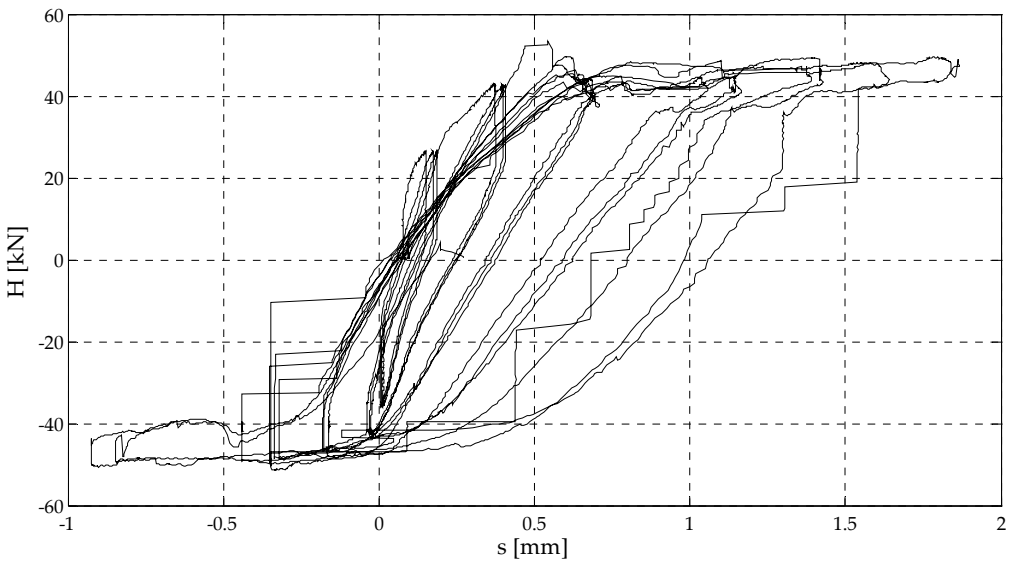
60
40
20
0
-20
-40
-60
H [kN]
-1
-0.5
0
0.5
1
1.5
2
s [mm]

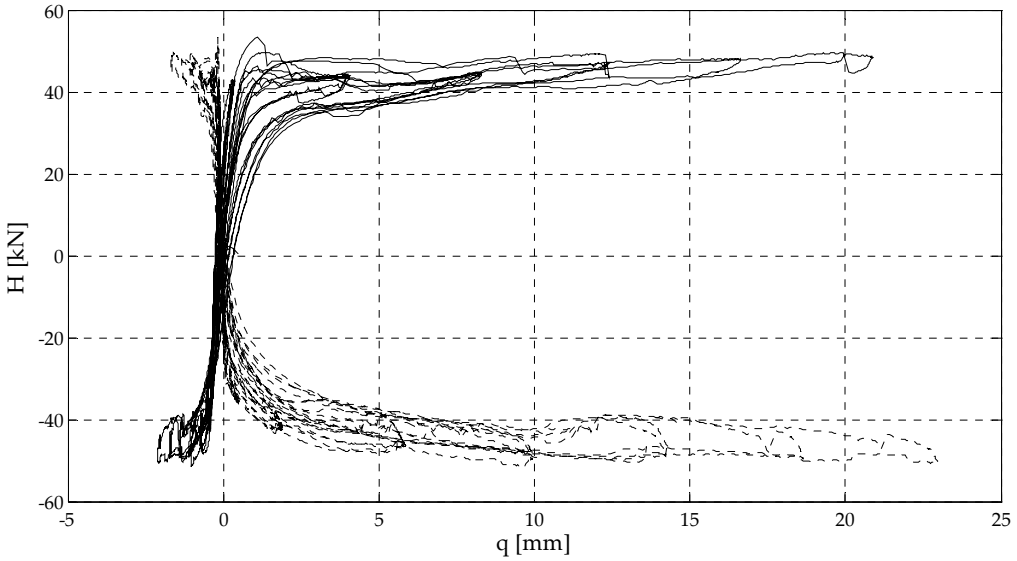
H [kN]
q [mm]

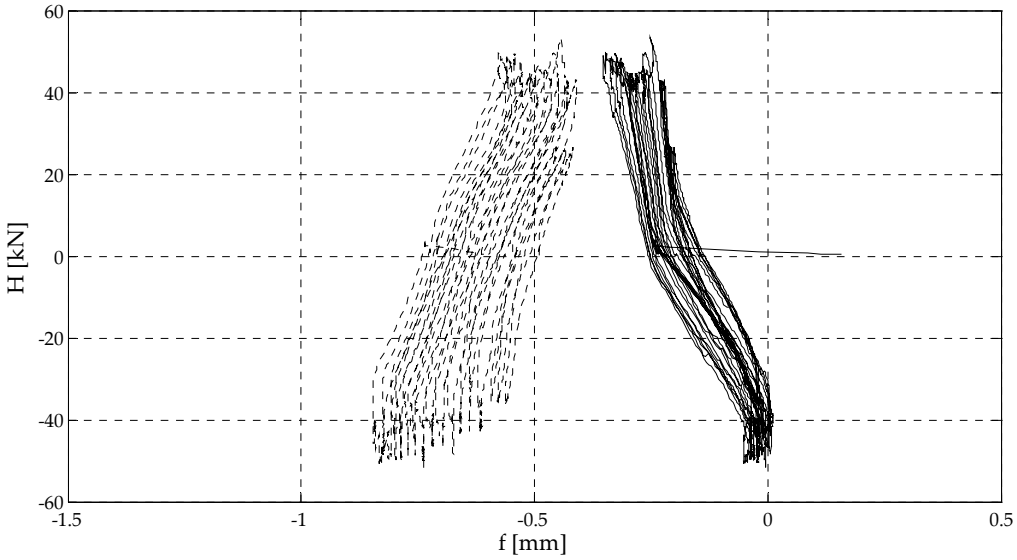
H [kN]
f [mm]

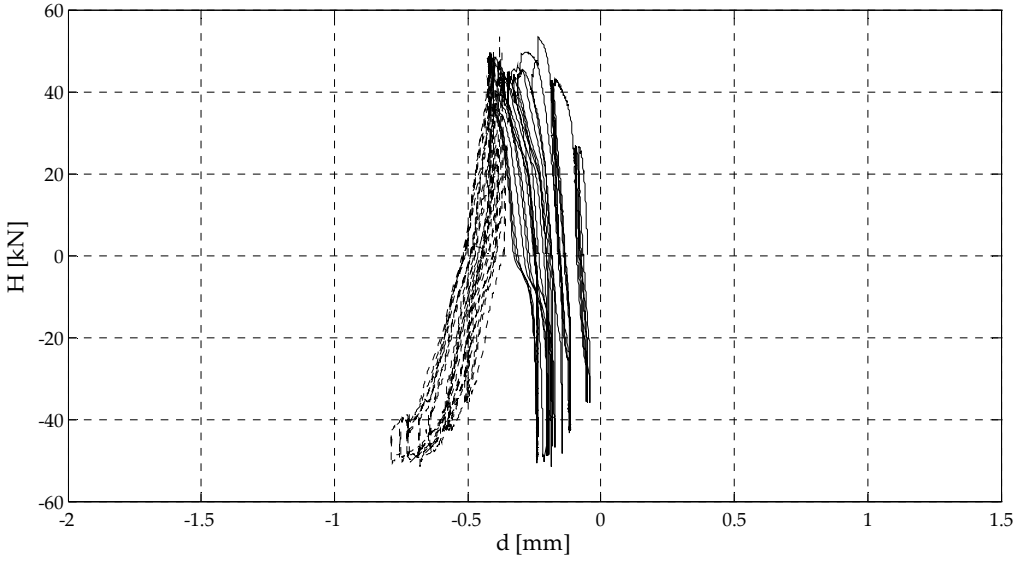
H [kN]
d [mm]

Appendix C: Crack patterns

Wallette A1_1

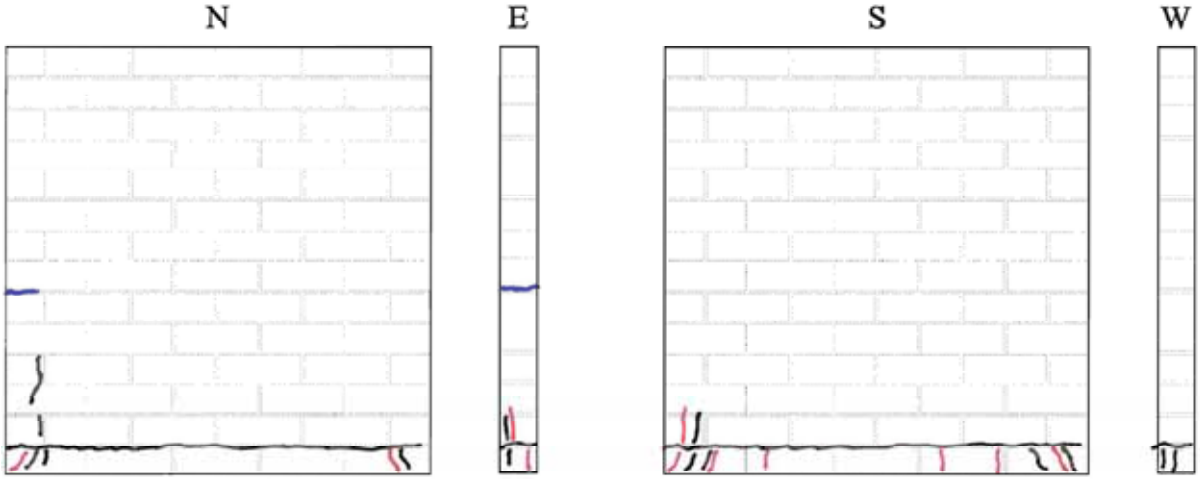

Wallette A1_2

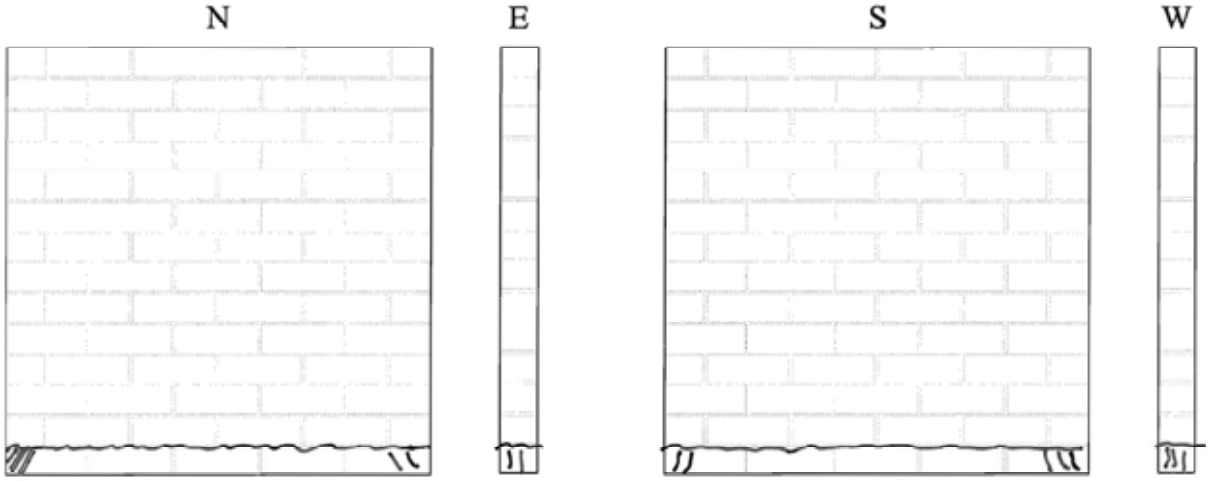

Wallette A1_3

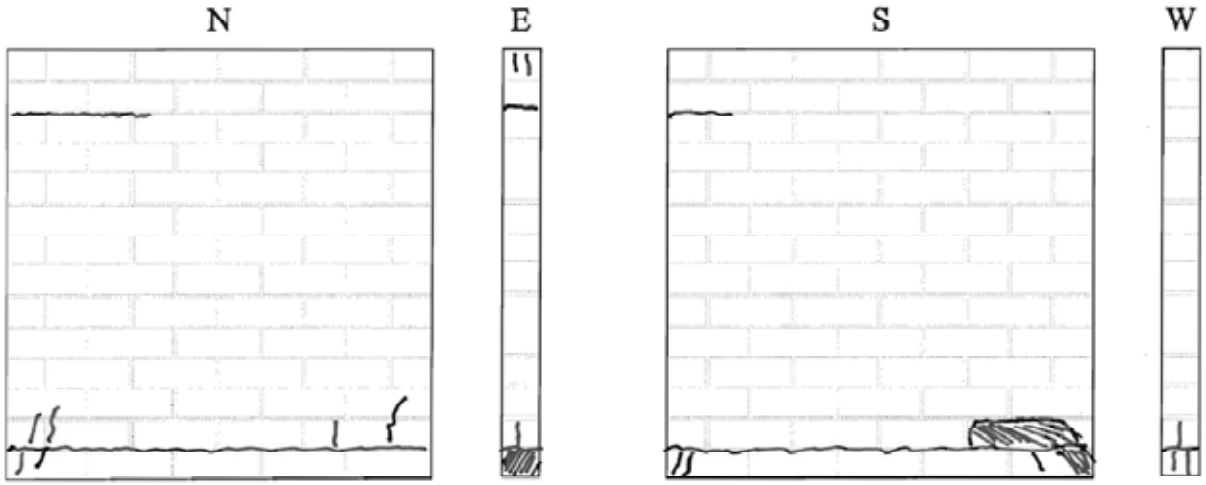

Wallette A2_1

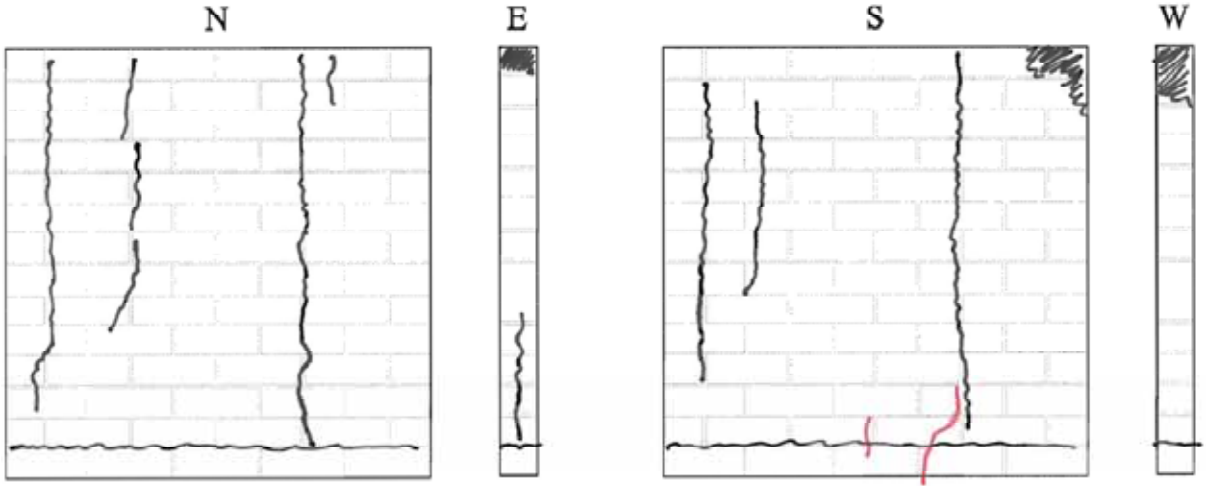

Wallette A2_2

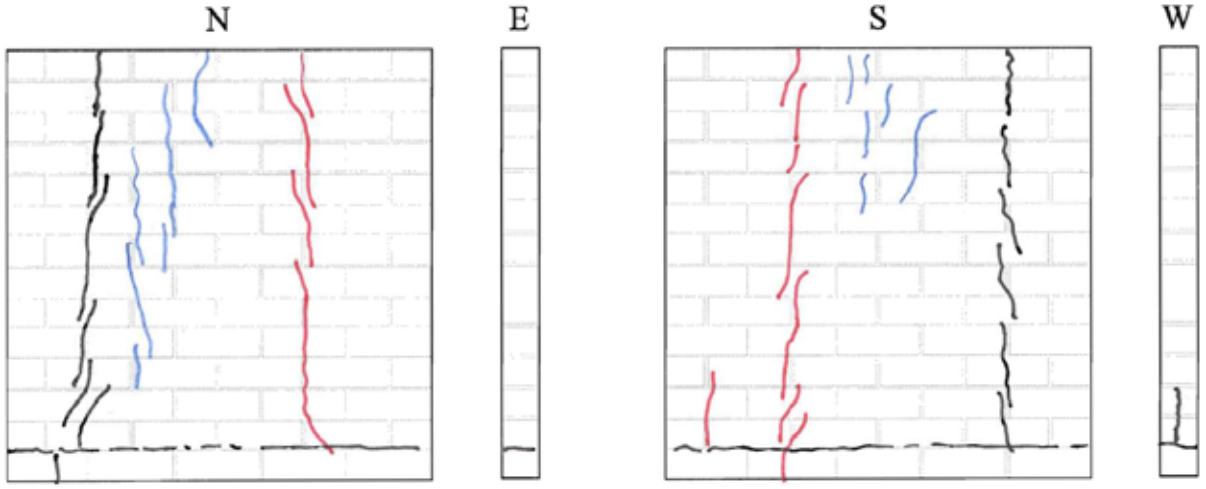

Wallette A2_3

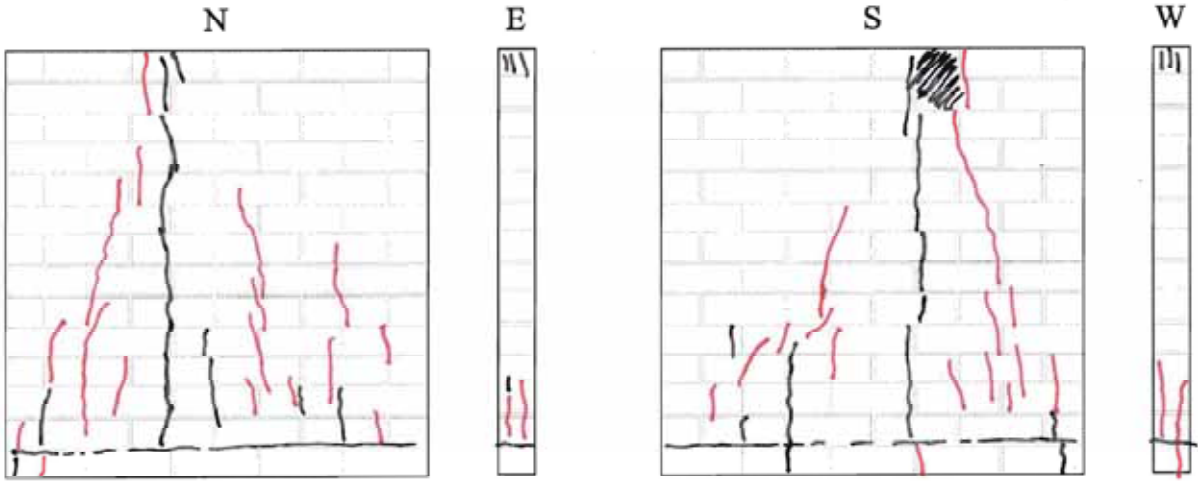

Wallette A3_1

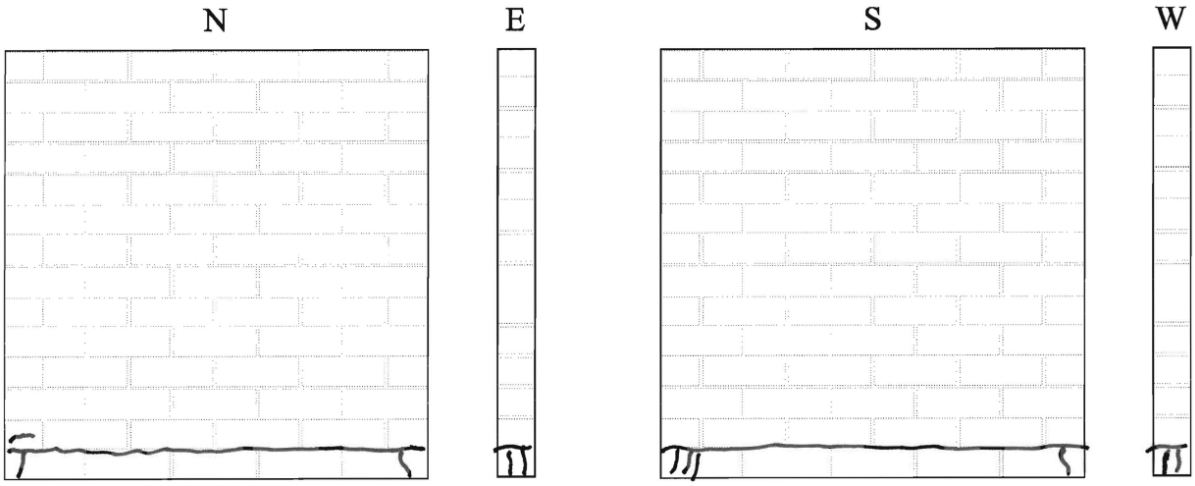

Wallette A3_2

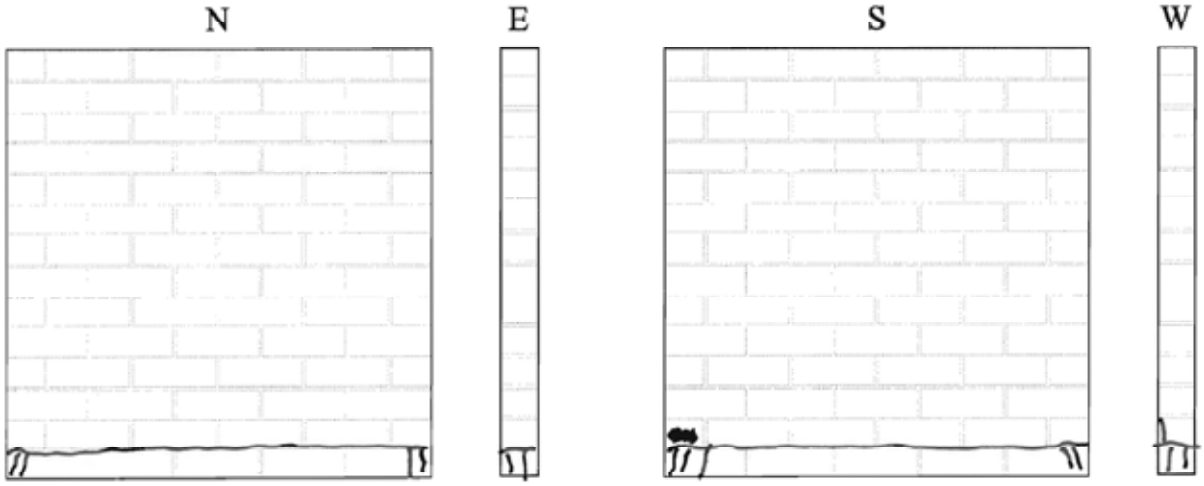

Wallette A3_3

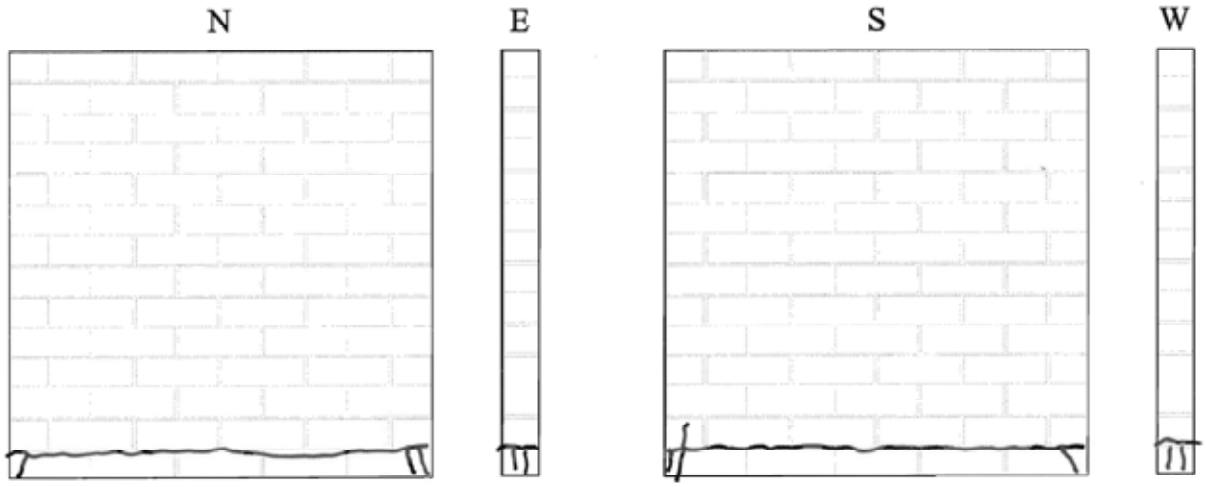

Wallette B1_1

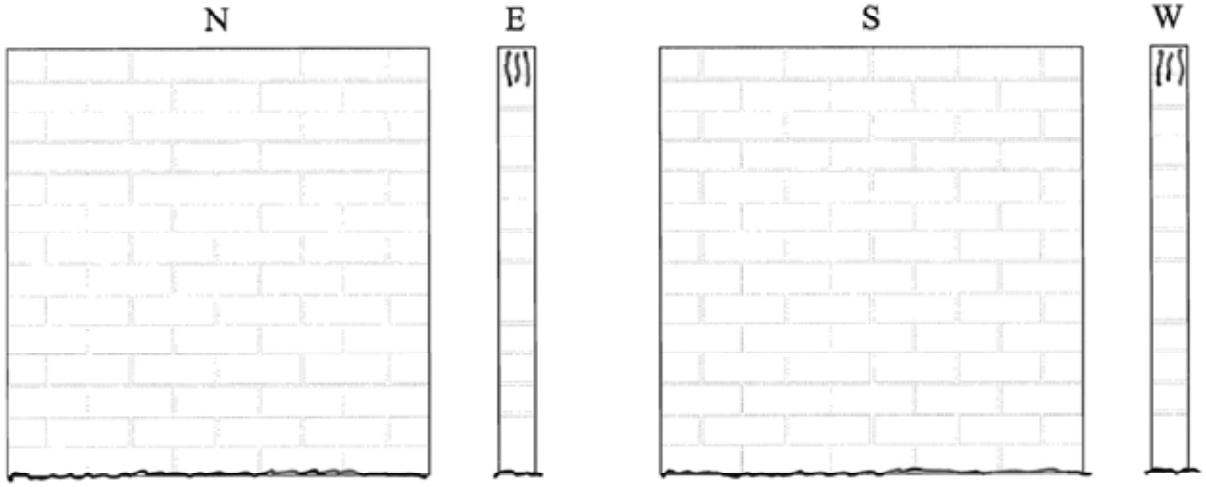

Wallette B1_2

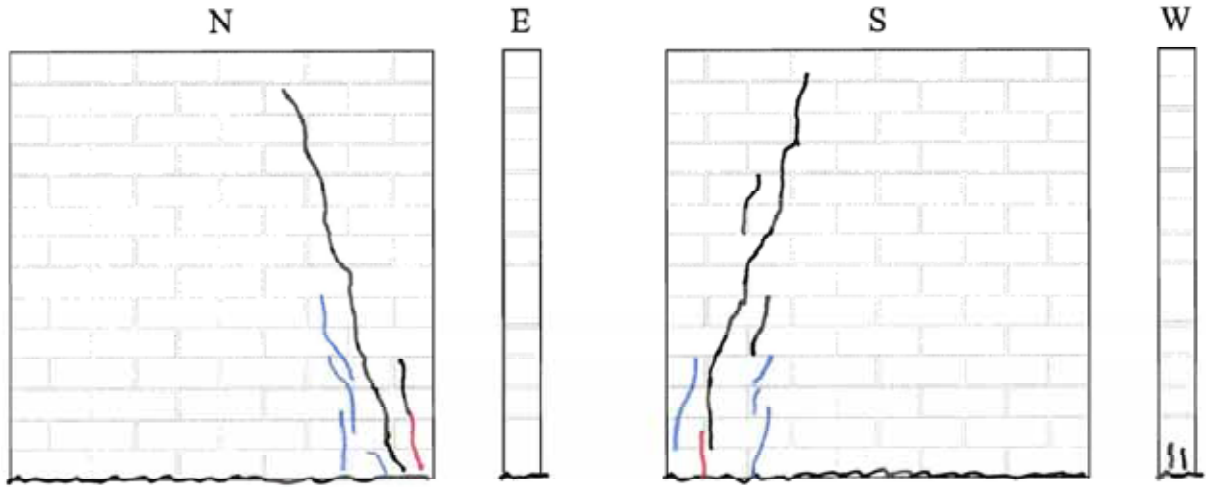

Wallette B1_3

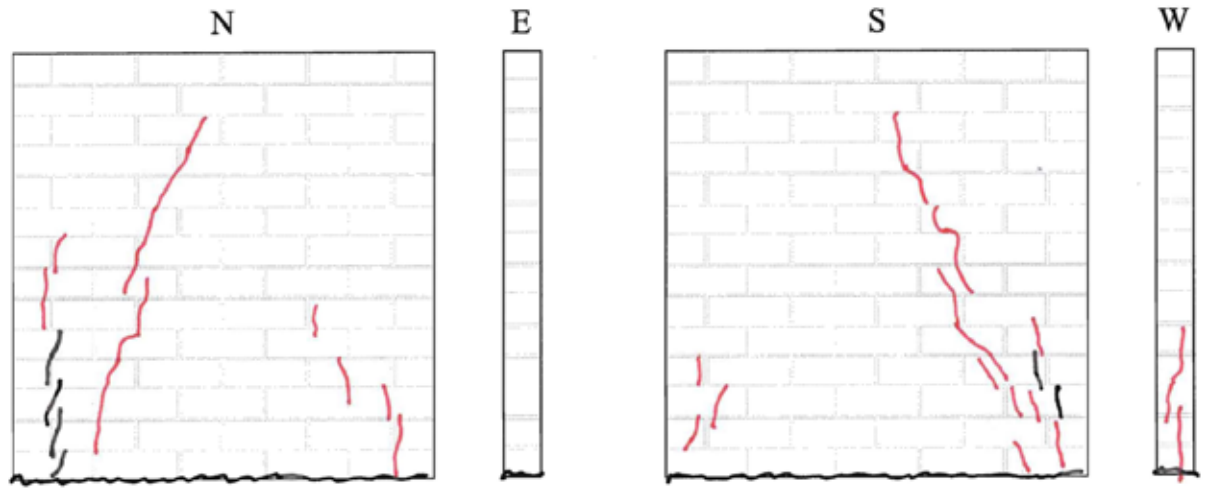

Wallette B2_1

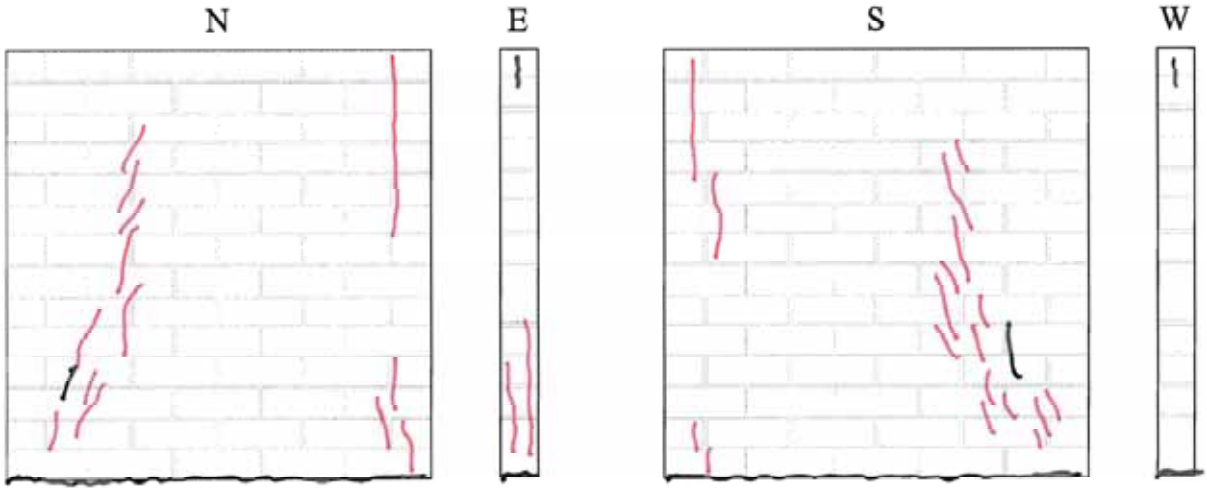

Wallette B2_2

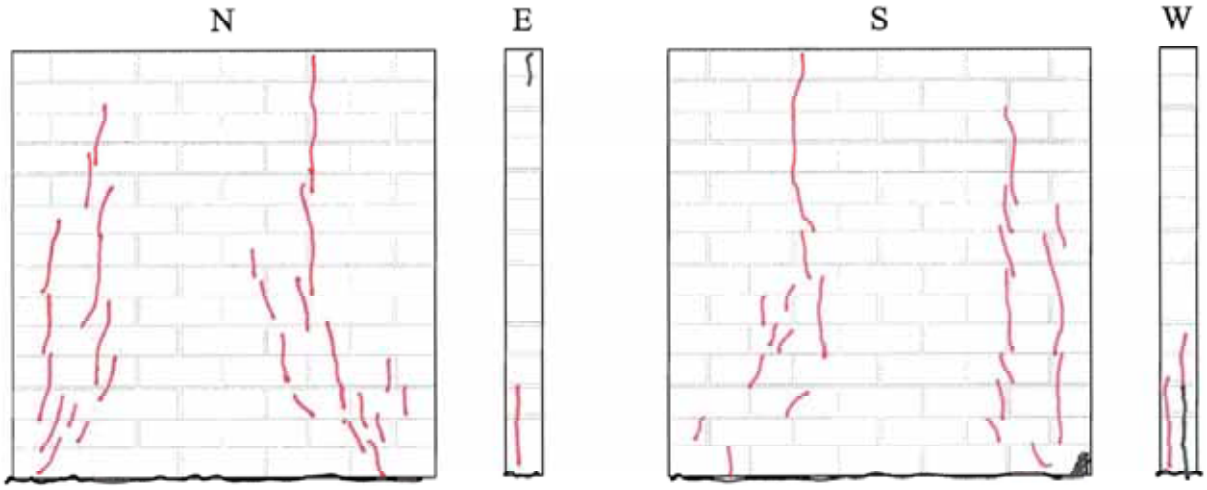

Wallette B2_3

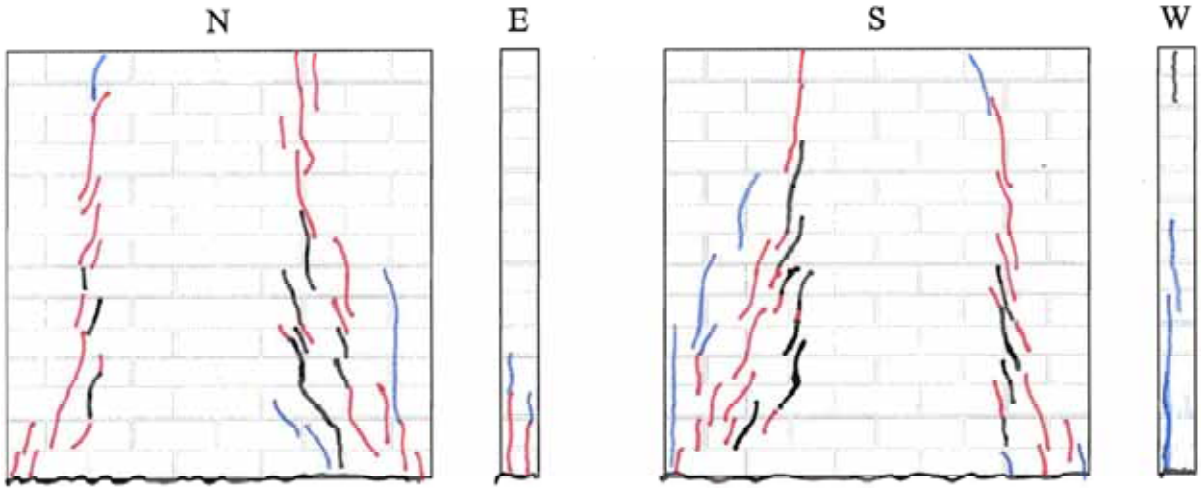

Wallette B3_1

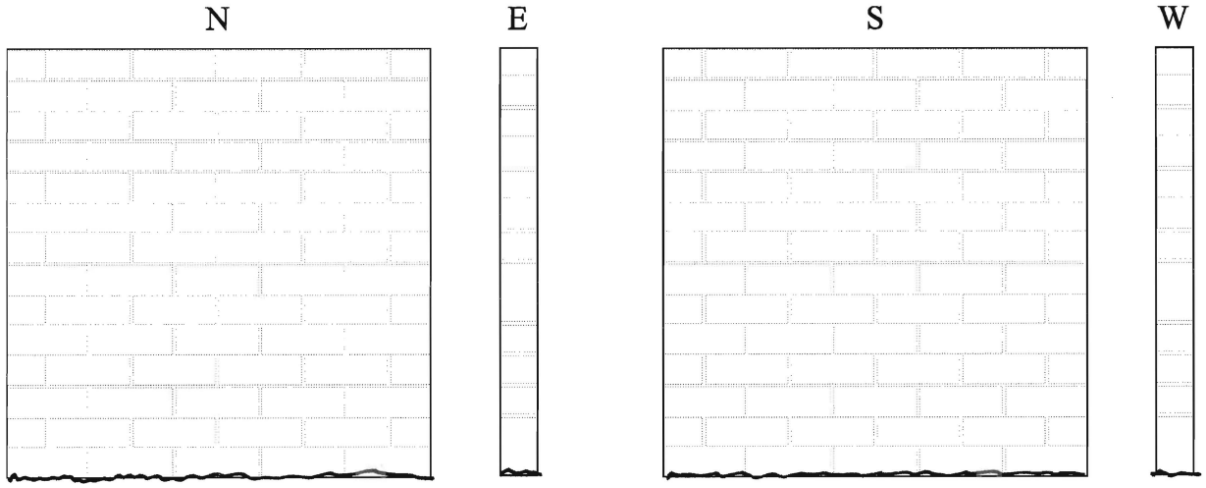

Wallette B3_2

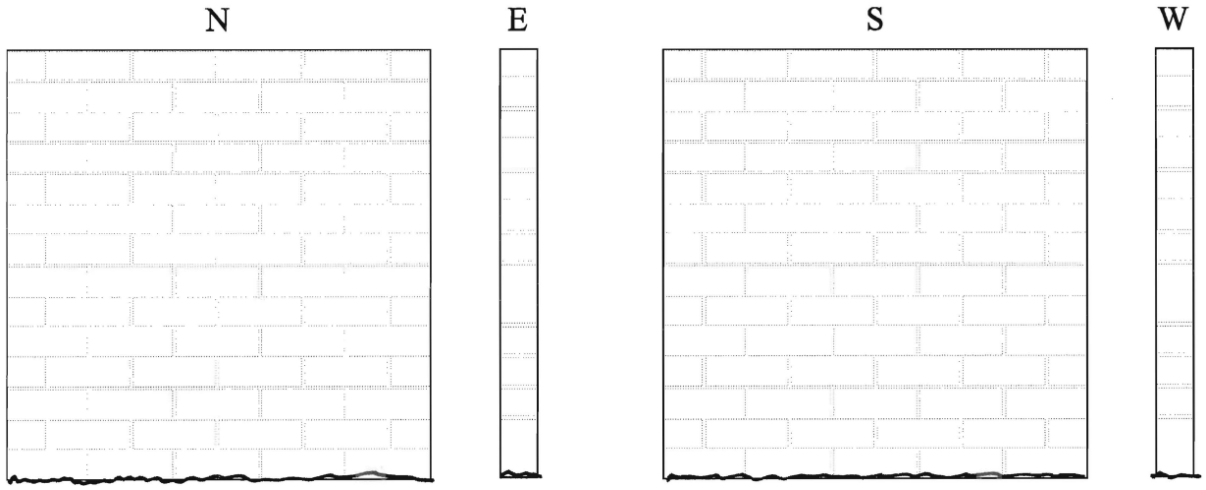

Wallette B3_3

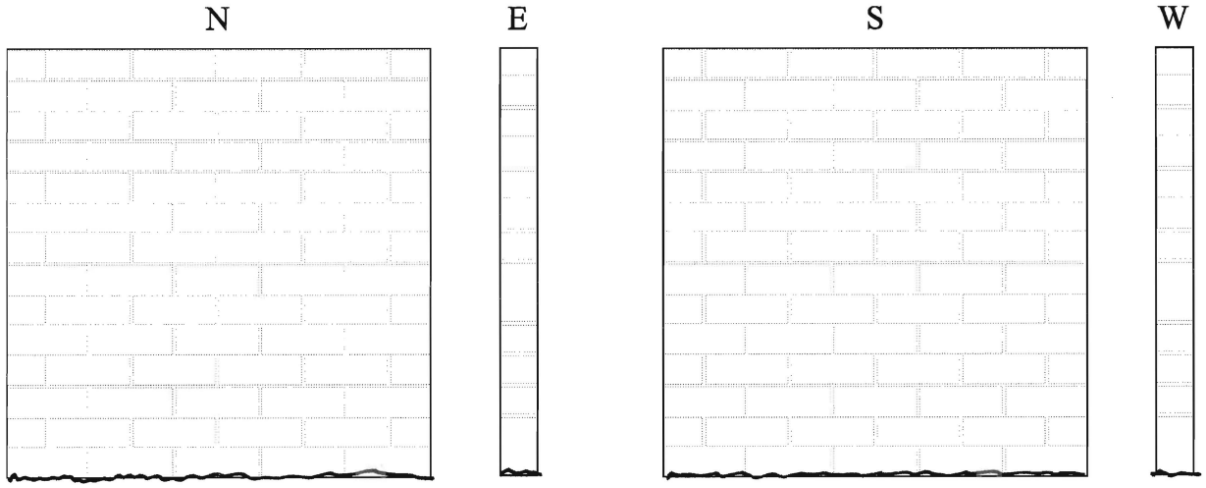

Wallette C1

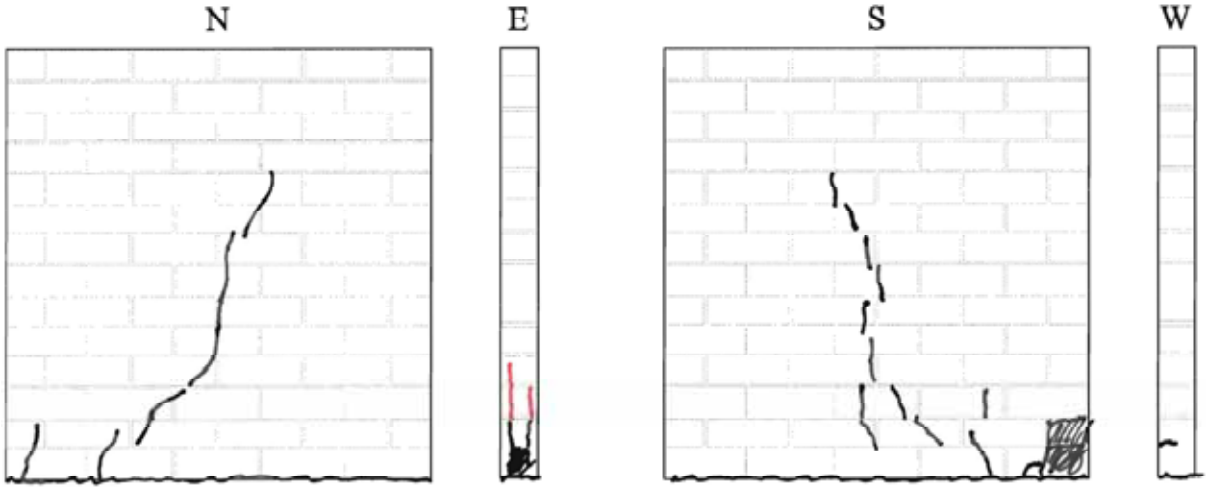

Wallette C2

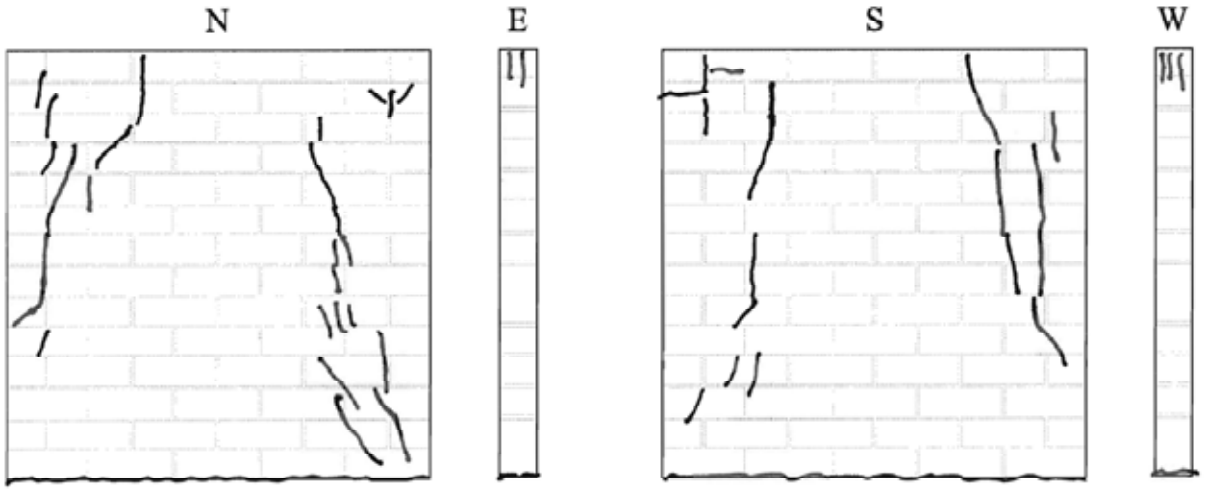

Wallette C3

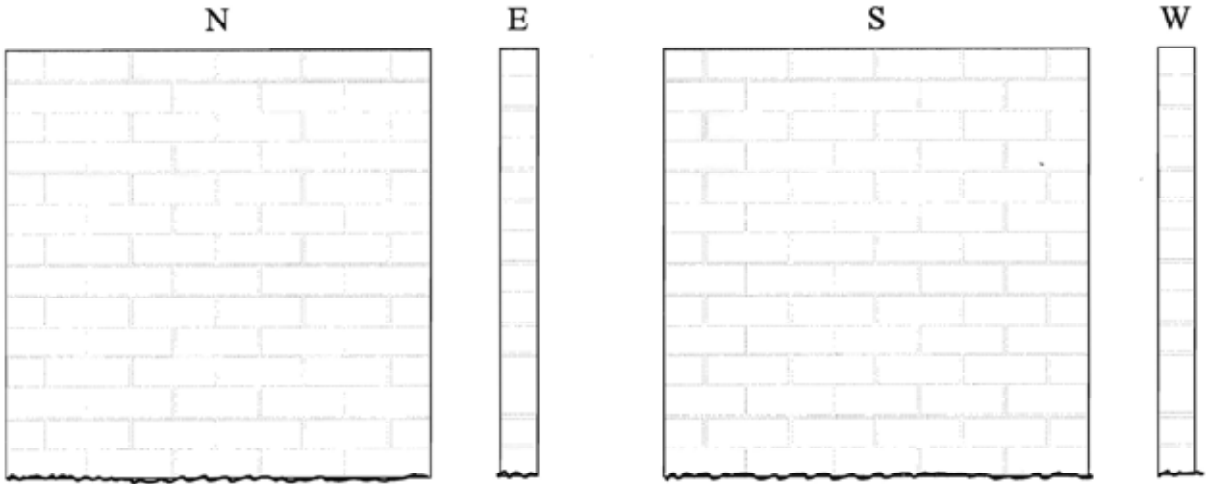

Appendix D: Photo archive

Wallette A1_1

Wallette A1_2

Wallette A1_3

Wallette A2_1



Wallette A2_2


Wallette A2_3


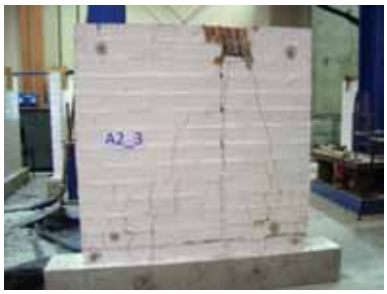

Wallette A3_1


Wallette A3_2

Wallette A3_3

Wallette B1_1

Wallette B1_2

Wallette B1_3


Wallette B2_1

Wallette B2_2

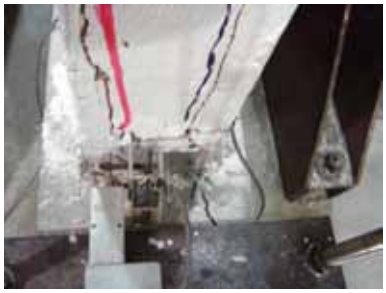


Wallette B2_3

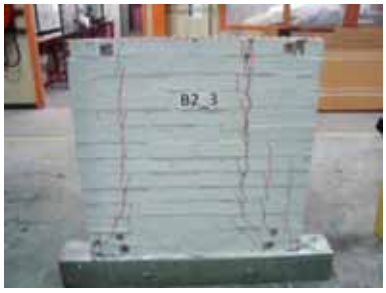

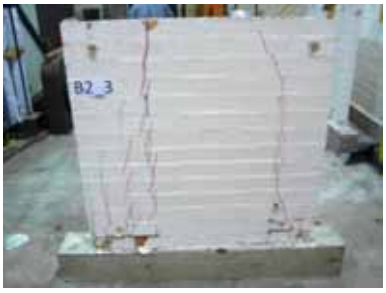

Wallette B3_1

Wallette B3_2

Wallette B3_3

Wallette C1

Wallette C2

Wallette C3